



UNIVERSIDADE ESTADUAL DE CAMPINAS
Faculdade de Engenharia de Alimentos

LEONARDO DO PRADO SILVA

Microbial inactivation by photodynamic treatment: from inactivation kinetics to vegetable applications

Inativação microbiana por tratamento fotodinâmico: da cinética de inativação às aplicações em vegetais

CAMPINAS
2020

LEONARDO DO PRADO SILVA

Microbial inactivation by photodynamic treatment: from inactivation kinetics to vegetable applications

Inativação microbiana por tratamento fotodinâmico: da cinética de inativação às aplicações em vegetais

Tese apresentada à Faculdade de Engenharia de Alimentos da Universidade Estadual de Campinas como parte dos requisitos exigidos para a obtenção do título de Doutor em Ciência de Alimentos.

Thesis presented to the Faculty of Food Engineering of the University of Campinas in partial fulfillment of the requirements for PhD in Food Science.

Orientador: Prof. Dr. Anderson de Souza Sant'Ana

Co-orientador: Prof. Dr. Gilberto Úbida Leite Braga

ESTE EXEMPLAR CORRESPONDE À VERSÃO FINAL DA TESE DEFENDIDA PELO ALUNO LEONARDO DO PRADO SILVA, ORIENTADO PELO PROF. DR. ANDERSON DE SOUZA SANT'ANA E CO-ORIENTADO PELO PROF. DR. GILBERTO ÚBIDA LEITE BRAGA

CAMPINAS

2020

Ficha catalográfica
Universidade Estadual de Campinas
Biblioteca da Faculdade de Engenharia de Alimentos
Claudia Aparecida Romano - CRB 8/5816

P882m Prado-Silva, Leonardo do, 1990-
Microbial inactivation by photodynamic treatment : from inactivation kinetics to vegetable applications / Leonardo do Prado Silva. – Campinas, SP : [s.n.], 2020.

Orientador: Anderson de Souza Sant'Ana.
Coorientador: Gilberto Ubida Leite Braga.
Tese (doutorado) – Universidade Estadual de Campinas, Faculdade de Engenharia de Alimentos.

1. Tecnologias emergentes. 2. *Bacillus cereus*. 3. *Alicyclobacillus acidoterrestris*. 4. Deterioração. 5. Patógeno. 6. Fotossensibilização. I. Sant'Ana, Anderson de Souza. II. Braga, Gilberto Ubida Leite. III. Universidade Estadual de Campinas. Faculdade de Engenharia de Alimentos. IV. Título.

Informações para Biblioteca Digital

Título em outro idioma: Inativação microbiana por tratamento fotodinâmico : da cinética de inativação às aplicações em vegetais

Palavras-chave em inglês:

Emerging technologies

Bacillus cereus

Alicyclobacillus acidoterrestris

Spoilage

Pathogen

Photosensitization

Área de concentração: Ciência de Alimentos

Titulação: Doutor em Ciência de Alimentos

Banca examinadora:

Anderson de Souza Sant'Ana [Orientador]

Adelaide de Almeida

Alessandra Regina da Silva

Poliana Mendes de Souza

Veronica Ortiz Alvarenga

Data de defesa: 05-08-2020

Programa de Pós-Graduação: Ciência de Alimentos

Identificação e informações acadêmicas do(a) aluno(a)

- ORCID do autor: <https://orcid.org/0000-0002-5181-3904>

- Currículo Lattes do autor: <http://lattes.cnpq.br/6332876092001571>

BANCA EXAMINADORA DA DEFESA DE DOUTORADO

Prof. Dr. Anderson de Souza Sant'Ana

Presidente/Orientador

FEA – UNICAMP

Profa. Dra. Adelaide Almeida

Membro

UAveiro – Portugal

Dra. Alessandra Regina da Silva

Membro

LABTERMO

Profa. Dra. Poliana Mendes de Souza

Membro

UFVJM

Profa. Dra. Verônica Ortiz Alvarenga

Membro

UFMG

Ata da defesa com as respectivas assinaturas dos membros encontra-se no SIGA/Sistema de Fluxo de Dissertação/Tese e na Secretaria do Programa da Unidade.

Dedicatória

Aos meus queridos pais, Mousart (*in memoriam*) e Graça, aos meus irmãos e à minha noiva, Paula, pelo apoio incondicional durante a trajetória.

Agradecimentos

À Deus, pelo dom da vida e por ser fonte inesgotável de esperança diante das dificuldades.

Ao Professor Anderson pela orientação, confiança, ensinamentos e oportunidades durante a realização deste trabalho. Muito obrigado!

Ao Professor Gilberto pela co-orientação, ensinamentos, auxílio e suporte essenciais para o desenvolvimento deste trabalho.

A todos os colaboradores da Universidade de Aveiro: Profa. Adelaide, Dra. Ana Gomes, Profa. Amparo, Profa. Graça Neves e Mariana pela fundamental contribuição e suporte desprendidos a este trabalho.

Ao meu pai Mousart (*in memoriam*) e minha mãe Graça pelos valiosos princípios de vida, amor e apoio incondicional, sem os quais eu não seria capaz de seguir em frente. Vocês sempre serão os meus maiores exemplos de dedicação, caráter e trabalho árduo!

A meus irmãos Márcio, Marcelo, Ana Paula (Papaula) e Adriano (Padrinho) por transmitirem boas energias e pelo orgulho demonstrado ao irmão caçula.

À minha noiva, Paula, por ser minha companheira de vida e maior incentivadora. Não tenho palavras para descrever o quão importante foi o seu apoio durante este período. Obrigado por tudo, em especial, pela confiança em mim depositada!

À minha Avó Terezinha (*in memoriam*) que sempre será luz e anjo da guarda.

À toda a minha família, em especial à minha Madrinha, Tia Lúcia, Tio Paulinho, Tio Luiz, Tia Ana, Tio Chicão (*in memoriam*), Tio Tião, Tia Dora (*in memoriam*), Tia Sônia, Tia Selma, Tio Juninho, Tia Léia, Cláudia, “Tí” Nardim, por sempre estarem presentes de alguma forma.

Ao Sr. Itamar, Dona Regina, Laís, Madi e Tia Landa pelo acolhimento à família de vocês, carinho e confiança.

À Dona Maria Rosa (Maricotinha) por ser um exemplo de vida a todos nós e por compartilharmos de uma mesma paixão: Coca-Cola®.

A todos os meus queridos amigos, em especial – Bruna, Henry, Verônica, Marcão, Bia, WJr, João Bosco, Tomoda e Nivaldo pelos momentos de diversão e companheirismo.

Aos companheiros de trabalho do Laboratório de Microbiologia Quantitativa de Alimentos, em especial – Fer, Mari, Ju, Lari, Mayara, Antônio e Syllas pela convivência e dedicação à ciência.

Aos meus amigos de Vittel – Leticia, César, Rony, Etienne, Adélie, Coralie, Christiane, Sylvie, Murielle e Romain pela acolhida e amizade.

A todos os funcionários da FEA pela amizade e auxílios prestados durante o doutorado.

A todos os membros da banca, titulares e suplentes, pela disponibilidade e contribuições ao trabalho.

À Universidade Estadual de Campinas (UNICAMP) e ao Departamento de Ciência de Alimentos da Faculdade de Engenharia de Alimentos pela oportunidade de desenvolvimento profissional e pessoal.

Ao Conselho Nacional de Desenvolvimento Científico e Tecnológico (CNPq) pela bolsa de doutorado concedida (número do processo: 140092/2017-0).

O presente trabalho foi realizado com apoio da Coordenação de Aperfeiçoamento de Pessoal de Nível Superior - Brasil (CAPES) - Código de Financiamento 001.

RESUMO

As bactérias *Bacillus cereus* e *Alicyclobacillus acidoterrestris* são ambas resistentes aos processos tradicionais de inativação térmica com elevado potencial patogênico e deteriorante, respectivamente. O tratamento fotodinâmico antimicrobiano (TFA) é uma alternativa promissora aos métodos convencionais de inativação microbiana. O TFA consiste no uso de um fotossensibilizador (FS) que ao entrar em contato com as células-alvo gera espécies reativas de oxigênio após exposição à luz visível. Inicialmente foi avaliada a eficácia do TFA com o FS fenotiazínico novo azul de metileno (NMB) nas células vegetativas e esporos de *B. cereus*. Inicialmente, a eficácia do TFA foi avaliada pela determinação da concentração inibitória mínima (CIM) do NMB em células vegetativas de 12 cepas diferentes de *B. cereus* através de um conjunto de 96 diodos emissores de luz (LED) vermelha com emissão de 631 nm e irradiância de 24,5 mW/cm². Os resultados da CIM permitiram selecionar 4 cepas de *B. cereus* (B3, 436, B63, ATCC 14579) através de uma análise de agrupamento com base na distância Euclidiana. Em seguida, foi realizado um estudo de sobrevivência ao TFA com NMB em três concentrações (5, 50 e 100 µM). Este estudo mostrou que o TFA reduziu a viabilidade tanto das células vegetativas como dos esporos das 4 cepas de *B. cereus* ($P < 0,05$) em todas as fluências aplicadas (0 - 450 J/cm²). As curvas de inativação de *B. cereus* apresentaram bom ajuste ao modelo de Weibull, o qual foi utilizado para estimar os parâmetros cinéticos δ e p de inativação fotodinâmica que correspondem à fluência necessária para a primeira redução decimal e ao parâmetro de curvatura, respectivamente. A cepa ATCC 14579 apresentou em todas as condições $p > 1$, indicando que as células vegetativas e esporos desta cepa foram progressivamente eliminadas pelo TFA. A cepa B3 obteve significativamente ($P < 0,05$) o menor valor de δ ($0,51 \pm 0,30$ J/cm²), indicando que havia uma população de células vegetativas muito sensível no início do TFA com NMB a 5 µM. No entanto, neste tratamento não foram alcançadas o mínimo de 4 reduções decimais (4D), o que demonstra que uma outra parcela da população foi mais resistente ao longo do TFA. Durante a avaliação do TFA com os esporos de *B. cereus* o NMB a 50 µM foi a única concentração capaz de atingir 4D para todas as cepas. Os resultados deste capítulo demonstraram que houve variabilidade entre as cepas de *B.*

cereus. No capítulo 3 o objetivo foi avaliar o TFA utilizando como FS uma porfirina tetracatiônica (Tetra-Py⁺-Me) e o NMB nos esporos de *A. acidoterrestris*. Os experimentos foram conduzidos como descrito a seguir: (I) *In vitro*, em tampão fosfato salina (PBS) com os FS Tetra-Py⁺-Me e NMB e exposição luminosa através de um LED com emissão de luz branca (400 – 700 nm) e irradiância de 140 mW/cm², (II) suco de laranja nas mesmas condições anteriores com a adição de iodeto de potássio (KI) como agente potencializador do TFA e (III) casca de laranja com apenas o uso do FS Tetra-Py⁺-Me com e sem a presença de KI e exposição luminosa através do LED e radiação solar, ambos à 65 mW/cm². Os experimentos em PBS com Tetra-Py⁺-Me a 10 µM resultaram em 7,3 reduções logarítmicas na viabilidade dos esporos de *A. acidoterrestris* após 5 h de TFA. Contrariamente, os ensaios em PBS com NMB não resultaram em reduções significativas. Em seguida, os resultados obtidos com Tetra-Py⁺-Me e NMB a 10 µM em suco de laranja na presença de KI resultaram em 5 reduções logarítmicas com ambos os FS após 10 h de TFA. Posteriormente, a inativação de esporos de *A. acidoterrestris* inoculados artificialmente em cascas de laranja foi realizada com Tetra-Py⁺-Me a 10 e 50 µM. Nenhum incremento significativo foi observado pelo uso de KI. A maior concentração de Tetra-Py⁺-Me (50 µM) causou 2,8 reduções logarítmicas na viabilidade dos esporos de *A. acidoterrestris* em cascas de laranja após 6 h exposição à radiação solar (65 mW/cm²). As características colorimétricas e nutricionais do suco de laranja e da casca foram significativamente (P < 0,05) influenciadas pela exposição à luz artificial e radiação solar. Os resultados deste estudo sugerem que o TFA é um método potencial para a redução microbiológica de *B. cereus* e *A. acidoterrestris*. No entanto, novos estudos são necessários para otimizar a aplicação do TFA pela indústria de alimentos.

Palavras-chave: Tecnologias emergentes, *Bacillus cereus*, *Alicyclobacillus acidoterrestris*, Deterioração, Patógeno, Fotossensibilização

ABSTRACT

The bacteria *Bacillus cereus* and *Alicyclobacillus acidoterrestris* are both resistant to conventional thermal microbial inactivation processes with high pathogenic and spoilage potential, respectively. Antimicrobial photodynamic treatment (aPDT) is a promising alternative to conventional microbial inactivation methods. aPDT is based on the use of a photosensitizer (PS) which in contact with the target cells, generate reactive oxygen species (ROS) after exposure to visible light. Initially was evaluated the efficacy of aPDT with the phenothiazinium PS new methylene blue (NMB) on the vegetative cells and spores of *B. cereus*. Initially, the effectiveness of aPDT was assessed by determining the minimum inhibitory concentration (MIC) of NMB on vegetative cells of 12 different strains of *B. cereus* using an array of 96 red light-emitting diodes (LED) with an emission peak of 631 nm and irradiance of 24.5 mW/cm². The results of the MIC allowed to select 4 strains of *B. cereus* (B3, 436, B63, ATCC 14579) through a cluster analysis based on the Euclidean distance. Then, a survival study of aPDT with NMB at three concentrations (5, 50, and 100 µM) was performed. This study showed that aPDT reduced the viability of both vegetative cells and spores of the 4 strains of *B. cereus* ($P < 0.05$) at all fluences (0 - 450 J / cm²). *B. cereus* inactivation curves presented a good fit to the Weibull model, which was used to estimate the kinetic parameters δ and p of photodynamic inactivation corresponding to the fluency required for the first decimal reduction and the curvature parameter, respectively. The strain ATCC 14579 presented in all conditions $p > 1$, indicating that the vegetative cells and spores of this strain were progressively eliminated by aPDT. The strain B3 obtained significantly ($P < 0.05$) the lowest value of δ (0.51 ± 0.30 J/cm²), indicating that there was a very sensitive vegetative cell population at the beginning of aPDT with 5 µM NMB. However, in this treatment, a minimum of 4 decimal reductions (4D) was not achieved, which demonstrates that another portion of the population was more resistant throughout the aPDT. During the aPDT with *B. cereus* spores, NMB at 50 µM was the only concentration capable to reach 4D for all strains. The results of this chapter demonstrated that there was variability between *B. cereus* strains. In chapter 3, the objective was to evaluate aPDT using a tetracationic porphyrin (Tetra-Py⁺-Me) and NMB in the spores of *A. acidoterrestris* as PS. The experiments were

conducted as follows: (I) *In vitro*, in phosphate-buffered saline (PBS) with PS Tetra-Py⁺-Me and NMB and light exposure through an LED with white light emission (400 – 700 nm) and irradiance of 140 mW/cm², (II) orange juice in the same conditions as before with the addition of potassium iodide (KI) as a potentiator agent of aPDT and (III) orange peel using only the PS Tetra-Py⁺-Me in the presence and absence of KI and exposition to LED and solar radiation, both at 65 mW/cm². The experiments in PBS with Tetra-Py⁺-Me at 10 µM resulted in 7.3 log reductions in the viability of *A. acidoterrestris* spores after 5 h of aPDT. Contrarily, the experiments with NMB did not result in significant reductions. Then, the results obtained with Tetra-Py⁺-Me and NMB at 10 µM in orange juice in the presence of KI resulted in 5 log reductions with both PS after 10 h of aPDT. Subsequently, the inactivation of *A. acidoterrestris* spores, artificially inoculated in orange peels, was performed with Tetra-Py⁺-Me at 10 and 50 µM. No significant increment was observed for the use of KI. The highest concentration of Tetra-Py⁺-Me (50 µM) caused 2.8 log reductions in the viability of *A. acidoterrestris* spores in orange peels after 6 h exposure to solar radiation (65 mW/cm²). The colorimetric and nutritional characteristics of orange juice and peel were significantly ($P < 0.05$) influenced by exposition to artificial light and solar radiation. The results of this study suggest that aPDT is a potential method for the microbiological reduction of *B. cereus* and *A. acidoterrestris*. However, further studies are required to optimize the application of aPDT in the food industry.

Keywords: Emerging technologies, *Bacillus cereus*, *Alicyclobacillus acidoterrestris*, Spoilage, Pathogen, Photosensitization

Lista de abreviaturas e siglas

ΔE	Total color change
δ	Time for first decimal reduction
$\bullet\text{OH}$	Hydroxyl radicals
$^1\text{O}_2$	Singlet oxygen
$^3\text{O}_2$	Triplet dioxygen
4D	Four decimal reductions
ABTS ⁺	2,2-Azino-bis(3-ethylbenzothiazoline)-6-sulponic acid
ALA	5-aminolevulinic acid
ANOVA	Analysis of variance
aPDT	Antimicrobial photodynamic treatment
ATCC	American type culture collection
Ca^{2+}	Calcium ions
CDC	Center for disease control and prevention
CFU	Colony forming unit
Chl	Chlorophyllin
CIM	Concentração inibitória mínima
DC	Dark control
DMMB	1,9-dimethylmethylene blue
DMSO	Dimethyl sulfoxide
DNA	Deoxyribonucleic acid
DPPH	2,2-difenil-1-picrilhidrazila
DSMZ	Deutsche Sammlung von Mikroorganismen und Zellkulturen
DTA	Doença transmitida por alimentos
e^-	Electron
EOY	Eosin Y
ERY	Erythrosine
FDA	Food and drug administration
FS	Fotossensibilizador
H_2O_2	Hydrogen peroxide
Hyp	Hypericin
I_2/I_3^-	Free molecular iodine

$I_2^{\bullet-}$	Iodine radicals
KI	Potassium iodide
L^*, a^*, b^*	Color coordinates
LC	Light control
LED	Light-emitting diode
MB	Methylene blue
Mg^{2+}	Magnesium ions
MIC	Minimal inhibitory concentration
NaBr	Sodium bromide
NaN_3	Sodium azide
NMB	New methylene blue
O_2	Oxygen
$O_2^{\bullet-}$	Superoxide anions
OMS	Organização mundial da saúde
ORAC	Oxygen radical absorbance capacity
ρ	Curvature parameter
PBS	Phosphate-buffered saline
PDT	Photodynamic therapy
PS	Photosensitizer
RB	Rose bengal
ROS	Reactive oxygen species
SCN^-	Thiocyanate
TBO	Toluidine blue O
Tetra-Py ⁺ -Me	5,10,15,20-tetrakis(1-methylpyridinium-4-yl) porphyrin tetra-iodide
TFA	Tratamento fotodinâmico antimicrobiano
TPC	Total phenolic content
UV	Ultraviolet
WHO	World health organization
YSG-A	Yeast starch glucose agar
YSG-B	Yeast starch glucose broth
$\Phi\Delta$	Quantum yield of singlet oxygen

Sumário

Introdução geral.....	17
Capítulo 1 – Revisão de Literatura.....	22
Antimicrobial photodynamic treatment (aPDT) as an innovative technology to control spoilage and pathogenic microorganisms in agrifood products: An updated review.....	22
Abstract.....	23
Research Highlights	24
1. Introduction	25
2. Concepts of antimicrobial photodynamic treatment.....	27
2.1. Mechanisms of action.....	28
2.2. Potentiation effect of inorganic salts on aPDT.....	31
2.3. Factors affecting the aPDT efficacy on foods.....	31
3. Photosensitizers.....	33
4. Sources of light	42
5. Inactivation efficacy of aPDT on the main foodborne microorganisms.....	43
5.1. Bacterial vegetative cells.....	44
5.2. Spore forming bacteria and biofilms.....	49
5.3. Yeasts and molds.....	52
5.4. Protozoa and viruses.....	53
6. Agrifood applications.....	59
6.1. Fruits and vegetables	59
6.2. Meat products	60
6.3. Milk.....	61
6.4. Plant diseases.....	62
7. Conclusions and future perspectives.....	66
Acknowledgements	67
8. References.....	67
Capítulo 2 – Inactivation kinetics of <i>Bacillus cereus</i> vegetative cells and spores from different sources by antimicrobial photodynamic treatment (aPDT)	93
Abstract.....	94

Research Highlights	95
1. Introduction	96
2. Material and methods.....	98
2.1 <i>Bacterial strains, cultivation and preparation of spore suspensions</i>	98
2.2 <i>Photosensitizer.....</i>	98
2.3 <i>Light source</i>	99
2.4 <i>Antimicrobial photodynamic treatment</i>	100
2.4.1 Evaluation of aPDT efficacies on vegetative cells of <i>B. cereus</i> based on the photosensitizer minimum inhibitory concentration (MIC)	100
2.4.2 aPDT resistance of vegetative cells and spores of selected <i>B. cereus</i> strains	100
2.5 <i>Modelling of aPDT inactivation data.....</i>	101
2.6 <i>Statistical analysis.....</i>	101
3. Results and discussion.....	102
Acknowledgment	112
4. References.....	113
Capítulo 3 - Antimicrobial photodynamic treatment as an alternative approach for Alicyclobacillus acidoterrestris inactivation	118
Abstract.....	119
Research Highlights	121
1. Introduction	122
2. Materials and Methods	125
2.1. <i>Spore cultivation and growth conditions.....</i>	125
2.2. <i>Photosensitizers.....</i>	125
2.3. <i>Light source</i>	126
2.4. <i>Antimicrobial photodynamic treatments</i>	127
2.4.1. <i>In vitro</i> photoinactivation of <i>A. acidoterrestris</i> spores.....	127
2.4.2. Photoinactivation of <i>A. acidoterrestris</i> spores in orange juice	128
2.4.3. Photoinactivation of <i>A. acidoterrestris</i> spores on orange peel.....	128
2.5. <i>Colorimetric analysis</i>	129
2.6. <i>Total phenolics content and antioxidant capacity of orange juice after aPDT.....</i>	130
2.6.1. Total phenolic content.....	130
2.6.2. Antioxidant capacity.....	130
2.7. <i>Statistical analysis.....</i>	131
3. Results	132
3.1. <i>aPDT of Alicyclobacillus spores.....</i>	132

3.1.1.	<i>In vitro</i> photoinactivation of <i>A. acidoterrestris</i> spores.....	132
3.1.2.	Photoinactivation of <i>A. acidoterrestris</i> spores in orange juice	133
3.1.3.	Photoinactivation of <i>A. acidoterrestris</i> spores on orange peel.....	135
3.2.	<i>Colorimetric analysis</i>	137
3.3.	<i>Phenolic content and antioxidant capacity of orange juice exposed to light</i>	137
4.	Discussion	139
	Acknowledgements	144
5.	References	144
	Discussão geral	155
	Conclusão geral	161
	Referências	163
	Anexos	171

Introdução geral

As doenças transmitidas por alimentos (DTAs) são uma das principais preocupações dos órgãos governamentais em relação à saúde pública. A presença de micro-organismos patogênicos em alimentos é responsável pela mortalidade e morbidade que afetam a vida das pessoas, a economia e o desenvolvimento social dos países. De acordo com a Organização Mundial da Saúde (OMS) 1 em cada 10 pessoas (≈ 600 milhões) adoecem após o consumo de alimentos contaminados em todo o mundo. Além disso, aproximadamente 420.000 pessoas morreram em decorrência de DTAs, das quais 125.000 são crianças menores de 5 anos de idade (WHO, 2015). Estima-se que as perdas econômicas em produtividade e tratamento clínico de DTAs ultrapassem US\$110 bilhões em países subdesenvolvidos (WORLD BANK, 2018). No entanto, grande parte das DTAs e suas consequências poderiam ser evitadas por meio de boas práticas de higiene em toda a cadeia de produção e consumo de alimentos.

Além das preocupações que envolvem a segurança dos alimentos, outro desafio enfrentado pela humanidade são as perdas de alimentos devido ao desperdício ou deterioração por micro-organismos (ODEYEMI et al., 2020). Um estudo conduzido pela Organização das Nações Unidas para a Alimentação e Agricultura revelou que aproximadamente 1,3 bilhão de toneladas de alimentos para o consumo humano é desperdiçado ou descartado por deterioração (FAO, 2011). Portanto, com o crescente aumento populacional, a demanda por alimentos para o consumo humano também segue o mesmo ritmo de crescimento.

Os micro-organismos estão amplamente distribuídos no ambiente e podem contaminar os alimentos por meio do contato direto com a água e o solo. Dentre os micro-organismos que são encontrados, pode-se destacar a bactéria *Bacillus cereus*, pela frequente associação a surtos de DTAs e deterioração de produtos lácteos (SPANU, 2016). Além disso, também destaca-se o gênero bacteriano *Alicyclobacillus* spp., considerado uma das principais preocupações da indústria de suco de frutas pelo seu elevado potencial de deterioração de produtos ácidos (HIPPCHEM; RÖLL; PORALLA, 1981; ORR et al., 2000).

B. cereus é uma bactéria gram-positiva, formadora de esporos, aeróbia facultativa e mesófila que pode ser frequentemente encontrada no solo e nas fezes de animais (CARLIN, 2011; HEYNDRICKX, 2011). As intoxicações alimentares causadas por *B. cereus* são caracterizadas principalmente por vômitos (toxina emética) e diarreia (enterotoxina) (BOTTONNE, 2010). Em produtos lácteos, *B. cereus* pode causar deterioração pela produção de enzimas como lipases, proteinases e fosfolipases que podem desencadear processos de coagulação e alteração de sabor (MEHTA et al., 2019).

As espécies do gênero *Alicyclobacillus* são bactérias Gram-positivas podendo também ser Gram-variáveis, termoacidófilas, formadora de esporos, móveis, aeróbias e caracterizadas pela presença de ácidos graxos ω -alicíclicos como principal componente lipídico da parede celular (TORLAK, 2014; WISOTZKEY et al., 1992; YAMAZAKI; TEDUKA; SHINANO, 1996). Dentre as espécies do gênero, *Alicyclobacillus acidoterrestris* é a espécie mais associada à deterioração desde o primeiro caso descrito, envolvendo suco de maçã (CERNY; HENNLICH; PORALLA, 1984; HU et al., 2020; VAN LUONG et al., 2019). Por meio do contato direto com o solo ou pela poeira, os esporos de *A. acidoterrestris* podem contaminar as frutas usadas na fabricação de suco. Assim, durante o processamento, esses esporos podem sobreviver às etapas de sanitização da superfície das frutas e pasteurização, permanecendo nos produtos finais (OTEIZA et al., 2011; SPINELLI et al., 2009). A deterioração de produtos ácidos como os sucos de frutas pela atividade metabólica de *Alicyclobacillus* é caracterizada por odores desagradáveis provenientes da produção de guaiacol e outros compostos halofenólicos (CHANG; KANG, 2004; SIEGMUND; PÖLLINGER-ZIERLER, 2006). Embora seja visualmente difícil detectar a deterioração pela ausência de produção de gás, a presença de tais compostos causa rejeição pelos consumidores e conseqüentemente perdas econômicas para as indústrias (SMIT et al., 2011).

Em complemento às políticas públicas de incentivo às boas práticas de higiene e orientações para evitar o desperdício, o processamento industrial contribui para a segurança e a qualidade dos alimentos. Dentre os processamentos estabelecidos pelas indústrias de alimentos, destacam-se os tratamentos térmico e químico. No

entanto, sabe-se que os processos térmicos podem causar efeitos indesejáveis aos alimentos como, por exemplo, perdas na qualidade sensorial e nutricional (UCHIDA; SILVA, 2017). Além disso, o uso de sanitizantes não é considerado ambientalmente correto, além de ser prejudicial aos seres humanos (ÖLMEZ; KRETZSCHMAR, 2009).

Desta forma, pesquisas na área de microbiologia de alimentos buscam por alternativas não térmicas e ambientalmente corretas que sejam capazes de reduzir a contaminação dos alimentos por micro-organismos com a mesma segurança dos métodos tradicionais. Na literatura existem várias tecnologias inovadoras de processamento moderado que foram desenvolvidas para suprir essa necessidade da indústria de alimentos (CEBRIÁN; MAÑAS; CONDÓN, 2016; FERRARIO; GUERRERO, 2018; KIM et al., 2017; REVERTER-CARRIÓN et al., 2018). Até o momento, as tecnologias mais estudadas são as que envolvem o uso da luz pulsada, da radiação UV, de campo elétrico pulsado, de plasma frio e do processamento de alta pressão (BARBA et al., 2017). No entanto, para a maioria das técnicas mencionadas os custos de instalação e manutenção são elevados (BARBA et al., 2017).

Assim, surgiu o interesse dos cientistas por uma técnica antimicrobiana promissora, que já é amplamente usada na área médica, denominada tratamento fotodinâmico antimicrobiano (TFA) (WAINWRIGHT et al., 2017). Essa técnica centenária permite que por meio da combinação de luz, oxigênio molecular e um composto fotossensibilizador seja possível matar células-alvos, como as células tumorais e os micro-organismos (JESIONEK; VON TAPPEINER, 1905; RAAB, 1900). A técnica evoluiu grandemente em termos de compostos fotossensibilizadores (FS) e tipos de fontes de luz, na área médica, principalmente para o tratamento de câncer (MANSOORI et al., 2019). O tratamento fotodinâmico destaca-se pela elevada capacidade de produção de espécies reativas de oxigênio, que atuam em múltiplos alvos celulares, como por exemplo, ácidos nucleicos, proteínas e lipídios (HAMBLIN; ABRAHAMSE, 2020). Por conta dessa característica houve o renascimento do tratamento fotodinâmico para a inativação microbiana, particularmente devido ao surgimento de micro-organismos resistentes aos antimicrobianos tradicionais (WAINWRIGHT et al., 2017). Além disso, o uso de compostos FS não tóxicos e de

fontes de luz que emitem no espectro visível, tornam o TFA uma alternativa segura e promissora para o setor de alimentos (PASKEVICIUTE; ZUDYTE; LUKŠIENE, 2019).

Nos últimos 10 anos vários estudos avaliaram os efeitos de diferentes tipos de FS e fontes de luz na redução da contaminação microbiana por meio do TFA (BARTOLOMEU et al., 2016; BEIRÃO et al., 2014; HUANG et al., 2020; LUKSIENE; PASKEVICIUTE, 2011; OLIVEIRA et al., 2009; RODRIGUES et al., 2019; VECCHIO et al., 2015; ŽUDYTE; LUKŠIENE, 2019). No entanto, mais estudos são necessários, principalmente em relação à inativação de micro-organismos termoresistentes como são os casos das bactérias *B. cereus* e *A. acidoterrestris*. Por conta da relevância em relação às DTAs (*B. cereus*) e deterioração de alimentos (*B. cereus* e *A. acidoterrestris*) ambas as bactérias são modelos interessantes para a aplicação do TFA.

Desta forma, no capítulo 1 foi realizada uma revisão de literatura com o objetivo de discutir os avanços mais recentes com TFA no setor agroalimentar. Os principais compostos FS e fontes de luz utilizados em TFA, bem como os mecanismos de inativação, os fatores que podem afetar a eficácia do tratamento e os efeitos de potencialização do TFA foram abordados. Além disso, os principais micro-organismos avaliados em TFA, potenciais aplicações do tratamento no setor agroalimentar e as perspectivas futuras do TFA também foram discutidas.

No capítulo 2, o objetivo do trabalho foi avaliar eficiência do TFA, com exposição à luz vermelha na presença do corante fenotiazínico novo azul de metileno (NMB) como PS, na inativação de células vegetativas e esporos de 12 diferentes cepas de *B. cereus*. Além disso, com os resultados deste capítulo foi possível estimar os parâmetros cinéticos de inativação fotodinâmica por meio do modelo de Weibull para 4 cepas selecionadas de acordo com a resistência ao tratamento.

No capítulo 3, objetivou-se investigar a eficiência do TFA com uma porfirina tetracatiônica (Tetra-Py⁺-Me) e NMB combinados com exposição à luz branca, na inativação esporos de *A. acidoterrestris* em três diferentes matrizes: PBS, suco de laranja e casca de laranja. O efeito da potencialização do tratamento pela adição de iodeto de potássio (KI) nos experimentos com suco de laranja e casca também foram

avaliados. Por fim, também foi avaliado o impacto do TFA nas características nutricionais e colorimétricas do suco de laranja e da casca após os tratamentos.

16 **Abstract**

17 Antimicrobial photodynamic treatment (aPDT) is a light-based method developed for
18 the inactivation of microorganisms. The advance of oncological diseases has made
19 photodynamic treatment widely used in the treatment of cancer. With the emergence
20 of antifungal and antibiotic-resistant microorganisms, the aPDT has been strongly
21 raised as a promising intervention to this global concern. The treatment involves the
22 combination of visible light, photosensitizer (PS) compounds, and the presence of
23 oxygen resulting in the generation of abundant reactive oxygen species (ROS), which
24 further attack multiple cellular targets of microbial cells and result in their death. The
25 multi-target mechanisms of action triggered by aPDT efficiently prevent the selection
26 of resistant microorganisms. The efficacy of aPDT for microbial inactivation on foods
27 can be affected by several factors such as type and characteristics of the PS, light
28 source features, food surface geometry, environmental aspects, and microbial
29 characteristics. The application of aPDT has spread rapidly in many types of agrifood
30 products and their associated processes, as food cultivation, industrial processing,
31 storage, distribution, and retail. Most of the *in vitro* aPDT studies have shown
32 significant results, including some cases in which up to 8 log CFU/mL reductions was
33 achieved. Strong antimicrobial performance of aPDT was also identified when the
34 investigation was carried out on various food matrixes, including fruits and vegetables
35 (1.5-5.0 log CFU/mL reductions), meat products (0.6-5.0 log CFU/mL reductions), and
36 milk (1.0-7.0 log CFU/mL reductions). This review aims to update information on the
37 advances of aPDT in the food and agriculture sectors, including photosensitizers,
38 source of light, microbial inactivation efficacy, affecting factors, potentiation effects,
39 inactivation mechanisms, possible applications on food and agriculture as well as the
40 future perspectives.

41

42 **Keywords:** Antimicrobial photodynamic treatment, emerging technologies,
43 photosensitization, reactive oxygen species, food safety, surface decontamination,
44 food spoilage

45 ***Research Highlights***

- 46 ○ Studies revealed the microbial reduction with different photosensitizers (PS)
- 47 ○ Chlorophyllin and curcumin are the most used natural PS
- 48 ○ The aPDT efficiency is dependent on PS formulation and source of light used
- 49 ○ aPDT effect can be enhanced by non-toxic compounds such as potassium
- 50 iodide
- 51 ○ Studies that evaluate the characteristics of food after photodynamic treatment
- 52 are still lacking

53 **1. Introduction**

54

55 Foodborne illness is one of the major global concerns in public health. The
56 contamination of foods with pathogens is responsible for mortality and morbidity that
57 impact on people's lives and countries' economies and in social development
58 (Havelaar et al., 2015). According to the Centers for Disease Control and Prevention
59 of the United States, 3,000 Americans die each year as a result of foodborne illnesses
60 (CDC, 2020a). The latest survey of foodborne outbreaks in Brazil in 2018 registered
61 597 outbreaks, 8,406 sick people, 916 hospitalizations, and 9 deaths (Saúde, 2019a).
62 Several bacterial (e.g., *Salmonella*, *Clostridium perfringens*, *Listeria monocytogenes*,
63 *Staphylococcus aureus*, *Bacillus cereus*, Shiga toxin-producing *Escherichia coli*),
64 fungal (e.g., *Aspergillus flavus*), viral (e.g., Norovirus, Rotavirus), protozoal (e.g.,
65 *Toxoplasma gondii*, *Giardia intestinalis*), and parasites (e.g., *Taenia saginata*, *T.*
66 *solium*) species can cause illnesses once present in food (WHO, 2015). In Brazil, most
67 foodborne illnesses are caused by bacteria (*E. coli* – 24.0%, *Salmonella* spp. – 11.2%,
68 *S. aureus* – 9.5%, *B. cereus* – 2.6%) and viruses (8.1%) from a total of 2,030 outbreaks
69 identified (Saúde, 2019b). The most common symptoms caused by foodborne
70 pathogens include nausea, vomiting, abdominal pain/discomfort, diarrhea, fever, and
71 lack of appetite (de Freitas Saccol et al., 2016). Food microbial contamination could
72 be avoided through good manufacturing practices, raw material control, and cold chain
73 at the industry and retail level (Jaffee et al., 2019). After four basic steps at home
74 (cleaning, separation, cooking, and cooling), people can be protected from food
75 poisoning (CDC, 2020b). There are still a few cases of human exposure to chemical
76 substances carried by food (0.2 %) from a total of 6,405 cases of chemical intoxication
77 (CIATox, 2018).

78 Another challenge facing humanity is related to food losses due to spoilage or
79 waste (Odeyemi et al., 2020). The global increase in the human population
80 consequently raises the demand for food as well. A study conducted by the Food and
81 Agriculture Organization of the United Nations revealed that one-third (1.3 billion tons
82 per year) of food production for human consumption is lost due to spoilage or waste
83 (FAO, 2011). For public health reasons, foodborne poisoning received more attention

84 than food spoilage. However, food spoilage also represents huge economic and
85 reputation losses for the food industry and also means fewer consumable foods for
86 humans (Lulietto et al., 2015). Any undesirable and unacceptable change in food quality
87 due to spoilage can lead to food rejection (Koutsoumanis, 2009). Even with the
88 application of modern preservation techniques, this is a frequent challenge faced by
89 the food and beverage industries (Remenant et al., 2015). The two main issues
90 involved with the inactivation of microorganisms are the antimicrobial resistance and
91 the heat effects on food quality caused by heat treatments. Antimicrobial resistant-
92 microbes can inhabit food, animals, people, and the environment. They can spread
93 easily among animals and food without sanitary measures and inadequate food
94 handling (WHO, 2018). For safety reasons, thermal treatment is the most widely used
95 method for microbial inactivation in the food and beverage industries. The deleterious
96 effects of thermal treatment on food and beverages have been observed, such as
97 sensorial and nutritional losses (Barba et al., 2017). Given the aforementioned
98 problems regarding antimicrobial resistance and undesirable effects of thermal
99 processes, several innovative mild processing technologies have been developed
100 (Cebrián et al., 2016; Ferrario & Guerrero, 2018; Kim & Kang, 2018; Min et al., 2017;
101 Reverter-Carrión et al., 2018). Among them, pulsed light, ultraviolet (UV) light radiation,
102 pulsed electric fields, cold plasma, and high-pressure processing are the most studied
103 techniques so far (Barba et al., 2017).

104 An innovative method has gained popularity in recent years among the scientific
105 community for microbial inactivation, namely photodynamic therapy (PDT). This is an
106 approved method for cancer treatment by the American Cancer Society (ACS, 2019),
107 and the European Academy of Dermatology and Venereology - EADV (Morton et al.,
108 2013). The advances in this area were transferred to the area of microbiology mainly
109 with the beginning of the era of antimicrobial resistance originating the term
110 antimicrobial photodynamic treatment – aPDT (Wainwright et al., 2017). Although its
111 discovery in 1900 has been reported for the inactivation of the protozoan *Paramecium*
112 *caudatum* by the combination of sunlight and dyes, its use for the treatment of tumor
113 cells in 1905 preceded the success of the PDT (Jesionek & von Tappeiner, 1905;
114 Raab, 1900). The elementary principle of aPDT depends on the combination of visible

115 or near-infrared light with a photosensitizer (PS) compounds in the presence of
116 molecular oxygen to generate reactive oxygen species (ROS), leading to cell death.
117 The multiple target action of ROS generated during aPDT reduces the chance of
118 selecting resistant microorganisms. Also, the use of non-toxic PS and harmless visible
119 light makes aPDT a promising alternative for the food applications. At present, aPDT
120 have focused the efforts on the inactivation of a broad spectrum of pathogenic
121 microorganisms as *Salmonella*, *E. coli*, *L. monocytogenes* and *B. cereus* (Josewin et
122 al., 2018; Oliveira et al., 2009; Santos et al., 2020; Vieira et al., 2019).

123 The current work aims to give a comprehensive report of the most recent advances
124 of aPDT on the food and agriculture sectors. The classifications of PSs and sources of
125 light used for aPDT, as well as the mechanisms of inactivated action including
126 potentiation effects caused by the addition of nontoxic inorganic salts, were discussed
127 in detail. Although the related topic has been reviewed before (Ghate et al., 2019;
128 Lukšiene, 2005; Lukšiene & Brovko, 2013; Lukšiene & Zukauskas, 2009; Silva et al.,
129 2018), a crescent number of studies recently published for agrifood reasons have been
130 observed. Therefore, an update is needed giving the advances in the knowledge
131 regarding aPDT. This review could assist the researchers in the development of aPDT-
132 associated approaches for reducing the food and agriculture microbial threats.

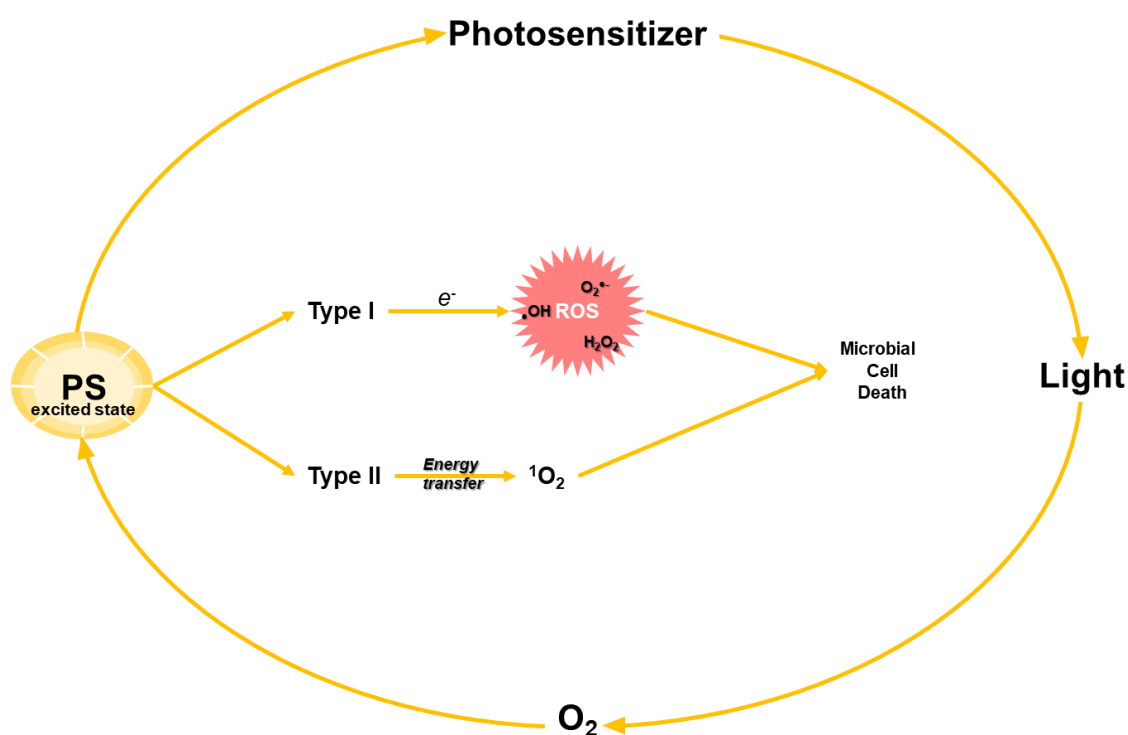
133

134 **2. Concepts of antimicrobial photodynamic treatment**

135

136 The basic concept of aPDT is the triggering of photochemical reactions through the
137 combination of visible or near-infrared light at a specific wavelength, a photosensitizer
138 compound, and molecular oxygen (Vieira et a., 2019). Both reactions (Type I and II)
139 presented in Fig. 1 occur after light exposure of the PSs compounds (endogenous or
140 exogenous) which absorb and transfer energy to the molecular oxygen forming the
141 reactive oxygen species (ROS) (Wainwright et al., 2017), such as singlet oxygen ($^1\text{O}_2$),
142 hydroxyl radicals ($\bullet\text{OH}$), superoxide anions ($\text{O}_2^{\bullet-}$), and hydrogen peroxide (H_2O_2). ROS
143 cause damages on microbial cells through the oxidation of essential molecular
144 components such as proteins, lipids, and nucleic acids (Broekgaarden et al., 2015;
145 Vatansever et al., 2013). This multitarget and unspecified mechanism of action make

146 aPDT an effective alternative for combating multidrug-resistant bacteria (Almeida et
 147 al., 2014; Cieplik, et al., 2018a). Also, some studies have investigated the potentiation
 148 of aPDT by adding inorganic salts as potassium iodide – KI (Vecchio et al., 2015; Vieira
 149 et al., 2018, 2019; Yuan et al., 2020; Zhang et al., 2015), sodium bromide – NaBr (Wu
 150 et al., 2016), sodium azide – NaN₃ (Huang et al., 2012), thiocyanate – SCN⁻ (St Denis
 151 et al., 2013), and preliminary studies of sodium nitrite and selenocyanate (Hamblin,
 152 2017).
 153



154

155 **Fig. 1.** Process of microbial cell death caused by the generation of reactive oxygen
 156 species (ROS) and singlet oxygen (¹O₂) after photosensitizer (PS) excitation by light
 157 exposure in the presence of oxygen molecules.

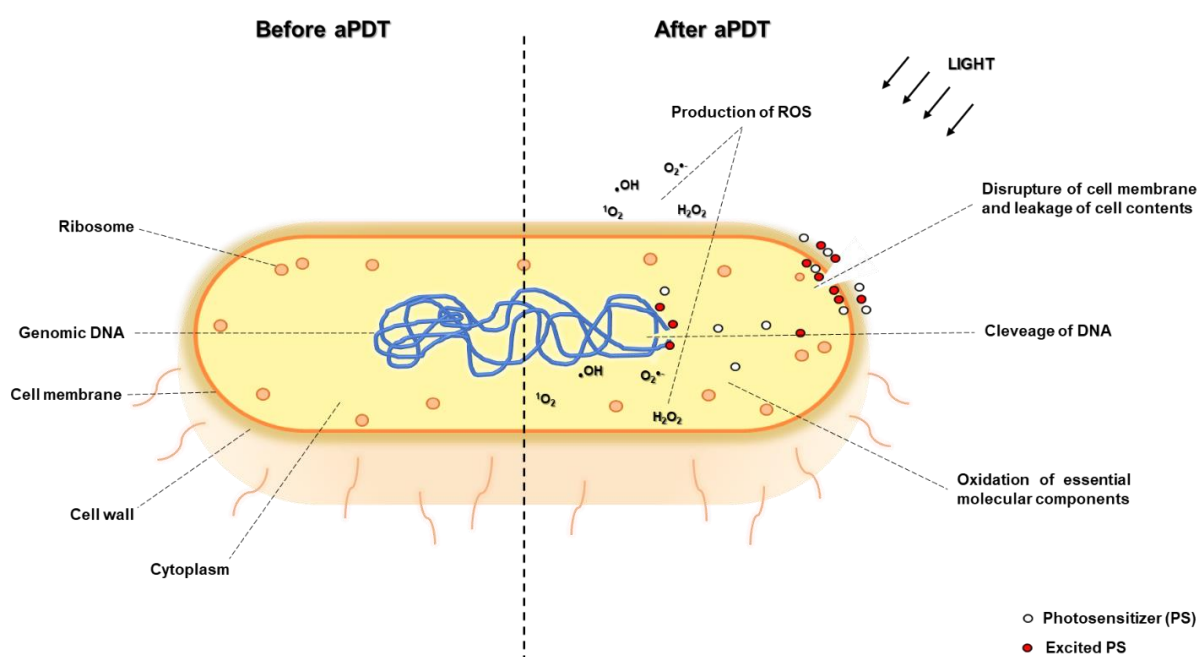
158

159 2.1. Mechanisms of action

160

161 The absorption of light by the PS can follow two alternative pathways, widely known
 162 as type I and II. Initially, the PS in the fundamental state can absorb light energy, further
 163 moving to an excited singlet state. This state can decay by fluorescence, heat

164 dissipation or to a longer-lived triplet state (most expected). The formation of the PS
 165 triplet state can return to the ground singlet state by phosphorescence or finally allows
 166 the interaction with oxygen by the electron transfer (Type I) from excited PS, forming
 167 ROS (e.g., $\cdot\text{OH}$, $\text{O}_2^{\cdot-}$, and H_2O_2); or transfer energy directly to a free oxygen molecule
 168 to produce $^1\text{O}_2$ in the process (Type II). The microbial cell killing depends on the excited
 169 PS characteristics (e.g., lipophilicity, amphiphilicity, ionic charge) which will influence
 170 its localization in the cell (e.g., microbial cell walls, lysosomes, mitochondria, lipid
 171 membranes, and nucleus) as demonstrated in the Fig. 2 (Brancini et al., 2016; Castano
 172 et al., 2004; de Menezes et al., 2014; Menezes et al., 2016; Wainwright et al., 2017).
 173 The localization of PS matters because it will only affect the cell structures that are
 174 near to the ROS production during aPDT (Castano et al., 2004). The singlet oxygen is
 175 considered much more destructive than other ROS, however, the combination of
 176 various ROS is desirable to enhance the antimicrobial efficiency (Maisch et al., 2005).
 177



178
 179 **Fig. 2.** Illustration of a generic bacterial cell before and after aPDT treatment and the
 180 involved mechanisms of photoinactivation.

181

182 The specific inactivation mechanism of aPDT has been explored by several authors
 183 and the cell membrane is the major inactivation target in the process (Alves et al.,

184 2013; Buchovec et al., 2017; Cieplik et al., 2018b; de Menezes et al., 2016; Kim & Yuk,
185 2017; Tonani et al., 2018). It was revealed that the membrane phospholipids of
186 *Staphylococcus warneri* were affected (e.g., the formation of lipid hydroxides and
187 hydroperoxides) by the aPDT with synthetic cationic porphyrin and artificial white light
188 (Alves et al., 2013). Also, some of these studies highlighted the cell membrane as the
189 main target of ROS action, promoting its disruption and the consequent release of
190 proteins and nucleic acids (Buchovec et al., 2017; Lin et al., 2012). Buchovec et al.
191 (2017) emphasized the role of singlet oxygen decreasing the inactivation of *S.*
192 *Typhimurium* by aPDT with Na-Chl and LED exposure at 405 nm by adding a singlet
193 oxygen quencher (NaN₃). Moreover, the gene expression evidenced that the process
194 of aPDT can upregulate some relevant genes (*OxyR*, *GrxA*, *AhpC*, *STM0225*, *AtpC*,
195 *groEL*, *SulA*) related to oxidative, extracytoplasmic, and acidic stress (Buchovec et al.,
196 2017). Another study found interesting results in terms of membrane depolarization
197 and permeability (efflux pump and glucose uptake activity), genomic DNA oxidation,
198 and gene expression of *S. Saintpaul* (LED-resistant) and *S. Enteritidis* (LED-sensitive)
199 strains by 405 nm LED illumination of endogenous PS (coproporphyrin) at 4°C (Kim &
200 Yuk, 2017). The authors also observed an increase of guanine oxidation, complete
201 inhibition of efflux pump activity (due to inhibition of ATPase), and glucose uptake
202 system disorders most likely because of the proximity to endogenous porphyrins. Such
203 mechanisms of action indicate that the aPDT inactivation is highly associated with
204 membrane depolarization and permeability (Cieplik et al., 2018b; de Menezes et al.,
205 206; Kim & Yuk, 2017; Tonani et al., 2018), membrane breakage (Buchovec et al.,
206 2017; Lin et al., 2012), phospholipids rearrangement (Alves et al., 2013) and
207 peroxidation (de Menezes et al., 2016; Tonani et al., 2018). The expression of five
208 genes (*oxyR*, *recA*, *rpoS*, *sodA*, and *soxR*) in non-illuminated and illuminated *S.*
209 *Saintpaul* and only one gene (*oxyR*) for *S. Enteritidis* cells, indicates that results were
210 more affected by low temperature than LED-illumination (Kim & Yuk, 2017). Such
211 published results are extremely important for a better understanding of the action
212 associated with aPDT on microbial cells, including the development of aPDT
213 resistance. A recent publication reviewed the main factors that can be addressed to
214 the aPDT resistance, including oxidative stress and antibiotic resistance mechanisms

215 (Kashef & Hamblin, 2017). Nevertheless, the development of resistance or tolerance
216 is highly unlikely given the unspecific characteristic of aPDT-induced cell death by ROS
217 production (Kashef & Hamblin, 2017).

218

219 **2.2. Potentiation effect of inorganic salts on aPDT**

220

221 The efficacy of aPDT can be enhanced by adding inorganic salt. The most powerful
222 and versatile is potassium iodide, which has been widely evaluated for the inactivation
223 of bacteria (Huang et al., 2018; Moreira et al., 2020; Vecchio et al., 2015; Vieira et al.,
224 2018, 2019; Yuan et al., 2020; Zhang et al., 2015), fungi (Freire et al., 2016; Zhang et
225 al., 2015) and virus (Vieira et al., 2019). The major antimicrobial inactivation
226 mechanism of potentiation is attributed to the reaction of potassium iodide with singlet
227 oxygen, forming highly oxidant free molecular iodine (I_2/I_3^-), iodine radicals (I_2^{\bullet}), and
228 H_2O_2 (Huang et al., 2017; Vieira et al., 2019). Another potentiation pathway involves
229 the oxidation of 2-electrons of iodide or bromide that occurs during the illumination of
230 titanium dioxide to form hypohalites (Huang et al., 2016; Wu et al., 2016). The third
231 mechanism of aPDT potentiation was discovered, paradoxically, by the addition of
232 NaN_3 , which is widely used as a singlet oxygen quencher (Huang et al., 2012). The
233 authors observed that the addition of NaN_3 to the menstruum of bacteria with MB and
234 red-light illumination potentiated the inactivation process, promoting the type I
235 mechanism (electron transfer) rather than acting as a singlet oxygen inhibitor.

236

237 **2.3.Factors affecting the aPDT efficacy on foods**

238

239 The efficacy of aPDT can be affected by various elements, including the nature of
240 the microorganisms, PS characteristics, light exposure period, and environmental
241 aspects (Gonzales et al., 2010). Besides these already well-documented factors, some
242 researchers are investigating the impact of some other factors such as liquid food
243 composition and geometry properties of solid foods.

244 The impact of the milk composition and their interaction with light and PS compound
245 on aPDT efficacy to reduce the viability of Gram-positive and Gram-negative bacteria

246 was investigated by Galstyan & Dobrindt (2019). It was demonstrated that abundant
247 components in milk as proteins, fat, and free cations (Ca^{2+} and Mg^{2+}) can impair the
248 aPDT antimicrobial efficacy. Such results were confirmed in the experiments where
249 the dilution of milk significantly impacted the bacterial photoinactivation. The authors
250 also detected a significant impact in the stability, generation of ROS, and aggregation
251 of MB as PS compound (Galstyan & Dobrindt, 2019).

252 Other food properties such as pH and water activity can affect the aPDT efficacy.
253 The influence of pH was investigated on the efficiency of PDT using LEDs, since the
254 acidity of the food can affect the treatment (Ghate et al., 2015). It was demonstrated in
255 this study that acidic and alkaline pH can enhance the effect of aPDT. The findings
256 showed that lower pH (4.5) can assist aPDT against Gram-positive bacteria (*L.*
257 *monocytogenes*) due to the absence of the outer membrane structure to protect the
258 permeation of hydrogen ions. In contrast, *E. coli* and *Salmonella* representing Gram-
259 negative bacteria were more vulnerable to the treatment at alkaline pH 9.5, most likely
260 due to the saponification of the membrane lipids (Ghate et al., 2015). As the pH of food
261 can vary, the findings of this study may contribute to optimizing the aPDT treatment
262 according to the pH of the food.

263 The effect of water activity on microbial resistance to the different methods of
264 inactivation has widely recognized from traditional methods to new emerging
265 technologies (Lee et al., 2020). The water content inside the cell is crucial for the
266 microbial survivals (Alvarenga et al., 2018). Also, resistant microbial forms, such as
267 spores of bacteria and fungi, help to survive in low water-activity foods. (e.g., dairy and
268 meat products, cereal and nut products) (Stevenson et al., 2015). However, studies
269 that assess the impact on the aPDT efficacy in different levels of water activity have
270 not be found in the literature, opening new horizons in this sense.

271 The physical factors (geometry and shadow effects) of solid food may have a
272 significant impact on the aPDT efficacy. The geometry characteristics of solid foods
273 such as fruits and vegetables have been recently investigated by Glueck et al. (2017).
274 The authors tested three types of food surface, namely flat, spherical, and complex, to
275 determine if the efficacy of a curcumin-based aPDT treatment was dependent on
276 superficial food geometry. A significant inactivation of more than 3 log CFU/mL of *E.*

277 *coli* were obtained on all flat surface produces, represented by cucumber, tomato and
278 lettuce. Inactivation of 3.7 log CFU/mL and 5 log CFU/mL of *E. coli* were observed on
279 the spherical surface of non-germinated mung beans and fenugreek seeds,
280 respectively, with the use of continuous rotation during the experiment. Only in the
281 complex geometry (multifaceted) represented by mung bean germlings did not reach
282 the minimum of 3 log CFU/mL reduction even with rotation (Glueck et al., 2017). In
283 technologies that are based on exposure to light, there is also a limiting factor known
284 as the shadow effect which is related to the food geometry (Condón-Abanto et al.,
285 2016). However, there are still no studies that have explored this effect in aPDT.

286

287 **3. Photosensitizers**

288

289 PSs are chemical compounds that can be natural or synthetic. Also, they can be
290 produced by microorganisms (endogenous) or administered externally (exogenous)
291 (Gábor et al., 2001). The choice of suitable PS is crucial to efficiently reduce microbial
292 loads during aPDT application. The principle of PS selection is based on the source of
293 light with the emission wavelength indicated for the absorption band of the PS to excite
294 the molecule (Hamblin, 2016). The optimization of photodynamic treatment is closely
295 related to the PS as it can increase the efficiency, selectivity, and safety of the
296 treatment (Ghate et al., 2019).

297 Some microorganisms (especially bacteria and fungi) present the ability of light
298 absorption because they are pigmented by compounds naturally produced inside the
299 cells (Kumar et al., 2015). Some of these compounds, namely porphyrins, are the first
300 generation of PSs classified as heterocyclic macromolecules including protoporphyrin,
301 coproporphyrin, and uroporphyrin (Ghate et al., 2019). This natural pigmentation
302 allows the photoinactivation of the microorganisms only by light exposure without the
303 application of exogenous PS (Demidova & Hamblin, 2004). The natural existing
304 porphyrins can be diverged based on quantity and composition among the species
305 (Kumar et al., 2015). According to these authors, the amount of coproporphyrin is
306 higher in Gram-positive than Gram-negative bacteria. The production of endogenous
307 porphyrins can be induced with the use of PS precursors such as 5-aminolevulinic acid

308 (ALA) (Le Marc et al., 2009; Lukšiene et al., 2009). ALA is an important component in
309 the heme biosynthesis pathway inside cells, leading to the production of porphyrins
310 endogenously (Fotinos et al., 2008). The strategy of microbial photoinactivation
311 triggering the production of endogenous PS with continuous light exposure is adequate
312 when fast inactivation is not required as in the case of food preservation during its
313 distribution and storage chain (Ghate et al., 2019).

314 However, microbial inactivation must be effective and fast to prevent the
315 propagation of undesirable microorganisms in food. Most research efforts are focused
316 to screen and evaluate promising candidates of PS to increase the rate of
317 photoinactivation in food matrixes. The ideal PS used for food decontamination should
318 present the following characteristics: (1) absence of toxicity; (2) solubility in non-toxic
319 compound; (3) photostability; (4) microbial cell affinity (positively charged PS can
320 achieve strong adhesion to negatively charged bacterial cell walls); (5) high production
321 of ROS and high quantum yield of singlet oxygen (Φ_{Δ}); and (6) wide spectrum of light
322 absorption (Alves et al., 2009; Cieplik et al., 2014; Ghate et al., 2019; Lukšiene &
323 Brovko, 2013; Lukšiene & Zukauskas, 2009). The absence of toxicity is essential to
324 keep the consumer safe and food without apparent damage. Especially when it is
325 increasingly desired to decrease food additives. In this sense, it is also required that a
326 suitable PS should be easily dissolved in water or any other non-toxic compound to
327 simplify the removal from the food surface. The photostability of the PS is an important
328 issue to be considered since it is desired to be stable when inside the microbial cells
329 for its inactivation. On the other hand, once the PS is free it will decay rapidly, avoiding
330 the persistence in the environment which is a frequent issue with conventional
331 insecticides (de Menezes et al., 2014b; Derosa & Crutchley, 2002). The microbial cell
332 affinity is also desirable to avoid the accumulation of the PS anywhere other than for
333 microbial inactivation (de Menezes et al., 2014a,b; 2016; Rodrigues et al., 2020). Once
334 inside the microbial cell, a good PS should be able to produce high amounts of ROS,
335 especially singlet oxygen species, that are highly cytotoxic (Gonzales et al., 2010;
336 Derosa & Crutchley, 2002).

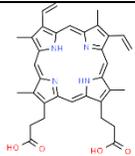
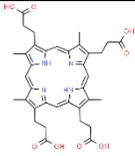
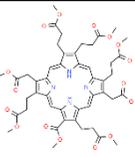
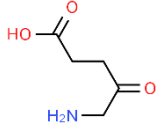
337 The exogenous PS used for aPDT can be synthesized or obtained from nature
338 (Table 1). The main synthetic PSs are the porphyrin derivatives (chlorins,

339 bacteriochlorins, phthalocyanine, tetraphenylporphine, iodide-based porphyrins), ALA
340 (endogenous porphyrin precursor), phenothiazinium dyes (toluidine blue, methylene
341 blue, new methylene blue, 1,9-dimethylmethylene blue), and xanthene dyes (rose
342 bengal, eosin Y, erythrosine) (Bartolomeu et al., 2016; Buchovec et al., 2010; de
343 Menezes et al., 2014b, 2016; Lukšiene & Brovko, 2013; Rodrigues et al., 2012a,b).
344 Most of the porphyrin derivatives are based on the tetrapyrrole nucleus including
345 chlorins, phthalocyanine, bacteriochlorins, phthalocyanine, and iodide-based
346 porphyrins. Their low toxicity in the absence of light and ability to enter into long-lived
347 triplet excited states contributes to its wide uses in aPDT (Demidova & Hamblin, 2004;
348 Lukšiene & Zukauskas, 2009). The phenothiazinium dyes, namely blue dyes, are the
349 most studied PSs against different microbial species (de Menezes et al., 2014; de
350 Menezes et al., 2016; Freire et al., 2016; Tonani et al., 2018; Wainwright et al., 1997;
351 Wainwright, 2004). Their molecular framework, in line with other linear tricyclic
352 heteroaromatics, is ideal for action against nucleic acids, due to their ability to bind to
353 guanosine residues forming 8-hydroxyguanosine causing DNA breakage (Schneider
354 et al., 1990; Wainwright, 1998; Wainwright et al., 2012). Xanthene dyes have been
355 extensively tested as PS to induce microbial photoinactivation due to their low cost,
356 high absorptivity, and abundant singlet oxygen generation (Bonin et al., 2018;
357 Yassunaka et al., 2015). Additionally, some xanthene derivatives have been approved
358 for pharmaceutical and food applications (Santos et al., 2019).

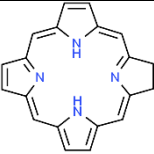
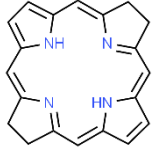
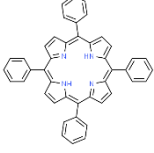
359 The use of natural PS grows as the demand for natural products increases,
360 following the recent desires of consumers. Some examples of PSs obtained from
361 nature are hypericin (Hyp), coumarins, furocoumarins, chlorophyllin (Chl), curcumin,
362 and riboflavin (vitamin B2) (Bonifácio et al., 2018; Dementavicius et al., 2016; Maisch
363 et al., 2014; Otieno et al., 2020; Paskeviciute et al., 2019). The Hyp extract is a natural
364 pigment obtained from the plant traditionally known as St John's wort (*Hypericum*
365 *perforatum*) widely used as natural PS and considered one of the most powerful PS in
366 nature (Lukšiene & Zukauskas, 2009). Also, Hyp is free of any toxic or genotoxic effects
367 (Feruszová et al., 2016; Okpanyi et al., 1990). Coumarins and furocoumarins
368 (psoralens) are naturally produced as secondary metabolites in a variety of plant
369 species, in particular of the Umbelliferae, Apiaceae, and Rataceae families (de

370 Menezes et al., 2014; Fracarolli et al., 2016). Plants produce these compounds to act
371 either via light-dependent or independent mechanisms, as antimicrobials (de Menezes
372 et al., 2014; Fracarolli et al., 2016). Chlorophyllin is a water-soluble derivative of
373 chlorophyll (not water-soluble) frequently used as a food additive (E-140 and E-141) in
374 dietary supplements and cosmetics (López-Carballo et al., 2008). Curcumin is a
375 natural yellow pigment obtained from the rhizome *Curcuma longa* widely used for
376 centuries as a food ingredient and is currently certified as a food additive (E-100). It is
377 also known by its antimicrobial, anti-inflammatory, anti-proliferative, antioxidant, and,
378 more recently, photosensitizing activities (Bonifácio et al., 2018; de Souza et al., 2019;
379 Eigner & Scholz, 1999; Ghosh et al., 2015; Huang et al., 2020). Riboflavin, also known
380 as vitamin B2, is an essential human nutrient (water-soluble) and frequently used in
381 the food industry as a colorant (E-101). It also can produce high amounts of singlet
382 oxygen after light exposure (Baier et al., 2006; Maisch et al., 2014). Also, riboflavin is
383 an important bioproduct photodegraded in the human body when exposed to visible
384 light (Cardoso et al., 2012; Schuyler, 2001), consequently can be considered safe for
385 food applications.

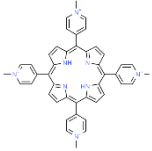
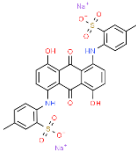
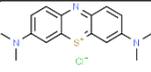
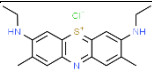
386 Table 1. Endogenous and exogenous (synthetic and natural) photosensitizers used on aPDT.

Photosensitizers	Chemical structure	Absorbance (nm)	Quantum yield of $^1\text{O}_2$ (Φ_Δ)	Molar absorptivity ($\text{L mol}^{-1} \text{cm}^{-1}$)	References
Endogenous:					
Protoporphyrin IX	 ChemSpider ID: 10469486	400-650	0.77 (phosphate buffer)	$\epsilon_{408\text{nm}} = 1.24 \times 10^5$	Balasubramaniam & Natarajan (1997); Nishimura et al. (2019)
Coproporphyrin III	 ChemSpider ID: 16736509	370-610	0.13 (ethanol) 0.18 (D ₂ O) 0.41 (D ₂ O + 2% Triton X-100)	N.A.	Murav'eva et al. (2018)
Uroporphyrin II	 ChemSpider ID: 4575518	546 nm	0.71 (phosphate buffer)	N.A.	Wilkinson et al. (1993)
Exogenous:					
5-aminolevulinic acid	 ChemSpider ID: 134		Precursor of endogenous porphyrins		Kennedy & Pottier (1992)

388 **Table 1.** Continued

Photosensitizers	Chemical structure	Absorbance (nm)	Quantum yield of $^1\text{O}_2$ (Φ_Δ)	Molar absorptivity ($\text{L mol}^{-1} \text{cm}^{-1}$)	References
Porphyrin derivatives:					
Chlorins	 ChemSpider ID: 58616	650	0.88-0.98 (toluene)	$\epsilon_{650\text{nm}} = 3.00 \times 10^4$	Pineiro et al. (2001)
Bacteriochlorins	 ChemSpider ID: 7827701	300-400	0.05 (phosphate buffer) 0.33 (DMPC liposome)	N.A.	Hoebeker & Damoiseau (2002)
Zinc phthalocyanine	 ChemSpider ID: 21169868	675	0.53 (tetrahydrofuran)	$\epsilon_{675\text{nm}} = 1.58 \times 10^5$	de Souza et al. (2018)
Tetraphenylporphine	 ChemSpider ID: 10291672	400-650	0.52 (DMSO)	$\epsilon_{516\text{nm}} = 14.08 \times 10^3$	da Silva et al. (2008)

390 **Table 1.** Continued

Photosensitizers	Chemical structure	Absorbance (nm)	Quantum yield of $^1\text{O}_2$ (Φ_Δ)	Molar absorptivity ($\text{L mol}^{-1} \text{cm}^{-1}$)	References
5,10,15,20-Tetrakis(1-methylpyridinium-4-yl)porphyrin tetraiodide (Tetra-Py ⁺ -Me)	 ChemSpider ID: 4086	600-750	N.A.	$\epsilon_{425\text{nm}} = 2.69 \times 10^5$ $\epsilon_{516\text{nm}} = 1.95 \times 10^4$ $\epsilon_{549\text{nm}} = 5.89 \times 10^3$ $\epsilon_{588\text{nm}} = 6.92 \times 10^3$ $\epsilon_{642\text{nm}} = 2.00 \times 10^3$	Simões et al. (2016)
Phenothiazinium dyes:					
Toluidine blue O (TBO)	 ChemSpider ID: 69136	600-680 627	0.44 (ethanol)	$\epsilon_{627\text{nm}} = 7.40 \times 10^4$	Bacellar et al. (2014)
Methylene blue (MB)	 ChemSpider ID: 5874	600-680 655	0.52 (ethanol)	$\epsilon_{655\text{nm}} = 9.60 \times 10^4$	Bacellar et al. (2014; Wilkinson et al. (1993)
New methylene blue N (NMB)	 ChemSpider ID: 16736255	600-680 550-650	N.A.	N.A.	Rodrigues et al. (2012)

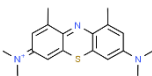
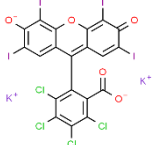
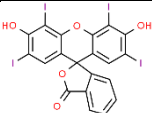
391

392

393

394

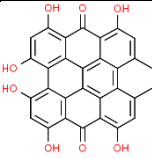
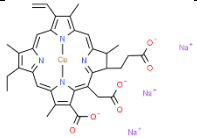
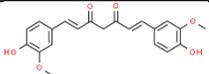
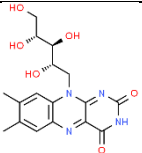
395 **Table 1.** Continued

Photosensitizers	Chemical structure	Absorbance (nm)	Quantum yield of $^1\text{O}_2$ (Φ_Δ)	Molar absorptivity ($\text{L mol}^{-1} \text{cm}^{-1}$)	References
1,9-dimethylmethylen blue (DMMB)	 ChemSpider ID: 110430	600-680 651	0.71 (ethanol)	$\epsilon_{651\text{nm}} = 7.80 \times 10^4$	Bacellar et al. (2014)
Xanthene dyes:					
Rose Bengal (RB)	 ChemSpider ID: 23773	480-550	0.76 (phosphate buffer)	$\epsilon_{543\text{nm}} = 10.90 \times 10^4$	Batistela et al. (2011); Lee & Rodgers (1987)
Eosin Y (EOY)	 ChemSpider ID: 10580	500-600	0.57 (phosphate buffer)	$\epsilon_{517\text{nm}} = 9.71 \times 10^4$	Batistela et al. (2011); Gandin et al. (1983)
Erythrosine (ERY)	 ChemSpider ID: 3144	500-600	0.63 (phosphate buffer)	$\epsilon_{532\text{nm}} = 9.66 \times 10^4$	Batistela et al. (2011); Gandin et al. (1983)

396

397

398 **Table 1.** Continued

Photosensitizers	Chemical structure	Absorbance (nm)	Quantum yield of $^1\text{O}_2$ (Φ_Δ)	Molar absorptivity ($\text{L mol}^{-1} \text{cm}^{-1}$)	References
<i>Natural compounds</i>					
Hypericin (Hyp)	 ChemSpider ID: 4444511	630	0.73 (ethanol)	$\epsilon_{630\text{nm}} = 1.31 \times 10^4$	Wilkinson et al. (1993)
Chlorophyllin (Chl) + cooper (Obtained from chlorophyll)	 ChemSpider ID: 21781827	400	0.57 (methanol)	$\epsilon_{400\text{nm}} = 2.08 \times 10^4$	Uchoa et al. (2015)
Curcumin	 ChemSpider ID: 839564	420	<0.01 (ethanol)	$\epsilon_{430\text{nm}} = 2.74 \times 10^4$	Chignell et al. (1994)
Riboflavin (Vitamin B2)	 ChemSpider ID: 431981	470-490	0.54-0.59 (methanol)	$\epsilon_{430\text{nm}} = 1.16 \times 10^4$	(Baier et al., 2006; Chacon, McLearn, & Sinclair, 1988)

399 N.A.: Not available

400 **4. Sources of light**

401

402 The light sources used in the photodynamic treatment are diverse according to their
403 emission spectrum. The main groups of light sources are the conventional lamps
404 (tungsten-halogen, metal–halide, xenon, etc.) (Calin & Parasca, 2009), light-emitting
405 diodes (LEDs) as the most recent alternative source of light for aPDT (Brancini et al.,
406 2016; Penha et al., 2017; Rodrigues et al., 2012; Silva et al., 2019; Yassunaka et al.,
407 2015), and lasers (light amplification by stimulated emission of radiation) (Gonzales et
408 al., 2010; Rodrigues et al., 2012; Rodrigues et al., 2020). Lasers are extremely efficient
409 alternatives and widely used in clinical treatments (Calin & Parasca, 2009), however,
410 their high cost makes them an impracticable option for the food sector. There are
411 several advantages related to LED usage, such as low driving voltage, lightness,
412 robustness, compactness, shock and vibration resistance, free of toxic compounds (i.e.
413 mercury), the flexibility of assemblage, narrow-band emission, and no residue of
414 undesirable spectral components (Lukšiene & Brovko, 2013). LEDs became more
415 attractive to the food industry (mainly for food production, postharvest storage, and
416 food safety) for its high cost-benefit, inexpensive maintenance, long life, and
417 nonthermal effects (D'Souza et al., 2015). The current choice for LEDs means the
418 delivery of a wide range of emission wavelengths from UVA (350 nm) to near-infrared
419 (1100 nm) and the output power can provide up to 150 mW/cm² of irradiance
420 (Brancaleon & Moseley, 2002). Most lamps can burn out abruptly making treatment
421 unfeasible. LEDs can maintain up to 70% of the initial irradiation output flux after
422 50.000 – 100.000 h of exposure (Lukšiene & Zukauskas, 2009). Recently, an emerging
423 alternative has been the use of sunlight in aPDT against foodborne (Miñán et al., 2015)
424 and plant pathogen (Fracarolli et al., 2016; Gonzales et al., 2017; Jesus et al., 2018)
425 microorganisms, besides clinical purposes (Wiegell et al., 2008). This method is
426 considered efficient, cheap, and environmentally friendly (Yang et al., 2019). As
427 sunlight is a limitless resource, its intelligent use has been increasingly demanded in
428 the field of photodynamic treatment due to its low cost and practicality (Fracarolli et al.,
429 2016; Gonzales et al., 2017). The choice of the appropriate light source is directly

430 associated to the PS selected for the aPDT. Each PS has a range of maximum
 431 absorbance (see Table 1) that can be emitted by several light sources. It is important
 432 to note that for maximum treatment efficiency, the emission wavelength must be
 433 correlated to the PS absorption spectrum (Lukšiene & Brovko, 2013). This is crucial
 434 for the generation of sufficient ROS (Type I) and $1O_2$ (Type II) to rapidly inactivate
 435 microorganisms.

436

437 **Table 2. Properties of the most frequently used sources of light on aPDT.¹**

Sources of light	Irradiance	Wavelength	Heating	Delivery
Tungsten filament	Up to 250 mW/cm ²	400 – 1100 nm	Yes	Direct
Diode laser	Up to 700 mW/cm ²	600 – 950 nm	Yes	Optical fiber
LED	Up to 150 mW/cm ²	350 – 1100 nm	Yes (low)	Direct

438

¹Data extracted from (Wilson & Patterson, 2008) and (Brancaleon & Moseley, 2002)

439

440 ***5. Inactivation efficacy of aPDT on the main foodborne*** 441 ***microorganisms***

442

443 It is widely known that the aPDT has been used to inactivate all classes of
 444 microorganism including bacteria (Gram-positive, Gram-negative, vegetative cells and
 445 spores), fungi (yeasts and molds), protozoa and viruses. Most of the studies published
 446 to date have dedicated the research mainly to photodynamic inactivation of bacteria
 447 as demonstrated by a recent comprehensive review focused on food safety (Ghate et
 448 al., 2019). Another interesting critical review summarized the studies of photodynamic
 449 inactivation of foodborne bacteria in planktonic and biofilm states (Silva et al., 2018).
 450 Although bacteria are important foodborne microorganisms, recent studies have
 451 shown that most foodborne outbreaks are caused by viruses (Bosch et al., 2018;
 452 EFSA, 2015; Painter et al., 2013). However, even the number of studies concerning
 453 aPDT of fungi species are higher than foodborne viruses (Ghate et al., 2019), mainly
 454 in clinical and agricultural areas (Freire et al., 2016; Gonzales et al., 2017; Rodrigues
 455 et al., 2012). The inactivation of protozoan parasites with the aPDT treatment is also

456 an important investigation field (Barbosa et al., 2020; Sepúlveda et al., 2020). The
457 most relevant studies described in this section are depicted in Table 3 and include only
458 studies that used exogenous PS.

459

460 **5.1. Bacterial vegetative cells**

461

462 Most of aPDT studies were focused on the inactivation of bacteria (e.g., antibiotic-
463 resistant, foodborne pathogens, spoilage strains, biofilms, and heat-resistant spores)
464 and this predominance can be attributed to bacterial susceptibility to the treatment and
465 the emergence of multidrug-resistant bacterial species. The efficacy of aPDT on
466 bacteria varies between Gram-positive and Gram -negative species, in all forms, such
467 as vegetative cells, spores, and biofilm (Silva et al., 2018). The majority of the studies
468 are dedicated to foodborne pathogenic bacteria instead of food spoilage bacteria. The
469 significant demand for the control of pathogenic bacteria for health issues is well
470 known; however, the spoilage bacteria also play a fundamental role in the food quality
471 of the industry.

472 Among the bacterial species frequently evaluated, Gram-negative bacteria are less
473 susceptible than Gram-positive bacteria. In a recent study, the authors confirmed that
474 Gram-negative bacteria (*Aeromonas hydrophila*, *E. coli*, *S. Typhimurium*, and
475 *Pseudomonas aeruginosa*) required higher concentrations of erythrosine and longer
476 exposure times than Gram-positive bacterium (*S. aureus*) did (Yassunaka et al., 2015).
477 The lower susceptibility of Gram-negative bacteria to aPDT is mainly related to the
478 outer membrane preventing the uptake of anionic and neutral PS (George et al., 2009).
479 The use of positively charged PS (e.g., porphyrin and phenothiazinium derivatives) has
480 been an efficient strategy to achieve significant photoinactivation of Gram-negative
481 species (Alves et al., 2009; Demidova & Hamblin, 2005; Simões et al., 2016). The use
482 of porphyrins (preferably cationic ones) has been extensively applied for a broad-
483 spectrum aPDT (Bartolomeu et al., 2016; Beirão et al., 2014; Moreira et al., 2020;
484 Pereira et al., 2014; Tomé et al., 2004). The main indicators of bacterial photodynamic

485 efficiency of porphyrin derivatives have been *S. aureus* (Gram-positive; including
486 methicillin-resistant strains) and *E. coli* (Gram-negative). Cells suspensions of six
487 different strains of *S. aureus* were irradiated for 60 min with Tetra-Py⁺-Me at 5 μM
488 reaching 5 log CFU/mL of reduction (Bartolomeu et al., 2016). A recent study evaluated
489 the photodynamic efficiency of the cationic porphyrin-imidazole against a
490 bioluminescent *E. coli* strain (Moreira et al., 2020). One of the porphyrin-imidazole
491 derivatives was evaluated in two different concentrations (5 and 20 μM) and reduced
492 the population of *E. coli* of 2.38 and 3.85 log CFU/mL, respectively, after 90 min of
493 irradiation (Moreira et al., 2020). Another study assessed how the outer structures
494 influenced the aPDT process in a diverse spectrum of Gram-positive and Gram-
495 negative bacteria (Pereira et al., 2014). The authors have documented that the
496 susceptibility of each bacterial strain to aPDT with Tetra-Py⁺-Me was dependent on
497 bacteria external structures, although Gram-positive bacteria with the complex multi-
498 layered outer structure were still more sensitive to aPDT than Gram-negative bacteria.
499 The authors explained that even multi-layer Gram-positive bacteria are still more
500 porous than gram-negative to the effects of aPDT. The use of porphyrins as PS is still
501 featured in other bacteria of food interest as *B. cereus*, *L. monocytogenes*, and *P.*
502 *aeruginosa* (Oliveira et al., 2009; Beirão et al., 2014; Romanova et a., 2003).

503 The use of phenothiazinium dyes (e.g. MB, TBO, NMB, DMMB) for photodynamic
504 inactivation of foodborne bacteria have been reported by several authors (Demidova
505 & Hamblin, 2005; Lin et al., 2012; Wainwright et al., 1997; Wainwright et al., 1998; Wu
506 et al., 2009). One of the earliest studies of aPDT with phenothiazinium derivatives
507 against foodborne pathogens tried to inactivate *S. aureus* (including MRSA), *B. cereus*,
508 *E. coli*, *P. aeruginosa*, and *Enterococcus faecalis* using a source of light (350-800 nm)
509 able to give a fluence of 6.3 J/cm² after 60-min exposure (Wainwright et al., 1997;
510 Wainwright et al., 1998). The minimum lethal concentrations required for several
511 bacterial species were significantly reduced by light exposure. This study did not
512 provide the results in log reductions. *L. monocytogenes* has also been effectively killed
513 by aPDT with MB excited by a tungsten-halogen lamp with an irradiance of 200

514 mW/cm² (Lin et al., 2012). The viability of *L. monocytogenes* was diminished by about
515 7 log CFU/mL after 10 min of exposure which corresponded to a fluence of 120 J/cm².

516 Another class of PS frequently used in aPDT processes is the xanthene dyes as
517 erythrosine which is an approved food colorant by the U.S. Food and Drug
518 Administration (FDA, 2020). Several studies have evaluated the photodynamic effects
519 of erythrosine and other xanthene dyes as RB, and EOY (Brovko et al., 2009; Silva et
520 al., 2018; Silva et al., 2019; Yassunaka et al., 2015). Brovko et al. (2009) reported the
521 use of RB at 5 µg/mL against *Bacillus* sp. and *L. monocytogenes* resulting in 5–6 log
522 CFU/mL reductions after 30 min of light exposure (0.81 J/cm²). However, to achieve
523 the same magnitude of reduction for *E. coli* and *S. Typhimurium*, the concentration of
524 RB had to be increased to 50 µg/mL in the same conditions of illumination. Moreover,
525 the authors also reported that an RB minimum bactericidal concentration of 5 µg/mL
526 for *L. monocytogenes* and 50 µg/mL for *Bacillus* sp. without light exposure. ERY at low
527 concentrations (1 µM) photoactivated by green LED exposure (510 nm) was able to
528 reduce the cell viability of *S. aureus* (4 log reduction) with a fluence of 40 J/cm²
529 (Yassunaka et al., 2015). The activity of EOY, another xanthene dye widely used as
530 PS for microbial photosensitization of foodborne bacteria was recently reported by
531 Bonin et al. (2018). The most and less susceptible species were *S. aureus* and *E. coli*,
532 respectively. *S. aureus* population was inactivated by ≈ 6 log CFU/mL with EOY at 5
533 µM and 5 min of irradiation while *E. coli* was inactivated only by 0.1-0.8 log CFU/mL.
534 *P. aeruginosa*, *B. cereus*, and *S. Typhimurium* presented intermediated resistances
535 with ≈ 6 log CFU/mL reduction at 10 µM EOY for 10 min, 4.3 log CFU/mL reduction at
536 7.5 µM EOY for 15 min, and 1.7 log CFU/mL reduction at 10 µM EOY for up to 15 min,
537 respectively (Bonin et al., 2018). Approximately 6 log CFU/mL and 7 log CFU/mL
538 reductions of vegetative cells of *S. Typhimurium* and *S. aureus* was achieved,
539 respectively with RB at 75 µM and 25 nM, respectively, after only 5 min of illumination
540 (Silva et al., 2019). The maximum concentration tested of ERY (500 nM) was needed
541 to reduce the populations of *S. aureus* to undetectable levels after 5 min, while a
542 reduction of only 2 log CFU/mL of *S. Typhimurium* have been achieved using ERY at
543 100 µM after 15 min (Silva et al., 2019). Recently, a study used response surface

544 methodology (RSM) to determine the optimum parameters for inactivation using EOY
545 combined with green LED light (Santos et al., 2020). The authors determined by RSM
546 that the highest inactivation rate ($> 4 \log \text{CFU/mL}$) of *S. aureus* was achieved using a
547 fluence of 9.98 J/cm^2 with EOY at 498 nm of concentration.

548 The use of natural compounds as PS against foodborne bacteria is an interesting
549 strategy of aPDT since compounds like curcumin, chlorophyllin, riboflavin, and
550 hypericin have been approved for use as food additives. aPDT with curcumin as PS
551 and blue LED against Gram-positive and Gram-negative foodborne bacteria has been
552 used by several authors (Huang et al., 2020; Penha et al., 2017). One of these studies
553 evaluated the effects of curcumin at $75 \mu\text{M}$ in the presence of blue LED (470 nm) on a
554 broad spectrum of foodborne bacteria (Penha et al., 2017). Curcumin-mediated aPDT
555 treatment induced $\approx 6 \log \text{CFU/mL}$ reductions of *S. aureus*, *A. hydrophila*, and *E. coli*
556 at fluence of 417 J/cm^2 . No reduction was observed for *P. aeruginosa* and only 2.82
557 $\log \text{CFU/mL}$ reduction was achieved for *S. Typhimurium* at the same fluence (Penha
558 et al., 2017). Another recent study showed a maximum reduction of 5.94 and $5.91 \log$
559 CFU/mL for *E. coli* and *S. aureus*, respectively, when treated with $20 \mu\text{M}$ of curcumin
560 and fluence of 13 J/cm^2 (Bhavaya & Hebbar, 2019a). The same authors also evaluated
561 the combinational effect of ultrasound (US) and aPDT with curcumin ($50\text{-}100 \mu\text{M}$) and
562 blue LED (70 J/cm^2) against *E. coli* and *S. aureus* in orange juice (Bhavaya & Hebbar,
563 2019b). However, despite having found an additional effect on the inactivation of *E.*
564 *coli* by US, the results of this work are still less effective than the previous one using
565 only aPDT. The authors attribute the minimal effect of sonication to the variation in
566 volume of orange juice (Bhavaya & Hebbar, 2019b). Photodynamic inactivation of *L.*
567 *monocytogenes* mediated by edible curcumin at low concentrations and fluence of 0.54
568 J/cm^2 was reported by Huang et al. (2020). Treatments with curcumin at $0.2 \mu\text{M}$ and at
569 $1.0 \mu\text{M}$ reduced the population of vegetative cells by more than $4 \log \text{CFU/mL}$ and 8
570 $\log \text{CFU/mL}$, respectively.

571 The photoactivity of a chlorophyllin derivative when combined with sodium (Na)
572 forms a water-soluble compound, which has been tested against food-borne bacteria

573 *in vitro* (Buchovec et al., 2017). In that study, the mechanism of inactivation of *S.*
574 *Typhimurium* by Na-Chl (15 μ M) with LED (405 nm) was evaluated in combination with
575 chitosan (CHS) and high-power pulsed UV light (HPPL). The aPDT process reduced
576 the population of *S. Typhimurium* by only 2.05 log CFU/mL at 46.1 J/cm². The
577 combination of CHS with Na-Chl and LED (17.3 J/cm²) increased the reductions to
578 7.28 log CFU/mL. Meanwhile, the combination of HPPL at 0.29 J/cm² with Na-Chl and
579 LED (46.1 J/cm²) was able to reduce more than 7 log CFU/mL of *S. Typhimurium*
580 vegetative cells (Buchovec et al., 2017).

581 Another plant-based PS that has been frequently used in aPDT processes against
582 foodborne bacteria is Hyp. Two studies from the same group evaluated the
583 effectiveness of aPDT with Hyp at 0.1 and 10 μ M and LED exposure (9.2 J/cm²)
584 against *L. monocytogenes*, *S. Typhimurium*, and *B. cereus* (Aponiene, Paskeviciute,
585 Reklaitis, & Lukšiene, 2015; Kairyte, Lapinskas, Gudelis, & Lukšiene, 2012). The
586 inactivation of *L. monocytogenes* after treatment with Hyp at 0.1 μ M achieved 7 log
587 CFU/mL, whereas *S. Typhimurium* was reduced by only 1 log CFU/mL with Hyp at 10
588 μ M. However, the authors tested the combination of ADPT with pulsed light at 0.023
589 J/cm² and viability of both species were reduced by 7 log CFU/mL (Kairyte et al., 2012).
590 In the same conditions mentioned above, the authors tested the inactivation of *B.*
591 *cereus in vitro* and on the surface of fruits and vegetables (Aponiene et al., 2015). Hyp-
592 based photosensitization reduced the population of *B. cereus* by 4.4 log CFU/mL *in*
593 *vitro* and by 0.77-1.3 log CFU/mL on the surface according to the type of fruit and
594 vegetable.

595 The micronutrient riboflavin or vitamin B2 is considered very sensitive to UV and
596 visible lights between 420 and 560 nm (Ottaway, 1993). In aPDT, riboflavin is usually
597 excited by visible light to avoid risks related to UV application. Two studies evaluated
598 the viability of *E. coli* after treatment with riboflavin and exposition to blue light (Liang
599 et al., 2013; Liang, Cheng, Yu, & Chen, 2015). DNA was found to be the main target
600 of the photochemical reactions triggered by the presence of riboflavin and its
601 derivatives.

602 Many studies are reporting some advance in the potentiation effect of non-toxic salt
603 (e.g., potassium iodide; KI) in aPDT as previously cited in this review in section 4.2. It
604 has been shown a significant potentiation effect for at least three different formulations
605 of porphyrin combined with KI against methicillin-resistant *S. aureus* (MRSA) and *E.*
606 *coli* (Huang et al., 2018; Moreira et al., 2020; Vieira et al., 2019). The authors reported
607 a drastic reduction in the irradiation time (Moreira et al., 2020; Vieira et al., 2019) as
608 well as the inactivation of *E. coli* using an anionic porphyrin which was unable to kill
609 the bacteria in the absence of KI (Huang et al., 2018). aPDT with phenothiazinium dyes
610 (especially MB) has been reported to be potentiated by the addition of inorganic or
611 halide salts such as KI, NaN_3 , and SCN^- (Huang et al., 2012; St Denis et al., 2013;
612 Vecchio et al., 2015; Yuan et al., 2020). The most common potentiator is KI, although
613 the addition of NaN_3 and SCN^- has shown interesting and even unexpected results.
614 Huang et al. (2012) observed that the combination between NaN_3 -MB and red-light
615 exposure can enhance the inactivation of *S. aureus* and *E. coli* up to 3 log CFU/mL.
616 Interestingly, NaN_3 increased the inactivation of *S. aureus* and *E. coli* even in the
617 absence of oxygen, instead of protection from killing as expected for its capacity to
618 quench singlet oxygen. One year later, St Denis et al. (2013) reported a potentiation
619 effect of SCN^- using 10 μM of MB in the populations of *S. aureus* and *E. coli*. The
620 authors observed that the SCN^- rapidly reacted with singlet oxygen producing both
621 sulfite and cyanide anions, responsible for bacterial death. The addition of KI in MB-
622 based aPDT to potentiate bacterial killing has been explored two years later by Vecchio
623 et al. (2015). The authors observed a consistent increase of red light-mediated
624 bacterial killing of *S. aureus* (4 log CFU/mL) and *E. coli* (2 log CFU/mL). The
625 combination of xanthene dyes and KI photoactivated by green light has been recently
626 evaluated against Gram-negative and Gram-positive bacteria (Santos et al., 2019;
627 Wen et al., 2017). Both studies from different research groups obtained similar and
628 promising results due to the presence of KI.

629

630 5.2. Spore forming bacteria and biofilms

631

632 The aPDT resistance of the spore forming bacterium *B. cereus* was evaluated in
633 the presence of different porphyrin derivatives (Oliveira et al., 2009). The authors
634 described a reduction of 3.5 log CFU/mL in the viability of the spores using a tricationic
635 porphyrin with a meso-pentafluorophenyl group (Tri-Py⁺-Me-PF) at 0.5 μM after 4 min
636 of irradiation. The group selected the same PS to investigate the susceptibility of other
637 spore forming *Bacillus* species such as *B. licheniformis*, *B. sphaericus*, and *B. subtilis*
638 as well as *B. cereus* as a model (da Silva et al., 2012). The study demonstrated that
639 more than 3 log CFU/mL reduction in viability was achieved for *B. cereus* and the other
640 species were considered less susceptible to aPDT with Tri-Py⁺-Me-PF at 10 μM after
641 4 min of irradiation. Despite the genetic similarity (Helgason et al., 2000), the authors
642 suggest that the reduction in the viability of *B. cereus* should not be considered a
643 surrogate for *B. anthracis* by aPDT. The authors concluded that there was no
644 significant difference in the adhesion of the PS to the spores of *Bacillus* regardless of
645 the structure of the exosporium (with or without glycoprotein layer). (da Silva et al.,
646 2012). To assess the effect of aPDT with porphyrins on *L. monocytogenes*, an
647 important foodborne causative agent of listeriosis, some authors have used *L. innocua*
648 as a surrogate of this pathogen (Bonifácio et al., 2018). The porphyrin tested was the
649 Tetra-Py⁺-Me at 23.7 mg/L, achieving only 1.1 log CFU/mL reductions of *L. innocua*
650 biofilm. The same research group had carried out studies on the inactivation of *L.*
651 *innocua* biofilms using a porphyrinic-chitosan antifouling complex during 24 h of
652 irradiation preventing the biofilm progress (Castro et al., 2017). The aPDT with Tetra-
653 Py⁺-Me at 20 μM and fluence of 64.8 J/cm² was able to reduce the viability of *P.*
654 *aeruginosa* and *S. aureus* by 2.8 and 6.3 log CFU/mL, respectively (Beirão et al.,
655 2014). The authors also reported a reduction of 81% in the polysaccharide content of
656 the *P. aeruginosa* biofilm matrix demonstrating that it can be the primary target of the
657 aPDT process for biofilms eradication.

658 Demidova and Hamblin (2005) studied the effects of aPDT with phenothiazinium
659 dyes and red light on the survival of spores of different *Bacillus* species. Their findings
660 revealed that *Bacillus* spores were susceptible to aPDT with phenothiazinium dyes at
661 low fluences of red light. It has been shown that in the presence of TBO, DMMB, and

662 MB (50 μM), the fluence of 40 J/cm^2 was able to achieve 5, > 3, and > 2 log CFU/mL
663 reductions of *B. cereus* spore viability, respectively, while NMB at the same
664 concentration only required 20 J/cm^2 to achieve a reduction of more than 5 log
665 CFU/mL. The team also discovered that the excess of PS, not bound to the spores,
666 can prejudice light delivery and impair inactivation efficiency (Demidova & Hamblin,
667 2005). The inactivation of *S. aureus*, *P. aeruginosa*, *E. coli*, and *Acinetobacter* sp.
668 biofilms was evaluated using a polyacrylamide (PAA) matrix loaded with MB
669 photoactivated by laser light (Wu et al., 2009). The results showed that the complex
670 PAA-MB damage the cell membrane, proteins, and DNA, killing all the species of
671 bacteria in both vegetative and biofilm forms as determined by plate count and
672 spectrophotometry, respectively (Wu et al., 2009). De Sordi et al. (2015) evaluated the
673 effect of aPDT using 665 nm red laser light (0.24 J/cm^2) on *Clostridium difficile*
674 vegetative cells, biofilm, and germinating spores. They observed that *C. difficile*
675 vegetative cells and biofilm were inactivated at least by 3 log CFU/mL in the presence
676 of MB and other PSs (e.g., chlorin e6) at 100 μM (for vegetative cells) and 1 mM (for
677 biofilm). They also achieved a slight reduction in viability of *C. difficile* spores (~ 1 log
678 CFU/mL), however, it was necessary to induce germination before aPDT (De Sordi et
679 al., 2015). The use of KI in combination with MB was also tested against the formation
680 of *E. faecalis* biofilms (Yuan et al., 2020). It was demonstrated that KI was able to
681 potentiate the aPDT of *E. faecalis* biofilm even in a hypoxic condition and absence of
682 light. Moreover, the presence of KI increases the photobleaching of MB after light
683 exposure which is desirable to reduce tooth staining by MB (Yuan et al., 2020) and
684 could be interesting for food applications.

685 The application of xanthene derivatives, RB and ERY as PS, in PDT study against
686 *S. Typhimurium* and *S. aureus* biofilm formation using a green LED was performed.
687 (Silva et al., 2019). A total of 8 log CFU/cm² reductions of *S. aureus* biofilms required
688 RB at 250 μM and ERY at 500 μM with 30 min of irradiation (Silva et al., 2019). In
689 contrast, the photoinactivation of *S. Typhimurium* biofilms (≥ 3 log CFU/cm²) only was
690 possible with RB at 50–1000 μM after the same 30 min of irradiation.

691 The use of natural compounds was also identified against the biofilm formation
692 (Bonifácio et al., 2018; Huang et al., 2020). The reduction of the biofilm formation or
693 structure disorder by curcumin-based aPDT is mainly promoted by DNA damage
694 (Huang et al., 2020). Another study used the spores of *B. atrophaeus* as surrogate of
695 foodborne spore forming bacteria such as *Bacillus* and *Clostridium* to evaluate
696 riboflavin positively charged as PS (Eichner et al., 2015). The spores were incubated
697 with the riboflavin derivatives and photoactivated with blue light at 70 J/cm². Depending
698 on the concentration of the PS, the spores were significantly reduced (3.5-4.4 log
699 CFU/mL) after only 10 s of irradiation and effectively killed when immobilized on PET
700 surface (7.0 log CFU/mL) by complete disruption of the coat and the outer membrane
701 (Eichner et al., 2015).

702

703 5.3. Yeasts and molds

704

705 The presence of fungi species is widespread but unlike bacteria and viruses, the
706 association with outbreaks of foodborne illnesses is rarely attributed to fungal species
707 (Fleet, 2007). Even though the application of aPDT against yeasts and molds is of
708 great relevance for the agrifood and medical sector. In a recent paper it was
709 demonstrated the inactivation of *Candida albicans* and *Candida tropicalis* with diode
710 laser and the compound aluminum phthalocyanine chloride as PS in nanoemulsion
711 (Rodrigues et al., 2019). The authors observed 5 log CFU/mL reduction in the viability
712 of *C. albicans* and 4-5 log CFU/mL reduction in the viability of *C. tropicalis* when the
713 nanoemulsion with PS was photoactivated. Another work also aimed to study the
714 photodynamic effect of phthalocyanines (Pcs) on *C. albicans* (Ozturk et al., 2020). After
715 illumination at 30 and 60 J/cm² with ZnPc, the cell viability was reduced by 5 and 2 log
716 CFU/mL, respectively. Another recent study of aPDT using porphyrin derivatives and
717 white light (380-700 nm) investigated its photodynamic effects against *C. albicans*, also
718 in the presence of KI (Vieira et al., 2019). It was demonstrated that a relatively low
719 concentration (0.5 µM) of the porphyrin derivatives in combination with KI and a fluence

720 of only 6.75 J/cm² were enough to achieve 6.7 log CFU/mL reduction of *C. albicans*
721 (Vieira et al., 2019).

722 Many filamentous fungi have also been investigated for their susceptibility to aPDT.
723 Recent findings on the effect of aPDT using phenothiazinium PSs and red light on the
724 survival of the filamentous fungi *Fusarium keratoplasticum* and *Fusarium moniliforme*
725 have been published (Paziani et al., 2019). aPDT with the PSs MB, NMB, and S137
726 can efficiently reduce the survival of both species. The susceptibility of the aflatoxin-
727 producing fungi species *Aspergillus flavus* to aPDT was evaluated (Temba et al.,
728 2019). In addition to the microbial reduction, the production of aflatoxin B₁ was lower
729 in the treated maize kernels than in the untreated samples.

730

731 **5.4. Protozoa and viruses**

732 Even though aPDT for the inactivation of protozoa and viruses do not have the
733 same emphasis as for the inactivation of bacteria and fungi species, its application has
734 presented satisfactory outcomes. It is important to remember that the first experiment
735 of aPDT was conducted precisely with a protozoan species (Raab, 1900). Given the
736 importance of the *Leishmania* and Chagas diseases caused by the infection with
737 protozoa species with apparent resistance to some of the currently used drugs, aPDT
738 has emerged as an alternative treatment. Recently, a study has focused the application
739 of aPDT for the inactivation of *Leishmania amazonensis* (Sepúlveda et al., 2020). The
740 authors investigated the efficacy of titanium dioxide (TiO₂) nanoparticles associated
741 with Zn and Hyp in combination with blue and red light (52.8 J/cm²). In the tests with
742 infected mice, aPDT was able to reduce the viability of *L. amazonensis* by 43% – 58%
743 (Sepúlveda et al., 2020). Although Chagas disease is considered endemic in Latin
744 American, the constant migration flow is worrying the specialists of public health. As
745 the causative agent of Chagas disease is the protozoan *Trypanosoma cruzi*, the effect
746 of aPDT with phenothiazine derivatives on the protozoan survival was recently
747 investigated (Barbosa et al., 2020). The trypanocidal effect of aPDT with MB and TBO
748 with diode laser illumination (660 nm, 4.2 J/cm²) was evaluated in infected
749 macrophages. The authors observed that MB at 2.6 µM and TBO at 1.2 µM caused a

750 reduction of 50% (IC₅₀) in the viability of *T. cruzi* without light exposition. However, the
751 photoactivation of the compounds contributed significantly to the reduction of the IC₅₀
752 values to 1.0 and 0.9 μM for MB and TBO, respectively (Barbosa et al., 2020). Recent
753 studies have shown the parasitical activity of some phenothiazinium dyes, even in the
754 dark (Pereira et al., 2020; Portapilla et al., 2019).

755 The application of aPDT for virus inactivation is not restricted to only one study, as
756 reported by Ghate et al., (2019). Several studies have been addressed to the
757 inactivation of different viruses, including the use of natural compounds as depicted in
758 a recently published review of the anti-infective properties of curcumin (Praditya et al.,
759 2019). Norovirus (NoV) is reported to be associated with the vast majority of cases of
760 foodborne illnesses in the USA (CDC, 2017). Recent findings of type 1 murine
761 norovirus (MNV-1) inactivation through aPDT using curcumin are available in the
762 literature (Wu et al., 2015; Randazzo et al., 2016). The photoinactivation of MNV-1 was
763 investigated *in vitro* in the presence of curcumin combined with blue light (470 nm) at
764 3.6 J/cm². Inactivation of MNV-1 increased in a dose-dependent manner and achieved
765 more than 3 log PFU/mL reductions at 20 μM of curcumin (Wu et al., 2015). Similarly,
766 other authors also investigated the aPDT efficacy of curcumin and blue light (464-474
767 nm) against MNV-1 and feline calicivirus (FCV-F9) (Randazzo et al., 2016). The FCV-
768 F9 with almost 5 log TCID₅₀/mL of reduction after 30 min was much more susceptible
769 than MNV-1 with only 0.73 log TCID₅₀/mL of inactivation after 120 min of treatment
770 (Randazzo et al., 2016). The variability in susceptibility to aPDT among different
771 viruses (bacteriophages MS2 and Qβ, bovine enterovirus type-2 (BEV-2) and MNV-1)
772 was assessed in a recent study using the compound 5, 10,15, 20-tetrakis (1-methyl-4-
773 pyridinio) porphyrin-tetra-*p*-toluene sulfonate (TMPyP) as PS combined with white light
774 (641-661 nm; 230.4 J/cm²) (Majiya et al., 2018; Majiya et al., 2019). The authors
775 observed approximately 8 log PFU/mL reductions of MS2 and Qβ within only 1 and 8
776 min of exposure, respectively, followed by 120 min of irradiation to achieve
777 approximately 4 log PFU/mL reductions of MNV-1 and BEV-2. Another recent study of
778 aPDT using porphyrin derivatives and white light (380-700 nm) investigated its effects
779 against a virus (T4-like bacteriophage) including in the presence of KI (Vieira et al.,
780 2019). It was demonstrated that low concentrations (0.1 μM) of the porphyrin

781 derivatives in combination with KI and a fluence of only 3 J/cm² were needed to achieve
782 approximately 8 log PFU/mL reductions of a T4-like phage (Vieira et al., 2019).
783

784 **Table 3. Overview of *in vitro* studies on aPDT against critical pathogenic and spoilage microorganisms.**

Photosensitizer	Microorganisms	Potentiator	Source of light (Wavelength and Irradiance)	Fluence	Log reduction	References
Porphyrin derivatives:						
Porphyrin Tetra-Py ⁺ -Me (5 µM)	<i>S. aureus</i> (MRSA)	No	Artificial white light: 380-700 nm 4 mW/cm ²	14.4 J/cm ²	> 5.0 log	Bartolomeu et al. (2016)
Porphyrin derivatives (5 and 20 µM)	<i>E. coli</i>	No	Artificial white light: 0.25 mW/cm ²	1.35 J/cm ²	5 µM: 2.38 log; 20 µM: 3.85 log	Moreira et al. (2020)
Porphyrin P3 (0.2 µM) + CHS	<i>L. innocua</i>	No	White LED: 400-800 nm 10 mW/cm ²	864 J/cm ²	8.0 log	Castro et al. (2017)
Porphyrin P2 (3 µM) + CHS	<i>E. coli</i> (bioluminescent)	No	Artificial white light: 380-700 nm 3 mW/cm ²	16.2 J/cm ²	4.0 log	Castro et al. (2019)
Porphyrin mixture (5 µM)	<i>S. aureus</i> (MRSA) <i>E. coli</i> (bioluminescent)	Yes, KI (100 mM)	Artificial white light: 380-700 nm 2.5 mW/cm ²	<i>S. aureus</i> : 0.75 J/cm ² <i>E. coli</i> : 11.25 J/cm ²	b.d.l	Vieira et a. (2019)
Phenothiazinium dyes:						
MB; TBO; NMB; DMMB (50 µM)	<i>B. cereus</i> spores	No	Red light: TBO and DMMN – 635 nm MB and NMB – 660 nm 200 mW/cm ²	TBO, MB and DMMB: 40 J/cm ² ; NMB: 20 J/cm ²	TBO: 5 log; MB: > 2 log; DMMB: > 3 log; NMB: > 5 log	Demidova & Hamblin (2005)
MB (100 µM)	<i>C. difficile</i> (vegetative cells, biofilm, and spores)	No	Laser light: 665 nm	0.24 J/cm ²	3.0 log	De Sordi et al. (2015)

CHS: Chitosan; b.d.l.: below detection limit

786 **Table 3. Continued**

Photosensitizer (concentration)	Microorganisms	Potentiator	Source of light (Wavelength and Irradiance)	Fluence	Log reduction	References
MB (100-200 µM)	<i>E. coli</i> <i>S. aureus</i>	Yes, NaN ₃ (10-100 µM)	Red light: 660 nm 100 mW/cm ²	8 J/cm ²	1-3 log	Huang et al. (2012)
MB (0.4 µM)	<i>E. faecalis</i>	Yes, KI (100 mM)	Red light: 660 nm 50 mW/cm ²	6.0 J/cm ²	8.0 log	Yuan et al. (2020)
Xanthene dyes:						
ERY (500 nM) RB (75 µM – 25 nM)	<i>S. Typhimurium</i> <i>S. aureus</i>	No	Green LED: 510 nm 10 mW/cm ²	3.0 J/cm ²	b.d.l	Silva et al. (2019)
EOY (498 nM)	<i>S. aureus</i>	No	Green LED: 530 nm 10 mW/cm ²	9.98 J/cm ²	> 4.0 log	Santos et al. (2020)
RB (10 µM)	<i>S. aureus</i> <i>E. coli</i> <i>P. aeruginosa</i> <i>C. albicans</i>	Yes, KI (100 mM)	Green Light: 540 nm 100 mW/cm ²	10-20.0 J/cm ²	> 6.0 log	Wen et al. (2017)
Natural compounds:						
Curcumin (0.2 and 1 µM)	<i>L. monocytogenes</i>	No	Blue LED: 455-460 nm 1.8 mW/cm ²	0.54 J/cm ²	0.2 µM: > 4.0 log 1 µM: b.d.l	Huang et al. (2020)
Curcumin (75 µM)	<i>S. aureus</i> <i>A. hydrophila</i> <i>S. Typhimurium</i> <i>E. coli</i> <i>P. aeruginosa</i>	No	Blue LED: 470 nm 1.2 W (1.77 cm ²)	417.0 J/cm ²	<i>S. aureus</i> , <i>A. hydrophila</i> and <i>E. coli</i> : b.d.l; <i>S. Typhimurium</i> : 2.82 log <i>P. aeruginosa</i> : No reductions	Penha et al. (2017)

b.d.l.: below detection limit

788 **Table 3. Continued**

Photosensitizer (concentration)	Microorganisms	Potentiator	Source of light (Wavelength and Irradiance)	Fluence	Log reduction	References
Chl (15 µM) + CHS	<i>S. Typhimurium</i>	No	LED: 405 nm 9.6 mW/cm ² HPPL UV light 260 nm	LED + Chl and HPPL: 46.1 J/cm ² and 0.29 J/cm ² ; LED + Chl + CHS: 17.3 J/cm ²	LED + Chl: 2.05 log; LED + Chl + CHS: 7.28 log; LED + Chl + HPPL: 7.5 log	Buchovec et al. (2017)
Hypericin (0.1 µM)	<i>B. cereus</i>	No	LED: 585 nm 3.84 mW/cm ²	9.2 J/cm ²	4.4 log	Aponiene et al. (2015)
Riboflavin (4 mM)	<i>B. atrophaeus</i> spores	No	Blue light: 320-500 nm 7 W/cm ²	70.0 J/cm ²	3.5-7.0 log	Eichner et al. (2015)

CHS: Chitosan

790 **6. Agrifood applications**

791

792 The development of environmentally friendly technologies is one of the main
793 objectives of the modern food industry, thus aPDT has been evaluated for a wide
794 application in several sectors of the food industry. According to a recent critical review,
795 most of the studies are focused on fruits, vegetables, and poultry (Ghate et al., 2019).
796 However, the same study notifies the concentrations of studies regarding food-related
797 surface. In the present review, the studies are mainly related to fruits and vegetables,
798 meat products, milk, and phytopathogen inactivation. Interestingly, recent studies from
799 the past two years mostly concentrated on two kinds of plant-based photosensitizers:
800 curcumin (Corrêa et al., 2020; de Oliveira et al., 2018; de Oliveira et al., 2018; Tao et
801 al., 2019; Temba et al., 2019; Tosati et al., 2018) and chlorophyllin (Josewin et al.,
802 2018; Paskeviciute et al., 2018; Paskeviciute et al., 2019; Žudyte & Lukšiene, 2019).
803 The main characteristics and results of these studies are depicted in Table 4.

804

805 **6.1. Fruits and vegetables**

806

807 It was demonstrated the bactericidal effect of aPDT with UV-A (320-400 nm) and
808 curcumin on *E. coli* and *L. innocua* cells inoculated on the surface of fresh produce (de
809 Oliveira et al. 2018a, b). Acidified curcumin at 10 mg/L was pulverized by conventional
810 spray-atomization or aerosolization on the inoculated surface of spinach, lettuce and
811 tomatoes before UV-A irradiation (de Oliveira, et al., 2018a). A reduction of 3 log
812 CFU/cm² by either conventional spray-atomization or aerosolization in both bacterial
813 populations tested was observed. The aPDT was also applied to prevent cross-
814 contamination of fresh produce from contaminated water of spinach and tomato after
815 washing (de Oliveira, et al., 2018b). A low concentration of curcumin (5 mg/L) was able
816 to inactivate more than 5 log CFU/mL after 10 and 5 min of UV-A light exposure for *E.*
817 *coli* and *L. innocua*, respectively (de Oliveira, et al., 2018b). The alternative curcumin-
818 based treatment has used 2 μM of PS to inactivate *E. coli* on the surface of apple slices
819 (Tao et al., 2019). Using a fluence of 152 J/cm², they observed inactivation of 0.96 log
820 CFU/g in the viability of *E. coli* on the surface of fresh-cut apple (Tao et al., 2019). At

821 relatively low fluence of 10 J/cm² with curcumin at 80 µM, an aPDT process on the
822 surface of apple achieved 2.0 log CFU/mL reductions of *S. aureus* (Corrêa et al., 2020).
823 These findings prove that the structure of Gram-positive bacteria is more susceptible
824 to aPDT.

825 The aPDT using Chl as PS has been investigated in real food matrices like
826 cantaloupe, cherry tomatoes, basil, and wheat sprouts. Josewin et al. (2018) used
827 cantaloupe rind in their study to evaluate the effectiveness of aPDT with Na-Chl for the
828 inactivation of *L. monocytogenes* and *Salmonella*. Na-Chl at 100 µM in combination
829 with exposure to 405 or 460 nm LED was used to evaluate the effects of
830 photosensitization at 4 and 20 °C, respectively. At both storage temperatures, a
831 fluence of 1,210 J/cm² (405 nm; LED) and 5,356 J/cm² (460 nm; LED) reached a
832 reduction in cell viability of 3 log CFU/cm² of *L. monocytogenes* in both cases whereas
833 the *Salmonella* cell viability was reduced by 1.1 and 3 log CFU/cm² for each
834 wavelength, respectively (Josewin et al., 2018). Two aPDT studies were conducted at
835 similar conditions of photosensitization with Chl at 150 µM and fluence of 3 J/cm², with
836 cherry tomatoes (Paskeviciute et al., 2018) and basil (Paskeviciute et al., 2019). The
837 viability of *B. cereus* and *L. monocytogenes*, artificially inoculated on the surface of
838 cherry tomatoes, was reduced by 1.5 and 1.6 log CFU/mL, respectively (Paskeviciute
839 et al., 2018). The aPDT in basil was able to reduce the viability of *L. monocytogenes*
840 by 1.6 log CFU/mL (Paskeviciute et al., 2019). A recent study aimed at the
841 decontamination of wheat sprouts by aPDT with Chl at high concentrations of 500 µM
842 combined with LED exposure of 18 J/cm² (Žudyte & Lukšiene, 2019). Under such
843 conditions of photosensitization against surface-attached *E. coli* and *Fusarium*
844 *oxysporum* (plant pathogen) in wheat sprouts, aPDT achieved reduction of 1.5 log
845 CFU/g for both pathogens.

846

847 **6.2. Meat products**

848

849 A researcher group attempted to prevent the growth of *S. aureus* and *E. coli* on the
850 surface of cut pieces of beef, chicken, and pork meat samples through aPDT (Corrêa
851 et al., 2020). The aPDT with curcumin at 40 µM and 15 J/cm² of UV-C irradiation

852 reduced the cell viability of *S. aureus* by 1.5, 1.4, and 0.6 log CFU/mL in beef, chicken,
853 and pork, respectively. The reductions of *E. coli* viability in beef, chicken, and pork was
854 1.0, 1.6, and 1.6 log CFU/mL at 3.9, 3.1, and 7.8 J/cm², respectively (Corrêa et al.,
855 2020). The authors emphasized the necessity for additional tests to assess the
856 nutritional and organoleptic effects of the aPDT. Another curcumin-based aPDT was
857 developed to avoid microbial growth on the surface of commercial sausages artificially
858 contaminated with *L. innocua* (Tosati et al., 2018). UV-A photoactivated edible coatings
859 with curcumin (5 mg/L) inactivated more than 5 log CFU/mL of *L. innocua* at a low dose
860 of 0.96 J/cm² (Tosati et al., 2018).

861

862 **6.3. Milk**

863

864 An interesting study aimed to photoinactivate *Staphylococcus* spp. and *E. coli*
865 vegetative cells was conducted in milk samples with 3.8 and 0.3% fat content (Galstyan
866 & Dobrindt, 2019). The suspensions of Gram-positive *S. aureus*, *S. hominis*, and *S.*
867 *warnei*, and Gram-negative *E. coli* isolates were artificially inoculated in diluted milk
868 samples (20%, 60%, and 90%). Firstly, the authors reported that the inactivation of
869 *Staphylococcus* spp. cells by aPDT with MB and silicon phthalocyanine derivative
870 (SiPc) at a higher fluence of 36 J/cm² achieved between 2-8 log CFU/mL reduction for
871 both PSs. To better understand the difference among the PSs, a lower fluence of 9
872 J/cm² was tested. The aPDT with SiPc at 10 µM reduced the viability of *Staphylococcus*
873 spp. by over 5 log CFU/mL in milk samples at the dilution rate of 20% and 60%, while
874 MB at the same concentration reduced the viability by only 1 log CFU/mL when the
875 milk content was 20% (Galstyan & Dobrindt, 2019). For the inactivation of *E. coli*, the
876 authors used the higher fluence of 36 J/cm² as Gram-negative bacteria are less
877 susceptible than Gram-positive bacteria to aPDT. In the milk samples with 0.3% and
878 3.8% fat content, the application of SiPc at 50 µM resulted in a reduction of 5-7 log
879 CFU/mL of the *E. coli* loads, while for MB they observed a lower reduction (2-4 log
880 CFU/mL) in the milk samples with 0.3% fat content (Galstyan & Dobrindt, 2019). The
881 authors did not evaluate the organoleptic and sensorial effects of the application of
882 aPDT on milk samples.

883

884 **6.4. Plant diseases**

885

886 The aPDT has also been employed to control plant-pathogenic fungi and bacteria
887 species for agricultural purposes avoiding the use of conventional antifungals and
888 bactericides, respectively (de Menezes et al., 2014; de Menezes et al., 2016; Fracarolli
889 et al., 2016; Gonzales et al., 2017; Jesus et al., 2018; Tonani et al., 2018). The
890 excessive use of chemicals is one of the major concerns for the environment. In this
891 way, some research dedicated to studying the effect of aPDT with phenothiazinium
892 dyes and natural plant-produced PSs in combination with artificial and solar radiation
893 has been explored against fungi species (*Colletotrichum* spp., *Fusarium* spp., and
894 *Neoscytalidium dimidiatum*) (de Menezes et al., 2014; Fracarolli et al., 2016; Gonzales
895 et al., 2017; Tonani et al., 2018). All of these studies showed positive results both *in*
896 *vitro* and *ex vivo* experiments against phytopathogens including some species able to
897 infect humans (*Neoscytalidium* spp.) (Machouart et al., 2013; Tonani et al., 2018). The
898 authors also demonstrated that aPDT did not damage the plant host. An interesting
899 study by Jesus et al. (2018) investigated the effect of aPDT on the control of
900 *Pseudomonas syringae* pv. *actinidiae* (Psa), a phytopathogenic bacterium. The
901 combination of porphyrin Tetra-Py⁺-Me, artificial light and solar radiation were
902 investigated using artificially contaminated kiwi leaves. Overall, it was demonstrated *in*
903 *vitro* and *ex vivo* an effective inactivation of Psa without any damage to the kiwi leaves
904 by the authors. However, all cited authors agree that further studies are needed under
905 field conditions to evaluate the environmental impact of this new technique as well as
906 to optimize the parameters of aPDT.

907 **Table 4. Some examples of *ex vivo* APDT studies on the inactivation of microorganisms for agrifood purposes.**

Agrifood applications	Microorganisms	Photosensitizer (concentration)	Source of light (Wavelength and Irradiance)	Fluence	Log reduction	References
<i>Fruit and vegetables:</i>						
Apple	<i>S. aureus</i>	Curcumin (80 µM)	LED: 450 nm 55 mW/cm ²	10 J/cm ²	2.0 log	Corrêa et al. (2020)
Spinach and cherry tomatoes	<i>E. coli</i> <i>L. innocua</i>	Curcumin (5 mg/L)	UV-A lamps: 320-400 nm 3.2 mW/cm ²	<i>E. coli</i> : 10 min (1.92 J/cm ²); <i>L. innocua</i> : 5 min (0.96 J/cm ²)	> 5.0 log	de Oliveira et al. (2018a)
Cantaloupe rind	<i>Salmonella</i> sp. <i>L. monocytogenes</i>	Chl (100 µM)	Blue LED 405 nm: 7 mW/cm ² 460 nm: 31 mW/cm ²	405 nm: 1210 J/cm ² 460 nm: 5356 J/cm ²	<i>L. monocytogenes</i> : 3 log (405 and 460 nm) <i>Salmonella</i> : 3 log – 405 nm and 1.1 log – 460 nm)	Josewin et al. (2018)
Maize kernels	<i>A. flavus</i>	Curcumin	Exon Arc lamp: 420 nm	60.0 J/cm ²	N.A. (Reduction of aflatoxin B1)	Temba et al. (2019)
Fresh-cut apples	<i>E. coli</i>	Curcumin (2 µM)	LED: 420 nm 298 mW/cm ²	152.0 J/cm ²	0.95 log	Tao et al. (2019)
Spinach, lettuce, and tomato	<i>E. coli</i> <i>L. innocua</i>	Acidified curcumin (10 mg/L)	UV-A lamps: 320-400 nm 0.68 mW/cm ²	2.0 J/cm ²	3.0 log	de Oliveira et al. (2018b)
Cherry tomatoes and basil	Mesophilic bacteria <i>B. cereus</i> <i>L. monocytogenes</i>	Chl (150 µM)	LED: 405 nm 10 mW/cm ²	3.0 J/cm ²	Mesophilic: 2.4 log (cherry tomatoes) and 1.3 log (basil); <i>B. cereus</i> : 1.5 log (cherry tomatoes); <i>L. monocytogenes</i> : 1.6 log (both)	Paskeviciute et al. (2018), (2019)

908 N.A.: Not available

909 **Table 4. Continued**

Agrifood applications	Microorganisms	Photosensitizer (concentration)	Source of light (Wavelength and Irradiance)	Fluence	Log reduction	References
Sprouted seeds	Mesophilic bacteria <i>E. coli</i> <i>F. oxysporum</i>	Chl (500 µM)	LED: 405 nm	18.0 J/cm ²	Mesophilic: 2.5 log; <i>E. coli</i> : 1.5 log ; <i>F. oxysporum</i> : 1.5 log	Žudyte & Lukšiene (2019)
Meat products:						
Sausage	<i>L. innocua</i>	Curcumin edible coating	UV-A lamps: 320-400 nm 3.2 mW/cm ²	0.96 J/cm ²	> 5.0 log	Tosati et al. (2018)
Beef, chicken, and pork.	<i>S. aureus</i>	Curcumin (40 µM)	LED: 450 nm 55 mW/cm ²	15 J/cm ²	Beef: 1.5 log; Chicken: 1.4 log; Pork: 0.6 log	Corrêa et al. (2020)
Milk	<i>S. aureus</i> <i>E. coli</i>	MB and SiPc (50 µM)	Red light 610 nm 10 mW/cm ²	9.0 – 36 J/cm ²	<i>S. aureus</i> : MB: 1.0 log (Milk 20%); SiPc: > 5.0 log (Milk 20% and 60%) <i>E. coli</i> : MB: 2.0-4.0 logs (Milk 20% / Fat content 0.3%); SiPc: 5.0-7.0 log (Milk 20% / Fat content 0.3% and 3.8%)	Galstyan & Dobrindt, (2019)
Plant diseases:						
Petals and leaves of <i>Citrus sinensis</i> Phytopathogen	<i>C. abscissum</i>	MB (25-50 µM)	Solar radiation 290-390 nm: 20.1-45.8 W/m ² ; Visible light 400-790 nm: 299.7-579.2 W/m ²)	30 min	Petals: 1.9-3.1 log Leaves: > 3.0 log	Gonzales et al. (2017)

911 **Table 4. Continued**

Agrifood applications	Microorganisms	Photosensitizer (concentration)	Source of light (Wavelength and Irradiance)	Fluence	Log reduction	References
Phytopathogen	<i>Neoscytalidium dimidiatum</i> <i>N. dimidiatum</i> var. <i>hyalinum</i>	NMB (10-200 μ M) S137 (10-25 μ M)	Red LED 631 nm 13.89 mW/cm ²	3.0 J/cm ²	NMB: 3-5 log S137: 2.0-3.5 log	Tonani et al. (2018)
Phytopathogen	<i>C. acutatum</i> <i>C. gleosporioides</i> A. <i>nidulans</i>	NMB (50 μ M) S137 (10 μ M)	Red LED 634 nm 9.20 mW/cm ²	15.0 J/cm ²	5.0 logs	de Menezes et al. (2014)
Kiwi leaves Phytopathogen	<i>P. syringae</i> pv. <i>actinidiae</i> (Psa)	Tetra-Py ⁺ -Me (50 μ M)	Artificial light: 400-800 nm 150 mW/cm ² Solar radiation: 65 mW/cm ²	90 min	Artificial light: 1.8-4.0 log Solar radiation: 1.5 log	Jesus et al. (2018)

912

913 **7. Conclusions and future perspectives**

914

915 The current status of aPDT as an innovative non-thermal technique designed for
916 microbial inactivation has gained increasing popularity in the last years among food
917 scientists. Researchers already know that the photodynamic procedure can inactivate
918 efficiently the most important microorganisms for food and agronomic interests, as
919 depicted in this review. Given the importance of food safety for the industry, aPDT can
920 in some cases still contribute to maintaining the organoleptic/nutritional characteristics
921 of foods. Thus, it is still necessary efforts to evaluated the effects of aPDT on the
922 nutritional and organoleptic features of food. The demand for healthy, fresh, and high-
923 quality food products has increased among consumers. Additionally, food products
924 without preservatives also possess an influence on the consumers in the supermarket.
925 The aPDT with natural PS, such as chlorophyllin and curcumin, has been widely
926 explored and can be an alternative for application in food.

927 The exploration of endogenous PSs, intrinsically produced by microorganisms, can
928 be particularly interesting in extending the shelf-life during the long-term storage of
929 foods in cold rooms, domestic refrigerators, and even in supermarket shelves. Most of
930 the studies developed for food applications so far are prototypes or methodologies only
931 on the laboratory scale. Despite the excellent results obtained even by the inactivation
932 of resistant forms (biofilms and spores) of foodborne bacteria and fungi species, it is
933 important to consider a scale-up of the technique to make it a reality in the food industry
934 as soon as possible. Some points should be considered to spark the interest of food
935 processors, such as the environmental, food-related, and engineering factors (Ghate
936 et al., 2019). Some of them can be mentioned as the dark period of incubation with
937 PS, the treatment temperature, surface roughness, and the right combination of PS
938 and light source. Photodynamic treatment is a promising technology to control harmful
939 microorganisms and could be used by industries and farms soon.

940 **Acknowledgements**

941 This work was supported by: Conselho Nacional de Desenvolvimento Científico e
942 Tecnológico (CNPq) (Grants #140092/2017-0, #302763/2014-7, #305804/2017-0,
943 445998, and 307738/2018-3); Fundação de Amparo à Pesquisa do Estado de São
944 Paulo (FAPESP) (Grant #2016/11386-5) and Coordenação de Aperfeiçoamento de
945 Pessoal de Nível Superior (CAPES) - Finance Code 001 for the financial support.

946

947 **Conflict of interest**

948 The authors declare no competing interests.

949

950 **8. References**

951 ACS. (2019). American Cancer Society. Getting Photodynamic Therapy. Retrieved
952 April 20, 2020, from [https://www.cancer.org/treatment/treatments-and-side-](https://www.cancer.org/treatment/treatments-and-side-effects/treatment-types/radiation/photodynamic-therapy.html)
953 [effects/treatment-types/radiation/photodynamic-therapy.html](https://www.cancer.org/treatment/treatments-and-side-effects/treatment-types/radiation/photodynamic-therapy.html)

954 Almeida, J., Tomé, J. P. C., Neves, M. G. P. M. S., Tomé, A. C., Cavaleiro, J. A. S.,
955 Cunha, A., Costa, L., Faustino, M.A.F, & Almeida, A. (2014). Photodynamic
956 inactivation of multidrug-resistant bacteria in hospital wastewaters: influence of
957 residual antibiotics. *Photochemical & Photobiological Sciences*, 13(4), 626.
958 <https://doi.org/10.1039/c3pp50195g>

959 Alvarenga, V. O., Brancini, G. T. P., Silva, E. K., da Pia, A. K. R., Campagnollo, F. B.,
960 Braga, G. Ú. L., Hubinger, M. D., & Sant'Ana, A. S. (2018). Survival variability of 12
961 strains of *Bacillus cereus* yielded to spray drying of whole milk. *International Journal of*
962 *Food Microbiology*, 286, 80–89. <https://doi.org/10.1016/j.ijfoodmicro.2018.07.020>

963 Alves, E., Costa, L., Carvalho, C. M., Tomé, J. P., Faustino, M. A., Neves, M. G., Tomé,
964 A. C., Cavaleiro, J. A. S., Cunha, Â., & Almeida, A. (2009). Charge effect on the
965 photoinactivation of Gram-negative and Gram-positive bacteria by cationic meso-
966 substituted porphyrins. *BMC Microbiology*, 9(1), 70. [https://doi.org/10.1186/1471-](https://doi.org/10.1186/1471-2180-9-70)
967 [2180-9-70](https://doi.org/10.1186/1471-2180-9-70)

968 Alves, E., Melo, T., Simões, C., Faustino, M. A. F., Tomé, J. P. C., Neves, M. G. P. M.
969 S., Cavaleiro, J. A. S., Cunha, Â., Gomes, N. C. M., Domingues, P., Domingues, M. R.

- 970 M., & Almeida, A. (2013). Photodynamic oxidation of *Staphylococcus warneri*
971 membrane phospholipids: new insights based on lipidomics. *Rapid Communications*
972 *in Mass Spectrometry*, 27(14), 1607–1618. <https://doi.org/10.1002/rcm.6614>
- 973 Aponiene, K., Paskeviciute, E., Reklaitis, I., & Lukšiene, Ž. (2015). Reduction of
974 microbial contamination of fruits and vegetables by hypericin-based
975 photosensitization: Comparison with other emerging antimicrobial treatments. *Journal*
976 *of Food Engineering*, 144, 29–35. <https://doi.org/10.1016/j.jfoodeng.2014.07.012>
- 977 Bacellar, I.O.L., Pavani, C., Sales, E.M., Itri, R., Wainwright, M., & Baptista, M.S.
978 (2014). Membrane damage efficiency of phenothiazinium photosensitizers.
979 *Photochemistry and Photobiology*, 90(4), n/a-n/a. <https://doi.org/10.1111/php.12264>
- 980 Baier, J., Maisch, T., Maier, M., Engel, E., Landthaler, M., & Bäuml, W. (2006).
981 Singlet oxygen generation by UVA light exposure of endogenous photosensitizers.
982 *Biophysical Journal*, 91(4), 1452–1459. <https://doi.org/10.1529/biophysj.106.082388>
- 983 Balasubramaniam, E., & Natarajan, P. (1997). Photophysical properties of
984 protoporphyrin IX and thionine covalently attached to macromolecules. *Journal of*
985 *Photochemistry and Photobiology A: Chemistry*, 103(3), 201–211.
986 [https://doi.org/10.1016/S1010-6030\(96\)04598-4](https://doi.org/10.1016/S1010-6030(96)04598-4)
- 987 Barba, F. J., Koubaa, M., Prado-Silva, L., Orlie, V., & Sant'Ana, A. S. (2017). Mild
988 processing applied to the inactivation of the main foodborne bacterial pathogens: A
989 review. *Trends in Food Science & Technology*, 66, 20–35.
990 <https://doi.org/10.1016/j.tifs.2017.05.011>
- 991 Barbosa, A. F. S., Santos, I. P., Santos, G. M. P., Bastos, T. M., Rocha, V. P. C., Meira,
992 C. S., Soares, M. B. P., Pitta, I. R., & Pinheiro, A. L. B. (2020). Anti-*Trypanosoma cruzi*
993 effect of the photodynamic antiparasitic chemotherapy using phenothiazine derivatives
994 as photosensitizers. *Lasers in Medical Science*, 35(1), 79–85.
995 <https://doi.org/10.1007/s10103-019-02795-4>
- 996 Bartolomeu, M., Rocha, S., Cunha, Â., Neves, M. G. P. M. S., Faustino, M. A. F., &
997 Almeida, A. (2016). Effect of photodynamic therapy on the virulence factors of
998 *Staphylococcus aureus*. *Frontiers in Microbiology*, 7, 1–11.

- 999 <https://doi.org/10.3389/fmicb.2016.00267>
- 1000 Batistela, V. R., Pellosi, D. S., de Souza, F. D., da Costa, W. F., de Oliveira Santin, S.
1001 M., de Souza, V. R., Caetano, W., de Oliveira, H. P. M., Scarminio, I. S., & Hioka, N.
1002 (2011). pKa determinations of xanthene derivates in aqueous solutions by multivariate
1003 analysis applied to UV–Vis spectrophotometric data. *Spectrochimica Acta Part A:
1004 Molecular and Biomolecular Spectroscopy*, 79(5), 889–897.
1005 <https://doi.org/10.1016/j.saa.2011.03.027>
- 1006 Beirão, S., Fernandes, S., Coelho, J., Faustino, M. A. F., Tomé, J. P. C., Neves, M. G.
1007 P. M. S., Tomé, A. C., Almeida, A., & Cunha, Â. (2014). Photodynamic inactivation of
1008 bacterial and yeast biofilms with a cationic porphyrin. *Photochemistry and
1009 Photobiology*, 90(6), 1387–1396. <https://doi.org/10.1111/php.12331>
- 1010 Bhavya, M. L., & Hebbar, H. U. (2019a). Efficacy of blue LED in microbial inactivation:
1011 Effect of photosensitization and process parameters. *International Journal of Food
1012 Microbiology*, 290, 296–304. <https://doi.org/10.1016/j.ijfoodmicro.2018.10.021>
- 1013 Bhavya, M. L., & Hebbar, H. U. (2019b). Sono-photodynamic inactivation of
1014 *Escherichia coli* and *Staphylococcus aureus* in orange juice. *Ultrasonics
1015 Sonochemistry*, 57, 108–115. <https://doi.org/10.1016/j.ultsonch.2019.05.002>
- 1016 Bonifácio, D., Martins, C., David, B., Lemos, C., Neves, M. G. P. M. S., Almeida, A.,
1017 Pinto, D. C. G. A., Faustino, M. A. F., & Cunha, Â. (2018). Photodynamic inactivation
1018 of *Listeria innocua* biofilms with food-grade photosensitizers: a curcumin-rich extract
1019 of *Curcuma longa* vs commercial curcumin. *Journal of Applied Microbiology*, 125(1),
1020 282–294. <https://doi.org/10.1111/jam.13767>
- 1021 Bonin, E., Ribeiro, L. H., Favero, M. E., Freitas, C. F. De, Caetano, W., & Hioka, N.
1022 (2018). Photodynamic inactivation of foodborne bacteria by eosin Y. *Journal of Applied
1023 Microbiology*, 124, 1617–1628. <https://doi.org/10.1111/jam.13727>
- 1024 Bosch, A., Gkogka, E., Le Guyader, F. S., Loisy-Hamon, F., Lee, A., van Lieshout, L.,
1025 Marthi, B., Myrmel, M., Sansom, A., Schultz, A.C., Winkler, A., Zuber, S., & Phister, T.
1026 (2018). Foodborne viruses: Detection, risk assessment, and control options in food
1027 processing. *International Journal of Food Microbiology*, 285, 110–128.

- 1028 <https://doi.org/10.1016/j.ijfoodmicro.2018.06.001>
- 1029 Brancaleon, L., & Moseley, H. (2002). Laser and non-laser light sources for
1030 photodynamic therapy. *Lasers in Medical Science*, 17(3), 173–186.
1031 <https://doi.org/10.1007/s101030200027>
- 1032 Broekgaarden, M., Weijer, R., van Gulik, T. M., Hamblin, M. R., & Heger, M. (2015).
1033 Tumor cell survival pathways activated by photodynamic therapy: a molecular basis
1034 for pharmacological inhibition strategies. *Cancer and Metastasis Reviews*, 34(4), 643–
1035 690. <https://doi.org/10.1007/s10555-015-9588-7>
- 1036 Brovko, L. Y., Meyer, A., Tiwana, A. S., Chen, W., Liu, H., Filipe, C. D. M., & Griffiths,
1037 M. W. (2009). Photodynamic treatment: a novel method for sanitation of food handling
1038 and food processing surfaces. *Journal of Food Protection*, 72(5), 1020–1024.
1039 <https://doi.org/10.4315/0362-028x-72.5.1020>
- 1040 Buchovec, I., Lukseviciūtė, V., Kokstaite, R., Labeikyte, D., Kaziukonyte, L., &
1041 Luksiene, Z. (2017). Inactivation of Gram (–) bacteria *Salmonella enterica* by
1042 chlorophyllin-based photosensitization: Mechanism of action and new strategies to
1043 enhance the inactivation efficiency. *Journal of Photochemistry and Photobiology B:*
1044 *Biology*, 172, 1–10. <https://doi.org/10.1016/j.jphotobiol.2017.05.008>
- 1045 Buchovec, I., Paskeviciute, E., & Luksiene, Z. (2010). Photosensitization-based
1046 inactivation of food pathogen *Listeria monocytogenes* in vitro and on the surface of
1047 packaging material. *Journal of Photochemistry and Photobiology B: Biology*, 99(1), 9–
1048 14. <https://doi.org/10.1016/j.jphotobiol.2010.01.007>
- 1049 Calin, M. A., & Parasca, S. V. (2009). Light sources for photodynamic inactivation of
1050 bacteria. *Lasers in Medical Science*, 24(3), 453–460. [https://doi.org/10.1007/s10103-](https://doi.org/10.1007/s10103-008-0588-5)
1051 [008-0588-5](https://doi.org/10.1007/s10103-008-0588-5)
- 1052 Cardoso, D. R., Libardi, S. H., & Skibsted, L. H. (2012). Riboflavin as a photosensitizer.
1053 Effects on human health and food quality. *Food & Function*, 3(5), 487.
1054 <https://doi.org/10.1039/c2fo10246c>
- 1055 Castano, A. P., Demidova, T. N., & Hamblin, M. R. (2004). Mechanisms in
1056 photodynamic therapy: Part one - Photosensitizers, photochemistry and cellular

- 1057 localization. *Photodiagnosis and Photodynamic Therapy*, 1(4), 279–293.
1058 [https://doi.org/10.1016/S1572-1000\(05\)00007-4](https://doi.org/10.1016/S1572-1000(05)00007-4)
- 1059 Castro, K. A. D. F., Moura, N. M. M., Fernandes, A., Faustino, M. A. F., Simões, M. M.
1060 Q., Cavaleiro, J. A. S., Nakagaki, S., Almeida, A., Cunha, Â., Silvestre, A. J. D., Freire,
1061 C. S. R., Pinto, R. J. B., & Neves, M. G. P. M. S. (2017). Control of *Listeria innocua*
1062 biofilms by biocompatible photodynamic antifouling chitosan based materials. *Dyes*
1063 *and Pigments*, 137, 265–276. <https://doi.org/10.1016/j.dyepig.2016.10.020>
- 1064 CDC. (2017). Center for Disease Control and Prevention. Norovirus: Facts for Food
1065 Workers. Retrieved April 29, 2020, from
1066 <https://www.cdc.gov/norovirus/downloads/foodhandlers.pdf>
- 1067 CDC. (2020a). CDC and Food Safety. Retrieved April 17, 2020, from
1068 <https://www.cdc.gov/foodsafety/cdc-and-food-safety.html>
- 1069 CDC. (2020b). Four steps for food safety. Retrieved April 19, 2020, from
1070 <https://www.cdc.gov/foodsafety/keep-food-safe.html>
- 1071 Cebrián, G., Mañas, P., & Condón, S. (2016). Comparative resistance of bacterial
1072 foodborne pathogens to non-thermal technologies for food preservation. *Frontiers in*
1073 *Microbiology*, 7, 1–17. <https://doi.org/10.3389/fmicb.2016.00734>
- 1074 Chacon, J. N., McLearnie, J., & Sinclair, R. S. (1988). Singlet oxygen yields and radical
1075 contributions in the dye-sensitised photo-oxidation in methanol of esters of
1076 polyunsaturated fatty acids (oleic, linoleic, linolenic and arachidonic). *Photochemistry*
1077 *and Photobiology*, 47(5), 647–656. [https://doi.org/10.1111/j.1751-](https://doi.org/10.1111/j.1751-1097.1988.tb02760.x)
1078 [1097.1988.tb02760.x](https://doi.org/10.1111/j.1751-1097.1988.tb02760.x)
- 1079 Chignell, C. F., Bilskj, P., Reszka, K. J., Motten, A. G., Sik, R. H., & Dahl, T. A. (1994).
1080 Spectral and photochemical properties of curcumin. *Photochemistry and Photobiology*,
1081 59(3), 295–302. <https://doi.org/10.1111/j.1751-1097.1994.tb05037.x>
- 1082 CIATox. Centro de Informação e Assistência Toxicológica – CIATox de Campinas –
1083 Faculdade de Ciências Médicas da UNICAMP (2018). Relatório de Atendimentos.
1084 Retrieved April 18, 2020, from
1085 https://www.fcm.unicamp.br/fcm/sites/default/files/2020/page/relatorio_de_atendimen

1086 tos_ciatox_2018_09jul2020.pdf

1087 Cieplik, F., Tabenski, L., Buchalla, W., & Maisch, T. (2014). Antimicrobial
1088 photodynamic therapy for inactivation of biofilms formed by oral key pathogens.
1089 *Frontiers in Microbiology*, 5, 1–17. <https://doi.org/10.3389/fmicb.2014.00405>

1090 Cieplik, F., Deng, D., Crielaard, W., Buchalla, W., Hellwig, E., Al-Ahmad, A., & Maisch,
1091 T. (2018a). Antimicrobial photodynamic therapy – what we know and what we don't.
1092 *Critical Reviews in Microbiology*, 44(5), 571–589.
1093 <https://doi.org/10.1080/1040841X.2018.1467876>

1094 Cieplik, F., Steinwachs, V.-S., Muehler, D., Hiller, K.-A., Thurnheer, T., Belibasakis, G.
1095 N., Buchalla, W., & Maisch, T. (2018b). Phenalen-1-one-mediated antimicrobial
1096 photodynamic therapy: antimicrobial efficacy in a periodontal biofilm model and flow
1097 cytometric evaluation of cytoplasmic membrane damage. *Frontiers in Microbiology*, 9.
1098 <https://doi.org/10.3389/fmicb.2018.00688>

1099 Condón-Abanto, S., Condón, S., Raso, J., Lyng, J. G., & Álvarez, I. (2016). Inactivation
1100 of *Salmonella* Typhimurium and *Lactobacillus plantarum* by UV-C light in flour powder.
1101 *Innovative Food Science and Emerging Technologies*, 35, 1–8.
1102 <https://doi.org/10.1016/j.ifset.2016.03.008>

1103 Corrêa, T. Q., Blanco, K. C., Garcia, É. B., Perez, S. M. L., Chianfrone, D. J., Morais,
1104 V. S., & Bagnato, V. S. (2020). Effects of ultraviolet light and curcumin-mediated
1105 photodynamic inactivation on microbiological food safety: A study in meat and fruit.
1106 *Photodiagnosis and Photodynamic Therapy*, 30, 101678.
1107 <https://doi.org/10.1016/j.pdpdt.2020.101678>

1108 D'Souza, C., Yuk, H., Khoo, G. H., & Zhou, W. (2015). Application of light-emitting
1109 diodes in food production, postharvest preservation, and microbiological food safety.
1110 *Comprehensive Reviews in Food Science and Food Safety*, 14(6), 719–740.
1111 <https://doi.org/10.1111/1541-4337.12155>

1112 da Silva, R. N., Tomé, A. C., Tomé, J. P. C., Neves, M. G. P. M. S., Faustino, M. A. F.,
1113 Cavaleiro, J. A. S., Oliveira, A., Almeida, A., & Cunha, Â. (2012). Photo-inactivation of
1114 *Bacillus* endospores: inter-specific variability of inactivation efficiency. *Microbiology*

- 1115 *and Immunology*, 56(10), 692–699. <https://doi.org/10.1111/j.1348-0421.2012.00493.x>
- 1116 de Freitas Saccol, A. L., Serafim, A. L., Hecktheuer, L. H., Medeiros, L. B., & Da Silva,
1117 E. A. (2016). Food safety in feeding services: a requirement in Brazil. *Critical Reviews*
1118 *in Food Science and Nutrition*, 56(8), 1363–1369.
1119 <https://doi.org/10.1080/10408398.2012.691917>
- 1120 de Menezes, H. D., Pereira, A. C., Brancini, G. T. P., de Leão, H. C., Massola Júnior,
1121 N. S., Bachmann, L., Wainwright, M., Bastos, J. K., & Braga, G. U. L. (2014a).
1122 Furocoumarins and coumarins photoinactivate *Colletotrichum acutatum* and
1123 *Aspergillus nidulans* fungi under solar radiation. *Journal of Photochemistry and*
1124 *Photobiology B: Biology*, 131, 74–83. <https://doi.org/10.1016/j.jphotobiol.2014.01.008>
- 1125 de Menezes, H. D., Rodrigues, G. B., Teixeira, S. de P., Massola, N. S., Bachmann,
1126 L., Wainwright, M., & Braga, G. Ú. L. (2014b). *In vitro* photodynamic inactivation of
1127 plant-pathogenic fungi *Colletotrichum acutatum* and *Colletotrichum gloeosporioides*
1128 with novel phenothiazinium photosensitizers. *Applied and Environmental Microbiology*,
1129 80(5), 1623–1632. <https://doi.org/10.1128/AEM.02788-13>
- 1130 de Menezes, H. D., Tonani, L., Bachmann L., Wainwright M., Braga, G. Ú. L., & Von
1131 Zeska Kress, M. R. (2016). Photodynamic treatment with phenothiazinium
1132 photosensitizers kills both ungerminated and germinated microconidia of the
1133 pathogenic fungi *Fusarium oxysporum*, *Fusarium moniliforme* and *Fusarium solani*.
1134 *Journal of Photochemistry and Photobiology B: Biology*, 164,1-12.
1135 <http://dx.doi.org/10.1016/j.jphotobiol.2016.09.008>
- 1136 de Oliveira, E. F., Tikekar, R., & Nitin, N. (2018a). Combination of aerosolized curcumin
1137 and UV-A light for the inactivation of bacteria on fresh produce surfaces. *Food*
1138 *Research International*, 114, 133–139. <https://doi.org/10.1016/j.foodres.2018.07.054>
- 1139 de Oliveira, E. F., Tosati, J. V., Tikekar, R. V., Monteiro, A. R., & Nitin, N. (2018b).
1140 Antimicrobial activity of curcumin in combination with light against *Escherichia coli*
1141 O157:H7 and *Listeria innocua* : Applications for fresh produce sanitation. *Postharvest*
1142 *Biology and Technology*, 137, 86–94.
1143 <https://doi.org/10.1016/j.postharvbio.2017.11.014>

- 1144 de Sordi, L., Butt, M. A., Pye, H., Kohoutova, D., Mosse, C. A., Yahioğlu, G., Stamati,
1145 I., Deonarain, M., Battah, S., Ready, D., Allan, E., Mullany, P., & Lovat, L. B. (2015).
1146 Development of photodynamic antimicrobial chemotherapy (PACT) for *Clostridium*
1147 *difficile*. *PLOS ONE*, 10(8), e0135039. <https://doi.org/10.1371/journal.pone.0135039>
- 1148 de Souza, T., Antonio, F., Zanotto, M., Homem-de-Mello, P., & Ribeiro, A. (2018).
1149 Photophysical and photochemical properties and aggregation behavior of
1150 phthalocyanine and naphthalocyanine derivatives. *Journal of the Brazilian Chemical*
1151 *Society*, 29(6), 1199–1209. <https://doi.org/10.21577/0103-5053.20170215>
- 1152 de Souza, L. M., Inada, N. M., Venturini, F. P., Carmona-Vargas, C. C., Pratavieira, S.,
1153 de Oliveira, K. T., Kurachi, C., & Bagnato, V. S. (2019). Photolarvicidal effect of
1154 curcuminoids from *Curcuma longa* Linn. against *Aedes aegypti* larvae. *Journal of Asia-*
1155 *Pacific Entomology*, 22(1), 151–158. <https://doi.org/10.1016/j.aspen.2018.12.016>
- 1156 Dementavicius, D., Lukseviciute, V., Gómez-López, V. M., & Lukšiene, Z. (2016).
1157 Application of mathematical models for bacterial inactivation curves using Hypericin-
1158 based photosensitization. *Journal of Applied Microbiology*, 120(6), 1492–1500.
1159 <https://doi.org/10.1111/jam.13127>
- 1160 Demidova, T. N., & Hamblin, M. R. (2004). Photodynamic therapy targeted to
1161 pathogens. *International Journal of Immunopathology and Pharmacology*, 17(3), 245–
1162 254. <https://doi.org/10.1177/039463200401700304>
- 1163 Demidova, T. N., & Hamblin, M. R. (2005). Photodynamic inactivation of *Bacillus*
1164 spores, mediated by phenothiazinium dyes. *Applied and Environmental Microbiology*,
1165 71(11), 6918–6925. <https://doi.org/10.1128/AEM.71.11.6918-6925.2005>
- 1166 Derosa, M. C., & Crutchley, R. J. (2002). Photosensitized singlet oxygen and its
1167 applications. *Coordination Chemistry Reviews*, 234, 351–371.
1168 [https://doi.org/10.1016/S0010-8545\(02\)00034-6](https://doi.org/10.1016/S0010-8545(02)00034-6)
- 1169 EFSA. (2015). The European Union summary report on trends and sources of
1170 zoonoses, zoonotic agents and food-borne outbreaks in 2014. *EFSA Journal*, 13(12).
1171 <https://doi.org/10.2903/j.efsa.2015.4329>
- 1172 Eichner, A., Gollmer, A., Späth, A., Bäumlner, W., Regensburger, J., König, B., &

- 1173 Maisch, T. (2015). Fast and effective inactivation of *Bacillus atrophaeus* endospores
1174 using light-activated derivatives of vitamin B2. *Photochemical & Photobiological*
1175 *Sciences*, 14(2), 387–396. <https://doi.org/10.1039/C4PP00285G>
- 1176 Eigner, D., & Scholz, D. (1999). *Ferula asa-foetida* and *Curcuma longa* in traditional
1177 medical treatment and diet in Nepal. *Journal of Ethnopharmacology*, 67(1), 1–6.
1178 [https://doi.org/10.1016/S0378-8741\(98\)00234-7](https://doi.org/10.1016/S0378-8741(98)00234-7)
- 1179 FAO. (2011). Food and Agricultural Organization. Global food losses and food waste
1180 – Extent, causes and prevention. Retrieved from <http://www.fao.org/3/a-i2697e.pdf>
- 1181 FDA. (2020). Food and Drug Administration. substances added to food (formerly
1182 EAFUS). Retrieved April 13, 2020, from
1183 <https://www.accessdata.fda.gov/scripts/fdcc/?set=FoodSubstances&id=FDCREDNO>
1184 3
- 1185 Ferrario, M. I., & Guerrero, S. N. (2018). Inactivation of *Alicyclobacillus acidoterrestris*
1186 ATCC 49025 spores in apple juice by pulsed light. Influence of initial contamination
1187 and required reduction levels. *Revista Argentina de Microbiologia*, 50(1), 3–11.
1188 <https://doi.org/10.1016/j.ram.2017.04.002>
- 1189 Feruszová, J., Imreová, P., Bodnárová, K., Ševcovicova, A., Kyzek, S., Chalupa, I.,
1190 Gálová, E., & Miadoková, E. (2016). Photoactivated hypericin is not genotoxic. *General*
1191 *Physiology and Biophysics*, 35(2), 223–230. https://doi.org/10.4149/gpb_2015045
- 1192 Fleet, G. H. (2007). Yeasts in foods and beverages: impact on product quality and
1193 safety. *Current Opinion in Biotechnology*, 18(2), 170–175.
1194 <https://doi.org/10.1016/j.copbio.2007.01.010>
- 1195 Fotinos, N., Convert, M., Piffaretti, J.-C., Gurny, R., & Lange, N. (2008). Effects on
1196 gram-negative and gram-positive bacteria mediated by 5-aminolevulinic acid and 5-
1197 aminolevulinic acid derivatives. *Antimicrobial Agents and Chemotherapy*, 52(4), 1366–
1198 1373. <https://doi.org/10.1128/AAC.01372-07>
- 1199 Fracarolli, L., Rodrigues, G. B., Pereira, A. C., Massola Júnior, N. S., Silva-Junior, G.
1200 J., Bachmann, L., Wainwright, M., Bastos, J. K., & Braga, G. U. L. (2016). Inactivation
1201 of plant-pathogenic fungus *Colletotrichum acutatum* with natural plant-produced

- 1202 photosensitizers under solar radiation. *Journal of Photochemistry and Photobiology B:*
1203 *Biology*, 162, 402–411. <https://doi.org/10.1016/j.jphotobiol.2016.07.009>
- 1204 Freire, F., Ferraresi, C., Jorge, A. O. C., & Hamblin, M. R. (2016). Photodynamic
1205 therapy of oral *Candida* infection in a mouse model. *Journal of Photochemistry and*
1206 *Photobiology B: Biology*, 159, 161–168.
1207 <https://doi.org/10.1016/j.jphotobiol.2016.03.049>
- 1208 Gábor, F., Szocs, K., Maillard, P., & Csík, G. (2001). Photobiological activity of
1209 exogenous and endogenous porphyrin derivatives in *Escherichia coli* and
1210 *Enterococcus hirae* cells. *Radiation and Environmental Biophysics*, 40(2), 145–151.
1211 <https://doi.org/10.1007/s004110100092>
- 1212 Galstyan, A., & Dobrindt, U. (2019). Determining and unravelling origins of reduced
1213 photoinactivation efficacy of bacteria in milk. *Journal of Photochemistry and*
1214 *Photobiology B: Biology*, 197, 111554.
1215 <https://doi.org/10.1016/j.jphotobiol.2019.111554>
- 1216 Gandin, E., Lion, Y., & Van de Vorst, A. (1983). Quantum yield of singlet oxygen
1217 production by xanthene derivatives. *Photochemistry and Photobiology*, 37(3), 271–
1218 278. <https://doi.org/10.1111/j.1751-1097.1983.tb04472.x>
- 1219 George, S., Hamblin, M. R., & Kishen, A. (2009). Uptake pathways of anionic and
1220 cationic photosensitizers into bacteria. *Photochemical & Photobiological Sciences*,
1221 8(6), 788. <https://doi.org/10.1039/b809624d>
- 1222 Ghate, V., Leong, A. L., Kumar, A., Bang, W. S., Zhou, W., & Yuk, H.-G. (2015).
1223 Enhancing the antibacterial effect of 461 and 521 nm light emitting diodes on selected
1224 foodborne pathogens in trypticase soy broth by acidic and alkaline pH conditions. *Food*
1225 *Microbiology*, 48, 49–57. <https://doi.org/10.1016/j.fm.2014.10.014>
- 1226 Ghate, V. S., Zhou, W., & Yuk, H. G. (2019). Perspectives and trends in the application
1227 of photodynamic inactivation for microbiological food safety. *Comprehensive Reviews*
1228 *in Food Science and Food Safety*, 18(2), 402–424. [https://doi.org/10.1111/1541-](https://doi.org/10.1111/1541-4337.12418)
1229 4337.12418
- 1230 Ghosh, S., Banerjee, S., & Sil, P. C. (2015). The beneficial role of curcumin on

- 1231 inflammation, diabetes and neurodegenerative disease: A recent update. *Food and*
1232 *Chemical Toxicology*, 83, 111–124. <https://doi.org/10.1016/j.fct.2015.05.022>
- 1233 Glueck, M., Schamberger, B., Eckl, P., & Plaetzer, K. (2017). New horizons in
1234 microbiological food safety: Photodynamic Decontamination based on a curcumin
1235 derivative. *Photochemical & Photobiological Sciences*, 16(12), 1784–1791.
1236 <https://doi.org/10.1039/C7PP00165G>
- 1237 Gonzales, F. P., da Silva, S. H., Roberts, D. W., & Braga, G. U. L. (2010).
1238 Photodynamic inactivation of conidia of the fungi *Metarhizium anisopliae* and
1239 *Aspergillus nidulans* with methylene blue and toluidine blue. *Photochemistry and*
1240 *Photobiology*, 86(3): 653-661. <https://doi.org/10.1111/j.1751-1097.2009.00689.x>
- 1241 Gonzales, J. C., Brancini, G. T. P., Rodrigues, G. B., Silva-Junior, G. J., Bachmann,
1242 L., Wainwright, M., & Braga, G. Ú. L. (2017). Photodynamic inactivation of conidia of
1243 the fungus *Colletotrichum abscissum* on *Citrus sinensis* plants with methylene blue
1244 under solar radiation. *Journal of Photochemistry and Photobiology B: Biology*, 176,
1245 54–61. <https://doi.org/10.1016/j.jphotobiol.2017.09.008>
- 1246 Hamblin, M. R. (2016). Antimicrobial photodynamic inactivation: a bright new technique
1247 to kill resistant microbes. *Current Opinion in Microbiology*, 33, 67–73.
1248 <https://doi.org/10.1016/j.mib.2016.06.008>
- 1249 Hamblin, M. R. (2017). Potentiation of antimicrobial photodynamic inactivation by
1250 inorganic salts. *Expert Review of Anti-Infective Therapy*, 15(11), 1059–1069.
1251 <https://doi.org/10.1080/14787210.2017.1397512>
- 1252 Havelaar, A. H., Kirk, M. D., Torgerson, P. R., Gibb, H. J., Hald, T., Lake, R. J., Praet,
1253 N., Bellinger, D. C., de Silva, N. R., Gargouri, N., Speybroeck, N., Cawthorne, A.,
1254 Mathers, C., Stein, C., Angulo, F. J., Devleeschauwer, B., Adegoke, G. O., Afshari,
1255 R., Alasfoor, D., Zeilmaker, M. (2015). World Health Organization Global Estimates
1256 and Regional Comparisons of the Burden of Foodborne Disease in 2010. *PLoS*
1257 *Medicine*, 12(12), p. 1001923. <https://doi.org/10.1371/journal.pmed.1001923>
- 1258 Helgason, E., Økstad, O. A., Caugant, D. A., Johansen, H. A., Fouet, A., Mock, M.,
1259 Hegna, I., & Kolstø, A. B. (2000). *Bacillus anthracis*, *Bacillus cereus*, and *Bacillus*

- 1260 *thuringiensis* – One species on the basis of genetic evidence. *Applied and*
1261 *Environmental Microbiology*, 66(6), 2627–2630.
1262 <https://doi.org/10.1128/AEM.66.6.2627-2630.2000>
- 1263 Hoebeke, M., & Damoiseau, X. (2002). Determination of the singlet oxygen quantum
1264 yield of bacteriochlorin a: a comparative study in phosphate buffer and aqueous
1265 dispersion of dimiristoyl-l- α -phosphatidylcholine liposomes. *Photochemical &*
1266 *Photobiological Sciences*, 1(4), 283–287. <https://doi.org/10.1039/b201081j>
- 1267 Huang, L., St. Denis, T. G., Xuan, Y., Huang, Y.Y., Tanaka, M., Zadlo, A., Sarna, T., &
1268 Hamblin, M. R. (2012). Paradoxical potentiation of methylene blue-mediated
1269 antimicrobial photodynamic inactivation by sodium azide: Role of ambient oxygen and
1270 azide radicals. *Free Radical Biology and Medicine*, 53(11), 2062–2071.
1271 <https://doi.org/10.1016/j.freeradbiomed.2012.09.006>
- 1272 Huang, Y.Y., Choi, H., Kushida, Y., Bhayana, B., Wang, Y., & Hamblin, M. R. (2016).
1273 Broad-spectrum antimicrobial effects of photocatalysis using titanium dioxide
1274 nanoparticles are strongly potentiated by addition of potassium iodide. *Antimicrobial*
1275 *Agents and Chemotherapy*, 60(9), 5445–5453. <https://doi.org/10.1128/AAC.00980-16>
- 1276 Huang, L., Szewczyk, G., Sarna, T., & Hamblin, M. R. (2017). Potassium iodide
1277 potentiates broad-spectrum antimicrobial photodynamic inactivation using photofrin.
1278 *ACS Infectious Diseases*, 3(4), 320–328. <https://doi.org/10.1021/acsinfecdis.7b00004>
- 1279 Huang, L., El-Husseini, A., Xuan, W., & Hamblin, M. R. (2018). Potentiation by
1280 potassium iodide reveals that the anionic porphyrin TPPS4 is a surprisingly effective
1281 photosensitizer for antimicrobial photodynamic inactivation. *Journal of Photochemistry*
1282 *and Photobiology B: Biology*, 178, 277–286.
1283 <https://doi.org/10.1016/j.jphotobiol.2017.10.036>
- 1284 Huang, J., Chen, B., Li, H., Zeng, Q.-H., Wang, J. J., Liu, H., Pan, Y., & Zhao, Y. (2020).
1285 Enhanced antibacterial and antibiofilm functions of the curcumin-mediated
1286 photodynamic inactivation against *Listeria monocytogenes*. *Food Control*, 108,
1287 106886. <https://doi.org/10.1016/j.foodcont.2019.106886>
- 1288 Iulietto, M. F., Sechi, P., Borgogni, E., & Cenci-Goga, B. T. (2015). Meat Spoilage: A

- 1289 Critical review of a neglected alteration due to ropy slime producing bacteria. *Italian*
1290 *Journal of Animal Science*, 14(3), 4011. <https://doi.org/10.4081/ijas.2015.4011>
- 1291 Jaffee, S., Henson, S., Unnevehr, L., Grace, D., & Cassou, E. (2019). The safe food
1292 imperative: accelerating progress in low- and middle-income countries. *Agriculture and*
1293 *Food Series*. Washington, DC: World Bank. License: Creative Commons Attribution
1294 CC BY 3.0 IGO. <https://doi:10.1596/978-1-4648-1345-0>
- 1295 Jesionek, A., & von Tappeiner, H. (1905). Zur behandlung der hautcarcinome mit
1296 fluorescierenden stoffen. *Arch Klin Med*, 82 (in German), 223.
- 1297 Jesus, V., Martins, D., Branco, T., Valério, N., Neves, M. G. P. M. S., Faustino, M. A.
1298 F., Reis, L., Barreal, E., Gallego, P. P., & Almeida, A. (2018). An insight into the
1299 photodynamic approach versus copper formulations in the control of *Pseudomonas*
1300 *syringae* pv. *Actinidiae* in kiwi plants. *Photochemical and Photobiological Sciences*,
1301 17(2), 180–191. <https://doi.org/10.1039/c7pp00300e>
- 1302 Josewin, S. W., Kim, M. J., & Yuk, H. G. (2018). Inactivation of *Listeria monocytogenes*
1303 and *Salmonella* spp. on cantaloupe rinds by blue light emitting diodes (LEDs). *Food*
1304 *Microbiology*, 76, 219–225. <https://doi.org/10.1016/j.fm.2018.05.012>
- 1305 Kairyte, K., Lapinskas, S., Gudelis, V., & Lukšiene, Ž. (2012). Effective inactivation of
1306 food pathogens *Listeria monocytogenes* and *Salmonella enterica* by combined
1307 treatment of hypericin-based photosensitization and high power pulsed light. *Journal*
1308 *of Applied Microbiology*, 112(6), 1144–1151. [https://doi.org/10.1111/j.1365-](https://doi.org/10.1111/j.1365-2672.2012.05296.x)
1309 [2672.2012.05296.x](https://doi.org/10.1111/j.1365-2672.2012.05296.x)
- 1310 Kashef, N., & Hamblin, M. R. (2017). Can microbial cells develop resistance to
1311 oxidative stress in antimicrobial photodynamic inactivation? *Drug Resistance Updates*,
1312 31(April), 31–42. <https://doi.org/10.1016/j.drup.2017.07.003>
- 1313 Kennedy, J. C., & Pottier, R. H. (1992). Endogenous protoporphyrin IX, a clinically
1314 useful photosensitizer for photodynamic therapy. *Journal of Photochemistry and*
1315 *Photobiology B: Biology*, 14(4), 275–292. [https://doi.org/10.1016/1011-](https://doi.org/10.1016/1011-1344(92)85108-7)
1316 [1344\(92\)85108-7](https://doi.org/10.1016/1011-1344(92)85108-7)
- 1317 Kim, D. K., & Kang, D. H. (2018). UVC LED irradiation effectively inactivates

- 1318 aerosolized viruses, bacteria, and fungi in a chamber-type air disinfection system.
1319 *Applied and Environmental Microbiology*, 84(17), 1–11.
1320 <https://doi.org/10.1128/AEM.00944-18>
- 1321 Kim, M. J., & Yuk, H.-G. (2017). Antibacterial mechanism of 405-nanometer light-
1322 emitting diode against Salmonella at refrigeration temperature. *Applied and*
1323 *Environmental Microbiology*, 83(5), 1–14. <https://doi.org/10.1128/AEM.02582-16>
- 1324 Koutsoumanis, K. (2009). Modeling food spoilage in microbial risk assessment. *Journal*
1325 *of Food Protection*, 72(2), 425–427. <https://doi.org/10.4315/0362-028x-72.2.425>
- 1326 Kumar, A., Ghate, V., Kim, M., Zhou, W., Hoon, G., & Yuk, H. (2015). Kinetics of
1327 bacterial inactivation by 405 nm and 520 nm light emitting diodes and the role of
1328 endogenous coproporphyrin on bacterial susceptibility. *Journal of Photochemistry &*
1329 *Photobiology, B: Biology*, 149, 37–44. <https://doi.org/10.1016/j.jphotobiol.2015.05.005>
- 1330 Le Marc, Y., Buchovec, I., George, S. M., Baranyi, J., & Lukšiene, Z. (2009). Modelling
1331 the photosensitization-based inactivation of *Bacillus cereus*. *Journal of Applied*
1332 *Microbiology*, 107(3), 1006–1011. <https://doi.org/10.1111/j.1365-2672.2009.04275.x>
- 1333 Lee, P. C. C., & Rodgers, M. A. J. (1987). Laser flash photokinetic studies of rose
1334 bengal sensitized photodynamic interactions of nucleotides and DNA. *Photochemistry*
1335 *and Photobiology*, 45(1), 79–86. <https://doi.org/10.1111/j.1751-1097.1987.tb08407.x>
- 1336 Lee, H. S., Park, H. H., & Min, S. C. (2020). Microbial decontamination of red pepper
1337 powder using pulsed light plasma. *Journal of Food Engineering*, 284, 110075.
1338 <https://doi.org/10.1016/j.jfoodeng.2020.110075>
- 1339 Liang, J.-Y., Yuann, J.-M. P., Cheng, C.-W., Jian, H.-L., Lin, C.-C., & Chen, L.-Y.
1340 (2013). Blue light induced free radicals from riboflavin on *E. coli* DNA damage. *Journal*
1341 *of Photochemistry and Photobiology B: Biology*, 119, 60–64.
1342 <https://doi.org/10.1016/j.jphotobiol.2012.12.007>
- 1343 Liang, J. Y., Cheng, C. W., Yu, C. H., & Chen, L. Y. (2015). Investigations of blue light-
1344 induced reactive oxygen species from flavin mononucleotide on inactivation of *E. coli*.
1345 *Journal of Photochemistry and Photobiology B: Biology*, 143, 82–88.
1346 <https://doi.org/10.1016/j.jphotobiol.2015.01.005>

- 1347 Lin, S., Hu, J., Tang, S., Wu, X., Chen, Z., & Tang, S. (2012). Photodynamic
1348 inactivation of methylene blue and tungsten-halogen lamp light against food pathogen
1349 *Listeria monocytogenes*. *Photochemistry and Photobiology*, 88(4), 985–991.
1350 <https://doi.org/10.1111/j.1751-1097.2012.01154.x>
- 1351 López-Carballo, G., Hernández-Muñoz, P., Gavara, R., & Ocio, M. J. (2008).
1352 Photoactivated chlorophyllin-based gelatin films and coatings to prevent microbial
1353 contamination of food products. *International Journal of Food Microbiology*, 126(1–2),
1354 65–70. <https://doi.org/10.1016/j.ijfoodmicro.2008.05.002>
- 1355 Lukšiene, Ž. (2005). New approach to inactivation of harmful and pathogenic
1356 microorganisms by photosensitization. *Food Technology and Biotechnology*, 43(4),
1357 411–418. <https://hrcak.srce.hr/110627>
- 1358 Lukšiene, Ž., & Brovko, L. (2013). Antibacterial photosensitization-based treatment for
1359 food safety. *Food Engineering Reviews*, 5(4), 185–199.
1360 <https://doi.org/10.1007/s12393-013-9070-7>
- 1361 Lukšiene, Ž., Buchovec, I., & Paskeviciute, E. (2009). Inactivation of food pathogen
1362 *Bacillus cereus* by photosensitization in vitro and on the surface of packaging material.
1363 *Journal of Applied Microbiology*, 107(6), 2037–2046. <https://doi.org/10.1111/j.1365-2672.2009.04383.x>
- 1365 Lukšiene, Ž., & Zukauskas, A. (2009). Prospects of photosensitization in control of
1366 pathogenic and harmful micro-organisms. *Journal of Applied Microbiology*, 107(5),
1367 1415–1424. <https://doi.org/10.1111/j.1365-2672.2009.04341.x>
- 1368 Machouart, M., Menir, P., Helenon, R., Quist, D., & Desbois, N. (2013). *Scytalidium*
1369 and scytalidiosis: What's new in 2012? *Journal de Mycologie Médicale*, 23(1), 40–46.
1370 <https://doi.org/10.1016/j.mycmed.2013.01.002>
- 1371 Maisch, T., Bosl, C., Szeimies, R.-M., Lehn, N., & Abels, C. (2005). Photodynamic
1372 effects of novel XF porphyrin derivatives on prokaryotic and eukaryotic cells.
1373 *Antimicrobial Agents and Chemotherapy*, 49(4), 1542–1552.
1374 <https://doi.org/10.1128/AAC.49.4.1542-1552.2005>
- 1375 Maisch, T., Eichner, A., Späth, A., Gollmer, A., König, B., Regensburger, J., & Bäumler,

- 1376 W. (2014). Fast and effective photodynamic inactivation of multiresistant bacteria by
1377 cationic riboflavin derivatives. *PLoS ONE*, 9(12).
1378 <https://doi.org/10.1371/journal.pone.0111792>
- 1379 Majiya, H., Adeyemi, O. O., Herod, M., Stonehouse, N. J., & Millner, P. (2018).
1380 Photodynamic inactivation of non-enveloped RNA viruses. *Journal of Photochemistry*
1381 *and Photobiology B: Biology*, 189, 87–94.
1382 <https://doi.org/10.1016/j.jphotobiol.2018.10.009>
- 1383 Majiya, H., Chowdhury, K. F., Stonehouse, N. J., & Millner, P. (2019). TMPyP
1384 functionalised chitosan membrane for efficient sunlight driven water disinfection.
1385 *Journal of Water Process Engineering*, 30, 100475.
1386 <https://doi.org/10.1016/j.jwpe.2017.08.013>
- 1387 Min, S. C., Roh, S. H., Niemira, B. A., Boyd, G., Sites, J. E., Uknalis, J., & Fan, X.
1388 (2017). In-package inhibition of *E. coli* O157:H7 on bulk Romaine lettuce using cold
1389 plasma. *Food Microbiology*, 65, 1–6. <https://doi.org/10.1016/j.fm.2017.01.010>
- 1390 Miñán, A., Lorente, C., Ipiña, A., Thomas, A. H., Fernández, M. L. de M., & Schilardi,
1391 P. L. (2015). Photodynamic inactivation induced by carboxypterin: a novel non-toxic
1392 bactericidal strategy against planktonic cells and biofilms of *Staphylococcus aureus*.
1393 *Biofouling*, 31(5), 459–468. <https://doi.org/10.1080/08927014.2015.1055731>
- 1394 Moreira, X., Santos, P., Faustino, M. A. F., Raposo, M. M. M., Costa, S. P. G., Moura,
1395 N. M. M., Gomes, A. T. P. C., Almeida, A., & Neves, M. G. P. M. S. (2020). An insight
1396 into the synthesis of cationic porphyrin-imidazole derivatives and their photodynamic
1397 inactivation efficiency against *Escherichia coli*. *Dyes and Pigments*, 178, 108330.
1398 <https://doi.org/10.1016/j.dyepig.2020.108330>
- 1399 Morton, C. A., Szeimies, R.-M., Sidoroff, A., & Braathen, L. R. (2013). European
1400 guidelines for topical photodynamic therapy part 1: treatment delivery and current
1401 indications - actinic keratoses, Bowen's disease, basal cell carcinoma. *Journal of the*
1402 *European Academy of Dermatology and Venereology*, 27(5), 536–544.
1403 <https://doi.org/10.1111/jdv.12031>
- 1404 Murav'eva, T. D., Dadeko, A. V., Kiselev, V. M., Kris'ko, T. K., Kislyakov, I. M., Kris'ko,

- 1405 A. V., Starodubtsev, A. M., Bagrov, I. V., Belousova, I. M., & Ponomarev, G. V. (2018).
1406 Comparative study of the photophysical properties of low-toxicity photosensitizers
1407 based on endogenous porphyrins. *Journal of Optical Technology*, 85(11), 709–721.
1408 <https://doi.org/10.1364/JOT.85.000709>
- 1409 Nishimura, T., Hara, K., Honda, N., Okazaki, S., Hazama, H., & Awazu, K. (2019).
1410 Determination and analysis of singlet oxygen quantum yields of talaporfin sodium,
1411 protoporphyrin IX, and lipidated protoporphyrin IX using near-infrared luminescence
1412 spectroscopy. *Lasers in Medical Science*. [https://doi.org/10.1007/s10103-019-02907-](https://doi.org/10.1007/s10103-019-02907-0)
1413 0
- 1414 Odeyemi, O. A., Alegbeleye, O. O., Strateva, M., & Stratev, D. (2020). Understanding
1415 spoilage microbial community and spoilage mechanisms in foods of animal origin.
1416 *Comprehensive Reviews in Food Science and Food Safety*, 19(2), 311–331.
1417 <https://doi.org/10.1111/1541-4337.12526>
- 1418 Okpanyi, S. N., Lidzba, H., Scholl, B. C., & Miltenburger, H. G. (1990). Genotoxicity of
1419 a standardized Hypericum extract. *Arzneimittelforschung*, 40(8), 851–855.
- 1420 Oliveira, A., Almeida, A., Carvalho, C. M. B., Tomé, J. P. C., Faustino, M. A. F., Neves,
1421 M. G. P. M. S., Tomé, A. C., Cavaleiro, J. A. S., & Cunha, Â. (2009). Porphyrin
1422 derivatives as photosensitizers for the inactivation of *Bacillus cereus* endospores.
1423 *Journal of Applied Microbiology*, 106(6), 1986–1995. [https://doi.org/10.1111/j.1365-](https://doi.org/10.1111/j.1365-2672.2009.04168.x)
1424 2672.2009.04168.x
- 1425 Otieno, W., Liu, C., Deng, H., Li, J., Zeng, X., & Ji, Y. (2020). Hypocrellin B-mediated
1426 photodynamic inactivation of gram-positive antibiotic-resistant bacteria: An *in vitro*
1427 study. *Photobiomodulation, Photomedicine, and Laser Surgery*, 38(1), 36–42.
1428 <https://doi.org/10.1089/photob.2019.4656>
- 1429 Ottaway P.B. (1993) Stability of vitamins in food. In: Ottaway P.B. (eds) *The*
1430 *Technology of Vitamins in Food*. Springer, Boston, MA. [https://doi.org/10.1007/978-1-](https://doi.org/10.1007/978-1-4615-2131-0_5)
1431 4615-2131-0_5
- 1432 Ozturk, I., Tunçel, A., Yurt, F., Biyiklioglu, Z., Ince, M., & Ocakoglu, K. (2020).
1433 Antifungal photodynamic activities of phthalocyanine derivatives on *Candida albicans*.

- 1434 *Photodiagnosis and Photodynamic Therapy*, 30, 101715.
1435 <https://doi.org/10.1016/j.pdpdt.2020.101715>
- 1436 Painter, J. A., Hoekstra, R. M., Ayers, T., Tauxe, R. V., Braden, C. R., Angulo, F. J., &
1437 Griffin, P. M. (2013). Attribution of foodborne illnesses, hospitalizations, and deaths to
1438 food commodities by using outbreak data, United States, 1998–2008. *Emerging*
1439 *Infectious Diseases*, 19(3), 407–415. <https://doi.org/10.3201/eid1903.111866>
- 1440 Paskeviciute, E., Zudyte, B., & Lukšiene, Ž. (2018). Towards better microbial safety of
1441 fresh produce: Chlorophyllin-based photosensitization for microbial control of
1442 foodborne pathogens on cherry tomatoes. *Journal of Photochemistry and*
1443 *Photobiology B: Biology*, 182, 130–136.
1444 <https://doi.org/10.1016/j.jphotobiol.2018.04.009>
- 1445 Paskeviciute, E., Zudyte, B., & Lukšiene, Ž. (2019). innovative nonthermal
1446 technologies: chlorophyllin and visible light significantly reduce microbial load on basil.
1447 *Food Technology and Biotechnology*, 57(1), 126–132.
1448 <https://doi.org/10.17113/ftb.57.01.19.5816>
- 1449 Paziani, M. H., Tonani, L., de Menezes, H. D., Bachmann, L., Wainwright, M., Braga,
1450 G. Ú. L., & von Zeska Kress, M. R. (2019). Antimicrobial photodynamic therapy with
1451 phenothiazinium photosensitizers in non-vertebrate model *Galleria mellonella* infected
1452 with *Fusarium keratoplasticum* and *Fusarium moniliforme*. *Photodiagnosis and*
1453 *Photodynamic Therapy*, 25, 197–203. <https://doi.org/10.1016/j.pdpdt.2018.12.010>
- 1454 Penha, C. B., Bonin, E., da Silva, A. F., Hioka, N., Zanqueta, É. B., Nakamura, T. U.,
1455 de Abreu Filho, B. A., Campanerut-Sá, P. A. Z., & Mikcha, J. M. G. (2017).
1456 Photodynamic inactivation of foodborne and food spoilage bacteria by curcumin. *LWT*
1457 - *Food Science and Technology*, 76, 198–202.
1458 <https://doi.org/10.1016/j.lwt.2016.07.037>
- 1459 Pereira, L. M., Mota, C. M., Baroni, L., Bronzon da Costa, C. M., Brochi, J. C. V.,
1460 Wainwright, M., Mineo, T. W. P., Braga, G. Ú. L., & Yatsuda, A. P. (2020). Inhibitory
1461 action of phenothiazinium dyes against *Neospora caninum*. *Scientific Reports*, 10(1),
1462 7483. <https://doi.org/10.1038/s41598-020-64454-x>

- 1463 Pereira, M. A., Faustino, M. A. F., Tomé, J. P. C., Neves, M. G. P. M. S., Tomé, A. C.,
1464 Cavaleiro, J. A. S., Cunha, Â., & Almeida, A. (2014). Influence of external bacterial
1465 structures on the efficiency of photodynamic inactivation by a cationic porphyrin.
1466 *Photochemical & Photobiological Sciences*, 13(4), 680.
1467 <https://doi.org/10.1039/c3pp50408e>
- 1468 Pineiro, M., Pereira, M. M., d'A Rocha Gonsalves, A. M., Arnaut, L. G., & Formosinho,
1469 S. J. (2001). Singlet oxygen quantum yields from halogenated chlorins: potential new
1470 photodynamic therapy agents. *Journal of Photochemistry and Photobiology A:
1471 Chemistry*, 138(2), 147–157. [https://doi.org/10.1016/S1010-6030\(00\)00382-8](https://doi.org/10.1016/S1010-6030(00)00382-8)
- 1472 Portapilla, G. B., Pereira, L. M., Bronzon da Costa, C. M., Voltarelli Providello, M.,
1473 Sampaio Oliveira, P. A., Goulart, A., Anchieta, N. F., Wainwright, M., Braga, G. Ú. L.,
1474 & Albuquerque, S. (2019). Phenothiazinium dyes are active against *Trypanosoma
1475 cruzi in vitro*. *BioMed Research International*, 2019, 1–9.
1476 <https://doi.org/10.1155/2019/8301569>
- 1477 Praditya, D., Kirchhoff, L., Brüning, J., Rachmawati, H., Steinmann, J., & Steinmann,
1478 E. (2019). Anti-infective properties of the golden spice curcumin. *Frontiers in
1479 Microbiology*, 10:912. <https://doi.org/10.3389/fmicb.2019.00912>
- 1480 Raab, O. (1900). Über die wirkung fluoreszcierender stoffe aus infusorien. *Ztg. Biol.*,
1481 39, 524.
- 1482 Randazzo, W., Aznar, R., & Sánchez, G. (2016). Curcumin-mediated photodynamic
1483 inactivation of norovirus surrogates. *Food and Environmental Virology*, 8(4), 244–250.
1484 <https://doi.org/10.1007/s12560-016-9255-3>
- 1485 Remenant, B., Jaffrès, E., Dousset, X., Pilet, M.-F., & Zagorec, M. (2015). Bacterial
1486 spoilers of food: Behavior, fitness and functional properties. *Food Microbiology*, 45,
1487 45–53. <https://doi.org/10.1016/j.fm.2014.03.009>
- 1488 Reverter-Carrión, L., Saucedo-Gálvez, J. N., Codina-Torrella, I., Hernández-Herrero,
1489 M. M., Gervilla, R., & Roig-Sagués, A. X. (2018). Inactivation study of *Bacillus subtilis*,
1490 *Geobacillus stearothermophilus*, *Alicyclobacillus acidoterrestris* and *Aspergillus niger*
1491 spores under Ultra-High Pressure Homogenization, UV-C light and their combination.

- 1492 *Innovative Food Science and Emerging Technologies*, 48, 258–264.
1493 <https://doi.org/10.1016/j.ifset.2018.06.011>
- 1494 Rodrigues, G. B., Ferreira, L. K. S., Wainwright, M., & Braga, G. U. L. (2012a).
1495 Susceptibilities of the dermatophytes *Trichophyton mentagrophytes* and *T. rubrum*
1496 microconidia to photodynamic antimicrobial chemotherapy with novel phenothiazinium
1497 photosensitizers and red light. *Journal of Photochemistry & Photobiology, B: Biology*,
1498 116, 89–94. <https://doi.org/10.1016/j.jphotobiol.2012.08.010>
- 1499 Rodrigues, G. B., Primo, F. L., Tedesco, A. C., & Braga, G. U. L. (2012b). *In vitro*
1500 photodynamic inactivation of *Cryptococcus neoformans* melanized cells with
1501 chloroaluminum phthalocyanine nanoemulsion. *Photochemistry and Photobiology*,
1502 88, 440–447. <https://doi.org/10.1111/j.1751-1097.2011.01055.x>
- 1503 Rodrigues, G. B., Dias-Baruffi, M., Holman, N., Wainwright, M., & Braga, G. U. L.
1504 (2013). *In vitro* photodynamic inactivation of *Candida* species and mouse fibroblasts
1505 with phenothiazinium photosensitisers and red light. *Photodiagnosics and*
1506 *Photodynamic Therapy*, 10(2), 141-149. <https://doi.org/10.1016/j.pdpdt.2012.11.004>
- 1507 Rodrigues, G. B., Brancini, G. T. P., Pinto, M. R., Primo, F. L., Wainwright, M.,
1508 Tedesco, A. C., & Braga, G. Ú. L. (2020). Photodynamic inactivation of *Candida*
1509 *albicans* and *Candida tropicalis* with aluminum phthalocyanine chloride nanoemulsion.
1510 *Fungal Biology*, 124(5), 297-303. <https://doi.org/10.1016/j.funbio.2019.08.004>
- 1511 Romanova, N. A., Brovko, L. Y., Moore, L., Pometun, E., Savitsky, A. P., Ugarova, N.
1512 N., & Griffiths, M. W. (2003). Assessment of photodynamic destruction of *Escherichia*
1513 *coli* O157:H7 and *Listeria monocytogenes* by using ATP bioluminescence. *Applied and*
1514 *Environmental Microbiology*, 69(11), 6393–6398.
1515 <https://doi.org/10.1128/AEM.69.11.6393-6398.2003>
- 1516 Santos, A. R., Batista, A. F. P., Gomes, A. T. P. C., Neves, M. G. P. M. S., Faustino,
1517 M. A. F., Almeida, A., Hioka, N., & Mikcha, J. M. G. (2019). The remarkable effect of
1518 potassium iodide in eosin and rose bengal photodynamic action against *Salmonella*
1519 *Typhimurium* and *Staphylococcus aureus*. *Antibiotics*, 8(4).
1520 <https://doi.org/10.3390/antibiotics8040211>

- 1521 Santos, A. R., da Silva, A. F., Batista, A. F. P., Freitas, C. F., Bona, E., Sereia, M. J.,
1522 Caetano, W., Hioka, N., & Mikcha, J. M. G. (2020). Application of response surface
1523 methodology to evaluate photodynamic inactivation mediated by Eosin Y and 530 nm
1524 LED against *Staphylococcus aureus*. *Antibiotics*, 9(3), 125.
1525 <https://doi.org/10.3390/antibiotics9030125>
- 1526 Saúde, Ministério da. (2019a). Surtos de Doenças Transmitidas por Alimentos no
1527 Brasil. Informe 2018. SINAN/SVS/Ministério da Saúde. Retrieved April 18, 2020, from
1528 [https://www.saude.gov.br/images/pdf/2019/maio/17/Apresentacao-Surtos-DTA-Maio-](https://www.saude.gov.br/images/pdf/2019/maio/17/Apresentacao-Surtos-DTA-Maio-2019.pdf)
1529 [2019.pdf](https://www.saude.gov.br/images/pdf/2019/maio/17/Apresentacao-Surtos-DTA-Maio-2019.pdf)
- 1530 Saúde, Ministério da. (2019b). Doenças transmitidas por alimentos. Retrieved April 18,
1531 2020, from [https://www.saude.gov.br/saude-de-a-z/doencas-transmitidas-por-](https://www.saude.gov.br/saude-de-a-z/doencas-transmitidas-por-alimentos)
1532 [alimentos](https://www.saude.gov.br/saude-de-a-z/doencas-transmitidas-por-alimentos)
- 1533 Schneider, J. E., Price, S., Maitt, L., Gutteridge, J. M. C., & Floyd, R. A. (1990).
1534 Methylene blue plus light mediates 8-hydroxy 2'-deoxyguanosine formation in DNA
1535 preferentially over strand breakage. *Nucleic Acids Research*, 18(3), 631–635.
1536 <https://doi.org/10.1093/nar/18.3.631>
- 1537 Schuyler, R. (2001). Use of riboflavin for photoinactivation of pathogens in blood
1538 components. *Transfusion and Apheresis Science*, 25(3), 189–190.
1539 [https://doi.org/10.1016/S1473-0502\(01\)00119-7](https://doi.org/10.1016/S1473-0502(01)00119-7)
- 1540 Sepúlveda, A. A. L., Arenas Velásquez, A. M., Patiño Linares, I. A., de Almeida, L.,
1541 Fontana, C. R., Garcia, C., & Graminha, M. A. S. (2020). Efficacy of photodynamic
1542 therapy using TiO₂ nanoparticles doped with Zn and hypericin in the treatment of
1543 cutaneous Leishmaniasis caused by *Leishmania amazonensis*. *Photodiagnosis and*
1544 *Photodynamic Therapy*, 30, 101676. <https://doi.org/10.1016/j.pdpdt.2020.101676>
- 1545 Silva, A. F., Borges, A., Giaouris, E., Mikcha, J. M. G., & Simões, M. (2018).
1546 Photodynamic inactivation as an emergent strategy against foodborne pathogenic
1547 bacteria in planktonic and sessile states. *Critical Reviews in Microbiology*, 44(6), 667–
1548 684. <https://doi.org/10.1080/1040841X.2018.1491528>
- 1549 Silva, A. F., Santos, A. R., Trevisan, D. A. C., Bonin, E., Freitas, C. F., Batista, A. F.

- 1550 P., Hioka, N., Simões, M., & Mikcha, J. M. G. (2019). Xanthene dyes and green LED
1551 for the inactivation of foodborne pathogens in planktonic and biofilm states.
1552 *Photochemistry and Photobiology*, 95(5), 1230–1238.
1553 <https://doi.org/10.1111/php.13104>
- 1554 Silva, A. R. da, Pelegrino, A. C., Tedesco, A. C., & Jorge, R. A. (2008). Photodynamic
1555 activity of chloro(5,10,15,20-tetraphenylporphyrinato)indium(III). *Journal of the*
1556 *Brazilian Chemical Society*, 19(3), 491–501. [https://doi.org/10.1590/S0103-](https://doi.org/10.1590/S0103-50532008000300017)
1557 [50532008000300017](https://doi.org/10.1590/S0103-50532008000300017)
- 1558 Simões, C., Gomes, M. C., Neves, M. G. P. M. S., Cunha, A., Tomé, J. P. C., Tomé,
1559 A. C., Cavaleiro, J. A. S., Almeida, A., & Faustino, M. A. F. (2016). Photodynamic
1560 inactivation of *Escherichia coli* with cationic meso-tetraarylporphyrins - The charge
1561 number and charge distribution effects. *Catalysis Today*, 266, 197–204.
1562 <https://doi.org/10.1016/j.cattod.2015.07.031>
- 1563 St Denis, T. G., Vecchio, D., Zadlo, A., Rineh, A., Sadasivam, M., Avci, P., Huang, L.,
1564 Kozinska, A., Chandran, R., Sarna, T., & Hamblin, M. R. (2013). Thiocyanate
1565 potentiates antimicrobial photodynamic therapy: In situ generation of the sulfur trioxide
1566 radical anion by singlet oxygen. *Free Radical Biology and Medicine*, 65, 800–810.
1567 <https://doi.org/10.1016/j.freeradbiomed.2013.08.162>
- 1568 Stevenson, A., Cray, J. A., Williams, J. P., Santos, R., Sahay, R., Neuenkirchen, N.,
1569 McClure, C. D., Grant, I. R., Houghton, J. D. R., Quinn, J. P., Timson, D. J., Patil, S.
1570 V., Singhal, R. S., Antón, J., Dijksterhuis, J., Hocking, A. D., Lievens, B., Rangel, D. E.
1571 N., Voytek, M. A., Gunde-Cimerman, N., Oren, A., Timmis, K. N., McGenity, T. J., &
1572 Hallsworth, J. E. (2015). Is there a common water-activity limit for the three domains
1573 of life? *The ISME Journal*, 9(6), 1333–1351. <https://doi.org/10.1038/ismej.2014.219>
- 1574 Tao, R., Zhang, F., Tang, Q.J, Xu, C.S, Ni, Z. J., & Meng, X.H. (2019). Effects of
1575 curcumin-based photodynamic treatment on the storage quality of fresh-cut apples.
1576 *Food Chemistry*, 274, 415–421. <https://doi.org/10.1016/j.foodchem.2018.08.042>
- 1577 Temba, B. A., Fletcher, M. T., Fox, G. P., Harvey, J., Okoth, S. A., & Sultanbawa, Y.
1578 (2019). Curcumin-based photosensitization inactivates *Aspergillus flavus* and reduces
1579 aflatoxin B1 in maize kernels. *Food Microbiology*, 82, 82–88.

- 1580 <https://doi.org/10.1016/j.fm.2018.12.013>
- 1581 Tomé, J. P. C., Neves, M. G. P. M. S., Tomé, A. C., Cavaleiro, J. A. S., Soncin, M.,
1582 Magaraggia, M., Ferro, S., & Jori, G. (2004). Synthesis and antibacterial activity of new
1583 Poly-S-lysine–Porphyrin conjugates. *Journal of Medicinal Chemistry*, 47(26), 6649–
1584 6652. <https://doi.org/10.1021/jm040802v>
- 1585 Tonani, L., Morosini, N. S., Dantas de Menezes, H., Nadaletto Bonifácio da Silva, M.
1586 E., Wainwright, M., Leite Braga, G. Ú., & von Zeska Kress, M. R. (2018). *In vitro*
1587 susceptibilities of *Neoscytalidium* spp. sequence types to antifungal agents and
1588 antimicrobial photodynamic treatment with phenothiazinium photosensitizers. *Fungal*
1589 *Biology*, 122(6), 436–448. <https://doi.org/10.1016/j.funbio.2017.08.009>
- 1590 Tosati, J. V., de Oliveira, E. F., Oliveira, J. V., Nitin, N., & Monteiro, A. R. (2018). Light-
1591 activated antimicrobial activity of turmeric residue edible coatings against cross-
1592 contamination of *Listeria innocua* on sausages. *Food Control*, 84, 177–185.
1593 <https://doi.org/10.1016/j.foodcont.2017.07.026>
- 1594 Uchoa, A. F., Konopko, A. M., & Baptista, M. S. (2015). Chlorophyllin derivatives as
1595 photosensitizers: synthesis and photodynamic properties. *Journal of the Brazilian*
1596 *Chemical Society*, 26(12), 2615–2622. <https://doi.org/10.5935/0103-5053.20150290>
- 1597 Vatansever, F., de Melo, W.C.M.A., Avci, P., Vecchio, D., Sadasivam, M., Gupta, A.,
1598 Chandran, R., Karimi, M., Parizotto, N.A, Yin, R., Tegos, G.P., & Hamblin, M.R. (2013).
1599 Antimicrobial strategies centered around reactive oxygen species – bactericidal
1600 antibiotics, photodynamic therapy, and beyond. *FEMS Microbiology Reviews*, 37(6),
1601 955–989. <https://doi.org/10.1111/1574-6976.12026>
- 1602 Vecchio, D., Gupta, A., Huang, L., Landi, G., Avci, P., Rodas, A., & Hamblin, M. R.
1603 (2015). Bacterial photodynamic inactivation mediated by methylene blue and red light
1604 is enhanced by synergistic effect of potassium iodide. *Antimicrobial Agents and*
1605 *Chemotherapy*, 59(9), 5203–5212. <https://doi.org/10.1128/AAC.00019-15>
- 1606 Vieira, C., Gomes, A. T. P. C., Mesquita, M. Q., Moura, N. M. M., Neves, G. P. M. S.,
1607 Faustino, A. F., & Almeida, A. (2018). An insight into the potentiation effect of
1608 potassium iodide on APDT efficacy. *Frontiers in Microbiology*, 9, 1–16.

- 1609 <https://doi.org/10.3389/fmicb.2018.02665>
- 1610 Vieira, C., Santos, A., Mesquita, M. Q., Gomes, A. T. P. C., Neves, M. G. P. M. S.,
1611 Faustino, M. A. F., & Almeida, A. (2019). Advances in aPDT based on the combination
1612 of a porphyrinic formulation with potassium iodide: Effectiveness on bacteria and fungi
1613 planktonic/biofilm forms and viruses. *Journal of Porphyrins and Phthalocyanines*,
1614 23(4–5), 534–545. <https://doi.org/10.1142/S1088424619500408>
- 1615 Wainwright, M. (2004). Photoinactivation of viruses. *Photochemical & Photobiological*
1616 *Sciences*, 3(5), 406. <https://doi.org/10.1039/b311903n>
- 1617 Wainwright, M., Phoenix, D. A., Marland, J., Wareing, D. R. A., & Bolton, F. J. (1997).
1618 A study of photobactericidal activity in the phenothiazinium series. *FEMS Immunology*
1619 *& Medical Microbiology*, 19(1), 75–80. [https://doi.org/10.1111/j.1574-](https://doi.org/10.1111/j.1574-695X.1997.tb01074.x)
1620 [695X.1997.tb01074.x](https://doi.org/10.1111/j.1574-695X.1997.tb01074.x)
- 1621 Wainwright, M. (1998). Photodynamic antimicrobial chemotherapy (PACT). *The*
1622 *Journal of Antimicrobial Chemotherapy*, 42(1), 13–28.
1623 <https://doi.org/10.1093/jac/42.1.13>
- 1624 Wainwright, M, Phoenix, D. A., Laycock, S. L., Wareing, D. R. A., & Wright, P. A.
1625 (1998). Photobactericidal activity of phenothiazinium dyes against methicillin-resistant
1626 strains of *Staphylococcus aureus*. *FEMS Microbiology Letters*, 160(2), 177–181.
1627 <https://doi.org/10.1111/j.1574-6968.1998.tb12908.x>
- 1628 Wainwright, Mark, Maisch, T., Nonell, S., Plaetzer, K., Almeida, A., Tegos, G. P., &
1629 Hamblin, M. R. (2017). Photoantimicrobials—are we afraid of the light? *The Lancet*
1630 *Infectious Diseases*, 17(2), e49–e55. [https://doi.org/10.1016/S1473-3099\(16\)30268-7](https://doi.org/10.1016/S1473-3099(16)30268-7)
- 1631 Wainwright, Mark, Smalley, H., Scully, O., & Lotfipour, E. (2012). Comparative
1632 photodynamic evaluation of new phenothiazinium derivatives against
1633 *Propionibacterium acnes*. *Photochemistry and Photobiology*, 88(3), 523–526.
1634 <https://doi.org/10.1111/j.1751-1097.2011.01021.x>
- 1635 Wen, X., Zhang, X., Szewczyk, G., El-Hussein, A., Huang, Y.-Y., Sarna, T., & Hamblin,
1636 M. R. (2017). Potassium iodide potentiates antimicrobial photodynamic inactivation
1637 mediated by rose bengal in *in vitro* and *in vivo* studies. *Antimicrobial Agents and*

- 1638 *Chemotherapy*, 61(7), 1–15. <https://doi.org/10.1128/AAC.00467-17>
- 1639 WHO. (2015). World Health Organization. WHO estimates of the global burden of
1640 foodborne diseases. Retrieved May 25, 2020, from
1641 [https://apps.who.int/iris/bitstream/handle/10665/199350/9789241565165_eng.pdf?se](https://apps.who.int/iris/bitstream/handle/10665/199350/9789241565165_eng.pdf?sequence=1)
1642 [quence=1](https://apps.who.int/iris/bitstream/handle/10665/199350/9789241565165_eng.pdf?sequence=1)
- 1643 WHO. (2018). World Health Organization. Antimicrobial resistance. Retrieved April 19,
1644 2020, from <https://www.who.int/news-room/fact-sheets/detail/antimicrobial-resistance>
- 1645 Wiegell, S. R., Hædersdal, M., Philipsen, P. A., Eriksen, P., Enk, C. D., & Wulf, H. C.
1646 (2008). Continuous activation of PpIX by daylight is as effective as and less painful
1647 than conventional photodynamic therapy for actinic keratoses; a randomized,
1648 controlled, single-blinded study. *British Journal of Dermatology*, 158(4), 740–746.
1649 <https://doi.org/10.1111/j.1365-2133.2008.08450.x>
- 1650 Wilkinson, F., Helman, W. P., & Ross, A. B. (1993). Quantum yields for the
1651 photosensitized formation of the lowest electronically excited singlet state of molecular
1652 oxygen in solution. *Journal of Physical and Chemical*, 22(1), 113–262.
1653 <https://doi.org/10.1063/1.555934>
- 1654 Wilson, B. C., & Patterson, M. S. (2008). The physics, biophysics and technology of
1655 photodynamic therapy. *Physics in Medicine and Biology*, 53(9), R61–R109.
1656 <https://doi.org/10.1088/0031-9155/53/9/R01>
- 1657 Wu, J., Xu, H., Tang, W., Kopelman, R., Philbert, M. A., & Xi, C. (2009). Eradication of
1658 bacteria in suspension and biofilms using methylene blue-loaded dynamic
1659 nanoplateforms. *Antimicrobial Agents and Chemotherapy*, 53(7), 3042–3048.
1660 <https://doi.org/10.1128/AAC.01604-08>
- 1661 Wu, J., Hou, W., Cao, B., Zuo, T., Xue, C., Leung, A. W., Xu, C., & Tang, Q. J. (2015).
1662 Virucidal efficacy of treatment with photodynamically activated curcumin on murine
1663 norovirus bio-accumulated in oysters. *Photodiagnosis and Photodynamic Therapy*,
1664 12(3), 385–392. <https://doi.org/10.1016/j.pdpdt.2015.06.005>
- 1665 Wu, X., Huang, Y.-Y., Kushida, Y., Bhayana, B., & Hamblin, M. R. (2016). Broad-
1666 spectrum antimicrobial photocatalysis mediated by titanium dioxide and UVA is

- 1667 potentiated by addition of bromide ion via formation of hypobromite. *Free Radical*
1668 *Biology and Medicine*, 95, 74–81. <https://doi.org/10.1016/j.freeradbiomed.2016.03.012>
- 1669 Yang, M., Yang, T., & Mao, C. (2019). Enhancement of photodynamic cancer therapy
1670 by physical and chemical factors. *Angewandte Chemie*, 58(40), 14066–14080.
1671 <https://doi.org/10.1002/anie.201814098>
- 1672 Yassunaka, N. N., de Freitas, C. F., Rabello, B. R., Santos, P. R., Caetano, W., Hioka,
1673 N., Nakamura, T. U., de Abreu Filho, B. A., & Mikcha, J. M. G. (2015). Photodynamic
1674 inactivation mediated by erythrosine and its derivatives on foodborne pathogens and
1675 spoilage bacteria. *Current Microbiology*. <https://doi.org/10.1007/s00284-015-0827-5>
- 1676 Yuan, L., Lyu, P., Huang, Y. Y., Du, N., Qi, W., Hamblin, M. R., & Wang, Y. (2020).
1677 Potassium iodide enhances the photobactericidal effect of methylene blue on
1678 *Enterococcus faecalis* as planktonic cells and as biofilm infection in teeth. *Journal of*
1679 *Photochemistry and Photobiology B: Biology*, 203, 111730.
1680 <https://doi.org/10.1016/j.jphotobiol.2019.111730>
- 1681 Zhang, Y., Dai, T., Wang, M., Vecchio, D., Chiang, L. Y., & Hamblin, M. R. (2015).
1682 Potentiation of antimicrobial photodynamic inactivation mediated by a cationic
1683 fullerene by added iodide: *In vitro* and *in vivo* studies. *Nanomedicine*, 10(4), 603–614.
1684 <https://doi.org/10.2217/nnm.14.131>
- 1685 Žudyte, B., & Lukšiene, Ž. (2019). Toward better microbial safety of wheat sprouts:
1686 Chlorophyllin-based photosensitization of seeds. *Photochemical and Photobiological*
1687 *Sciences*, 18(10), 2521–2530. <https://doi.org/10.1039/c9pp00157c>

1 **Capítulo 2 – Inactivation kinetics of *Bacillus cereus* vegetative cells**
2 **and spores from different sources by antimicrobial photodynamic**
3 **treatment (aPDT)**

4
5 Leonardo do Prado-Silva^a, Verônica O. Alvarenga^b, Gilberto Ú.L. Braga^c, Anderson
6 S. Sant'Ana^a

7
8 ^aDepartment of Food Science, Faculty of Food Engineering, University of Campinas
9 (UNICAMP), Campinas, SP, Brazil

10 ^bDepartment of Food, Faculty of Pharmacy - Federal University of Minas Gerais, Belo
11 Horizonte, MG, Brazil

12 ^cDepartment of Clinical, Toxicological and Bromatological Analysis, School of
13 Pharmaceutical Sciences of Ribeirão Preto, University of São Paulo, Ribeirão Preto,
14 SP, Brazil

15

16

17 Capítulo formatado de acordo com as normas de submissão da revista:

18 ***LWT – Food Science and Technology.***

19 **Abstract**

20 Antimicrobial photodynamic treatment (aPDT) is a promising alternative to
21 conventional thermal inactivation methods. This study aimed to evaluate the
22 inactivation of *Bacillus cereus* vegetative cells and spores by aPDT with new
23 methylene blue (NMB) as photosensitizer (PS) using red light. The efficacy of aPDT
24 was determined, initially by minimal inhibitory concentration (MIC) of NMB at different
25 concentrations and fluences. Cluster analysis from the results of MIC grouped *B.*
26 *cereus* strains according to their aPDT resistance. Then, four strains (B63, B3, 436,
27 and ATCC 14579) were selected for a survival study of aPDT with NMB in three
28 concentrations (5, 50, and 100 μM). The viability of *B. cereus* vegetative cells and
29 spores was reduced in all tested fluences. The strain ATCC 14579 (vegetative cells
30 and spores) was the most susceptible to aPDT at relatively low fluence (25 J/cm^2). The
31 Weibull model presented a good fit for the inactivation data estimating the kinetic
32 parameters δ (first decimal reduction) and p (shape parameter). This study contributes
33 to the knowledge on the behavior of different strains of *B. cereus* regarding an
34 emerging method of microbial inactivation. The variability of inactivation among strains
35 will allow the development of more reliable processes.

36

37 **Keywords:** Emerging technology, Nonthermal treatment, Pathogen, Spoilage,
38 Phenothiazine dye

39 **Research Highlights**

- 40 ○ Antimicrobial photodynamic treatment (aPDT) for inactivation of *B. cereus* is
- 41 effective
- 42 ○ Cluster analysis grouped strains according to aPDT resistance
- 43 ○ Variability among the strains of the same origin was observed
- 44 ○ The Weibull model was able to estimate the inactivation kinetic parameters of
- 45 aPDT

46 **1. Introduction**

47

48 The contamination of foods with pathogens is responsible for mortality and
49 morbidity that impact on people's lives, countries' economies, and in social
50 development (WHO, 2015). According to the Center for Disease Control and
51 Prevention (CDC) from the United States, 1 in 6 Americans get sick from food
52 poisoning each year (CDC, 2020). *Bacillus cereus* is a Gram-positive spore-forming
53 rod-shaped bacterium commonly found in soil environments and associated with
54 foodborne illnesses and food spoilage (Spanu, 2016). Food poisonings caused by *B.*
55 *cereus* is mainly characterized by vomiting (emetic toxin) and diarrhea (enterotoxin)
56 (Bottone, 2010). In dairy products, *B. cereus* can also cause food spoilage by the
57 production of lipase, proteinase, and phospholipases that causes off-flavour,
58 coagulation, and bitterness (Heyndrickx, 2011; Mehta, Metzger, Hassan, Nelson, &
59 Patel, 2019; Spanu, 2016).

60 Food industries seek for nonthermal and environmentally friendly alternatives to
61 reduce or avoid the contamination of the products and, consequently, to diminish
62 foodborne diseases. Antimicrobial photodynamic treatment (aPDT) is a promising
63 technology that can effectively reduce microbial counts from the surface of foods and
64 related materials (Gonzales et al., 2017; Luksiene, Buchovec, & Paskeviciute, 2009).

65 Mostly, the microbial inactivation is obtained through thermal and chemical
66 treatment and controlled by good manufacturing, transportation, and storage practices.
67 Even though conventional thermal methodologies are effective, it is known that they
68 cause undesirable effects as losses in the sensory and nutritional quality of food (Barba
69 et al., 2017; Uchida & Silva, 2017). Besides that, the use of chemical products as
70 sanitizers is not considered environmentally friendly also being harmful to humans
71 (Ölmez & Kretzschmar, 2009).

72 The mechanism of action of aPDT is based on the combination of three nontoxic
73 components: visible light, oxygen and a photosensitizer (PS). Visible light with the
74 appropriate wavelength excites the PS molecule to a high-energy electronic state. This
75 excited state reacts with the oxygen molecules nearby producing reactive oxygen
76 species (ROS) such as singlet oxygen, superoxide, and radicals (Demidova &

77 Hamblin, 2005). These cytotoxic compounds produced can oxidize many
78 biomolecules, such as proteins, lipids, and nucleic acids causing cell death (Almeida,
79 Faustino, & Tomé, 2015; Brancini et al., 2016; Tonani et al., 2018; Žudyte & Lukšiene,
80 2019).

81 aPDT has been known since the mid-1900s as a treatment capable to reduce
82 microbial counts after light exposition in the presence of dyes (Wainwright, 1998).
83 Some studies have investigated the effect of different classes of PS as well light source
84 on the reduction of microbial contamination (Buchovec, Vaitonis, & Luksiene, 2009;
85 Demidova & Hamblin, 2005; Le Marc, Buchovec, George, Baranyi, & Luksiene, 2009;
86 Oliveira et al., 2009). It has been demonstrated the efficiency of aPDT with
87 phenothiazinium dyes, such as toluidine blue O (TBO), methylene blue (MB) and new
88 methylene blue (NMB), against *B. cereus* spores and vegetative cells (Demidova &
89 Hamblin, 2005). Therefore, *B. cereus* comprises an interesting microorganism to be
90 employed as a model for aPDT.

91 The current work aimed to evaluate the efficiency of aPDT using NMB and red
92 light against *B. cereus* vegetative cells and spores from different sources. Also, this
93 study also estimated the aPDT inactivation kinetics for both forms of selected strains
94 using the Weibull model. Also, when possible the fluence for 4D (fluence needed for
95 four decimal reductions) was calculated.

2. Material and methods

2.1 Bacterial strains, cultivation and preparation of spore suspensions

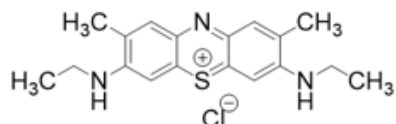
All strains of *B. cereus* (n = 12) used in this study were obtained from Fundação Oswaldo Cruz (Rio de Janeiro, Brazil). The strains used were isolated from the following sources: ATCC 14579 – “**Standard strain**”; 432 and 436 – “**Chocolate**”; 511, 512, 540 – “**Dairy products**”; B3 and B94 – “**Milk**”; B18 – “**Starch**”; B51 – “**Meat**”; B63 – “**Ready meal**”; and B86 – “**Corn flour**”. Cells were grown in nutrient broth (Kasvi, Italy) at 30 °C for 48 h, after centrifugation (Sorvall Legend XTR, Thermo Fisher Scientific, Waltham, MI, USA) the pure cells were stored at – 80 °C (Revco EXF, Thermo Fisher Scientific, Marietta, OH, USA) in cryotubes with 20% (w/w) glycerol until further use.

The spore suspensions were prepared according to Pflug (1999) and confirmed by Alvarenga et al., 2018. Briefly, roux bottles were filled with approximately 200 mL of nutrient agar (Kasvi, Italy) supplemented with manganese sulfate (10 ppm) (Synth, Diadema, Brazil). After inoculation, the roux bottles were incubated at 30 °C for 30 days. The sporulation progress was frequently microscopically observed with malachite green staining to evaluate the spore formation. After such a period of incubation, the suspensions were gently collected scraping the agar surface with sterile deionized water followed by centrifugation (1500 x g for 20 min at 4 °C). After five rounds of centrifugation, the spore suspensions were resuspended in sterile deionized water and heat-shocked (80 °C for 30 min) to kill any vegetative cells and enumerate the initial concentration of the spores and, finally, stored at – 20 °C until further use.

2.2 Photosensitizer

The phenothiazinium dye new methylene blue N zinc chloride double salt (NMB; Fig. 1) was purchased from Sigma-Aldrich, Inc. (St. Louis, MO, USA). A stock solution at the concentration of 500 µM was prepared in phosphate-buffered saline (PBS; pH

126 7.4) and stored in the dark at $-20\text{ }^{\circ}\text{C}$. Dilutions were prepared with PBS on the same
127 day of the experiments.



128

129 **Figure 1.** Chemical structure of the new methylene blue (NMB) used as
130 photosensitizer in the study.

131

132 2.3 Light source

133

134 Light was provided by an in-house-made array of 96 red light-emitting diodes
135 (red LED96) with an emission peak at 631 nm. The measured irradiance from 400 to
136 700 nm was 24.50 mW/cm^2 . Light measurements were performed according to de
137 Menezes et al., 2016 using a cosine-corrected irradiance probe (CC-3-UV, Ocean
138 Optics, Dunedin, FL, USA) screwed onto the end of an optical fiber coupled to an
139 USB4000 spectroradiometer (Ocean Optics, Dunedin, FL, USA). Light intensity was
140 measured inside the well to reduce external interference. The choice of this light source
141 was based on previous results obtained by the application of phenothiazinium
142 photosensitizers and red light (Rodrigues et al 2012). The emission spectrum for the
143 light source can be seen in a previous publication (Rodrigues et al 2012).

144 The fluences provided by the red LED96 calculated by the Eq. 1:

145

$$\mathbf{f} = \mathbf{I} \times \mathbf{t} \quad \text{Eq. (1)}$$

146 where, \mathbf{f} = fluence in J/cm^2 , \mathbf{I} = irradiance in W/cm^2 , and \mathbf{t} = time of irradiation in s.

147 **2.4 Antimicrobial photodynamic treatment**

148

149 **2.4.1 Evaluation of aPDT efficacies on vegetative cells of *B. cereus* based** 150 **on the photosensitizer minimum inhibitory concentration (MIC)**

151

152 The efficacy of aPDT with NMB combined with different fluences on vegetative
153 cells of 12 strains of *B. cereus* was evaluated by determining the MIC of the PS at each
154 fluence as previously described (Rodrigues, Ferreira, Wainwright, & Braga, 2012).
155 Briefly, 50 μL of the bacterial cell suspension ($\approx 10^5$ CFU/mL) and 50 μL of NMB were
156 added to each well of sterile 96-well flat-bottomed plates (NEST Biotechnology, China).
157 The final concentrations of NMB were 0, 1, 2.5, 5, 10, 12.5, 25, 50, 75, 100, and 200
158 μM . Plates were kept in the dark for 30 min at 30 °C and exposed to light fluences of
159 4.41 (3 min), 8.82 (6 min), 13.23 (9 min), and 22.05 J/cm² (15 min) using the red LED96
160 array as the light source (irradiance of 24.5 mW/cm²) or kept in the dark. The light and
161 dark controls were performed to determine the effects of the light and NMB separately.
162 After the exposures, 100 μL of nutrient broth (Kasvi, Italy) was added to each well
163 followed the incubation of the plates at 30 °C for 48 h. MIC was considered the lowest
164 PS concentration, for each fluence, which inhibited the visible growth. Two
165 independent experiments were performed in quadruplicate.

166

167 **2.4.2 aPDT resistance of vegetative cells and spores of selected *B. cereus*** 168 **strains**

169

170 Vegetative cells from selected *B. cereus* strains (B3, B63,436, and ATCC
171 14579) were grown overnight in nutrient broth (Kasvi, Italy) at 30 °C and cell
172 concentration was adjusted to 10^{6-8} CFU/mL in PBS using a McFarland turbidimeter
173 (MS Tecnopon, Brazil). Spore suspensions of the selected strains at 10^7 spores/mL
174 were prepared as previously described. Experiments were performed in 12-well flat-
175 bottomed plates (NEST Biotechnology, China). Five mL of cell or spore suspensions
176 and the solution of NMB were added to each well. The final concentrations of NMB
177 were 5, 50, and 100 μM , which were selected based on previous MIC experiments.

178 Plates were kept in the dark for 30 min at 30 °C before light exposition (24.5 mW/cm²).
179 Vegetative cells and spores were illuminated for up to 120 min and 300 min,
180 respectively. Aliquots of 100 µL were serial diluted and the counts (CFU/mL) were
181 determined by drop-plating onto nutrient agar (Kasvi, Italy) followed by overnight
182 incubation at 30 °C. Three independent experiments were performed.

183

184 **2.5 Modelling of aPDT inactivation data**

185

186 Survival curves were obtained by plotting the logarithmical population counts
187 (log CFU/mL or spores/mL) versus the fluence (J/cm²). The inactivation data were
188 analyzed by GlnaFiT Excel[®] add-in according to Geeraerd, Valdramidis, & Van Impe,
189 2005.

190 The Weibull model (Mafart, Couvert, Gaillard, & Leguerinel, 2002) was used
191 with modifications according to Izquier & Gómez-López, 2011 (Eq. 2):

$$192 \quad \log_{10}N(t) = \log_{10}N(0) - \left(\frac{f}{\delta}\right)^p \quad Eq (2)$$

193 where $N(t)$ (CFU/mL or spores/mL) is the number of survivors at referred time, $N(0)$
194 (CFU/mL or spores/mL) is the initial population of vegetative cells or spores, f is the
195 fluence (J/cm²), δ (J/cm²) is the fluence needed for the first decimal reduction, and p
196 is the shape parameter (dimensionless) (Mafart et al., 2002).

197

198 **2.6 Statistical analysis**

199

200 All graphics and statistics were made using GraphPad Prism 6 (GraphPad
201 Software, USA). To evaluate the differences between the conditions tested the data
202 were submitted to analysis of variance (ANOVA) followed by post-hoc Tukey test. P
203 values of <0.05 were considered significant. A cluster analysis was performed using
204 Ward's algorithm of the ape package in software R, determining the Euclidean distance
205 (Alvarenga et al., 2018).

206 3. Results and discussion

207

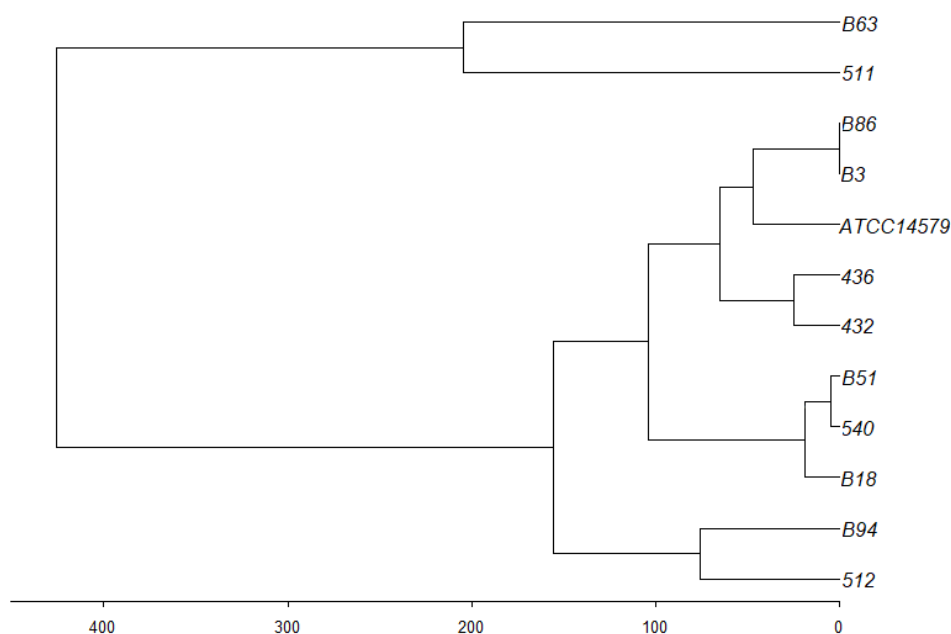
208 Given the importance of *B. cereus* commonly associated with foodborne
 209 illnesses, being also able to spoil food products (Mehta et al., 2019) in the present
 210 study were evaluated 12 strains from different sources for their resistance to aPDT.
 211 The efficacy of aPDT was firstly evaluated determining the MIC for NMB at different
 212 fluences (4.41, 8.82, 13.23, and 22.05 J/cm²). Exposure to red light in the absence of
 213 the PS did not inhibit the growth of any strain independent of the fluence used (data
 214 not shown). As well as the dark control of the NMB at concentrations up to 200 µM did
 215 not inhibit the growth of any strain. The MIC of the NMB for all the fluences is depicted
 216 in Table 1. Only after 6 min of exposure corresponding to 8.82 J/cm² was possible to
 217 determine the MIC for all strains. The MIC varied among strains and for most of them
 218 was possible to observe a decrease while fluence increases. The strain B63 was less
 219 susceptible to all fluences. The strains 432, B3, and B86 showed the same survival at
 220 fluences 4.41, 8.82, and 22.05 J/cm². These strains survived in 200, 50, and 10 µM of
 221 NMB in the respective fluences. The strains B18, B51, B94, and ATCC 14579
 222 (standard) presented the same MIC (25 µM) at 8.82 J/cm².

223

224 **Table 1.** Minimal inhibitory concentration of the NMB at concentrations from 0 to 200
 225 µM illuminated by an array of 96 red light-emitting diodes (LED) at different fluences
 226 (J/cm²).

Strains	Source	Fluences (J/cm ²)				
		(Dark control)	4.41	8.82	13.23	22.05
432	Chocolate	>200	200	50	25	10
436		>200	>200	75	25	10
511		>200	>200	200	25	10
512	Dairy products	>200	>200	100	25	75
540		>200	75	25	10	5
B3	Milk	>200	200	50	50	10
B94		>200	200	25	12.5	75
B18	Starch	>200	200	25	25	5
B51	Meat	>200	200	25	10	10
B63	Ready meal	>200	200	200	100	200
B86	Corn flour	>200	200	50	50	10
ATCC 14579	Standard	>200	200	25	75	12.5

227 According to the cluster analysis of such strains, two main groups could be
 228 observed based on their MIC (Fig. 2). The strains B63 (ready meal) and 511 (dairy
 229 products) were considered the less susceptible strains. These strains survived in a
 230 concentration of 200 μM at fluences of 22.05 and 8.82 J/cm^2 , respectively. The second
 231 group is formed by four subgroups. In the first subgroup (less susceptible) was
 232 composed by the strains B3 (milk), B86 (corn flour), and ATCC 14579 (standard strain)
 233 from different sources. These strains survived in a concentration of 200 μM at a fluence
 234 of 4.41 J/cm^2 . The second subgroup, composed by the strains 432 and 436 (chocolate)
 235 presenting the same MIC of 200 and 25 μM using fluences of 4.41 and 13.23 J/cm^2 ,
 236 respectively. The third subgroup, composed of the strains B18 (starch), B51(meat),
 237 and 540 (dairy products) presented the same MIC of 25 μM at fluences of 8.82 J/cm^2 .
 238 The fourth subgroup, B94 (milk) and 512 (dairy products) composed by the strains
 239 were considered the most susceptible. These strains survived in concentrations of 25
 240 and 12.5 μM , respectively, at a fluence of 13.23 J/cm^2 . The heterogeneity of the strains
 241 with different levels of aPDT resistance revealed a significative variability among the
 242 strains. This behavior was previously described by Alvarenga et al., 2018 with the
 243 same strains.



244

245 **Figure 2.** Cluster analysis based on the MIC of *B. cereus* vegetative cells.

246 From the MIC results and the cluster analysis, 4 strains (B3, 436, B63, ATCC
247 14579) were selected according to their aPDT resistance. For such strains, the aPDT
248 with NMB and red light was conducted with vegetative cells and spores. The
249 inactivation curves are presented as the $\log(N/N_0)$ of each strain, to avoid small
250 variation in the initial populations, as a function of the fluence (J/cm^2).

251 As presented in Fig. 3, Fig. 4, the inactivation data of *B. cereus* vegetative cells
252 and spores did not follow a log-linear inactivation in most cases. Therefore, the Weibull
253 model with modifications (Izquier & Gómez-López, 2011) was used to fit inactivation
254 data and estimate the aPDT inactivation kinetic parameters. From the Weibull model,
255 it is possible to determine the δ -value which was initially described by Mafart et al.,
256 (2002) as the time for first decimal reduction and adapted by Izquier & Gómez-López
257 (2011) as the fluence (J/cm^2) needed for the first decimal reduction. Also, the Weibull
258 model provides the p -value (shape parameter) which contributes to the understanding
259 of microbial behavior. The R^2 obtained were higher than 0.87, indicating a good fit of
260 the Weibull model to the data.

261 Fig. 3 shows the inactivation curves of the strains *B. cereus* vegetative cells
262 submitted to aPDT. As expected, the less susceptible strain (B63; Fig. 3B) showed the
263 lowest reduction in the viability at concentrations of 50 and 100 μM compared to the
264 other strains ($P < 0.05$). At the same concentrations (50 and 100 μM), strains B3 (Fig.
265 3A), 436 (Fig. 3C), and ATCC 14579 (Fig. 3D) showed 4 and 5 log CFU/mL reductions
266 when exposed to fluences of 73.50 and 88.20 J/cm^2 , respectively. For the most
267 susceptible strain (ATCC 14579), it was only necessary 29.40 J/cm^2 , corresponding to
268 20 min of exposure to light, and 5 μM of NMB to achieve around 4 log CFU/mL
269 reductions in cell viability. In previous studies, the viability of *B. cereus* was reduced
270 by 4.4 log CFU/mL reductions after aPDT with the PS hypericin and approximately 40
271 min of light exposure (9.2 J/cm^2) (Aponiene, Paskeviciute, Reklaitis, & Luksiene,
272 2015). The use of 5-aminolevulinic acid (ALA) as a precursor of endogenous PSs at 3
273 and 7.5 mmol/L reduced the viability of *B. cereus* from 4 to 6 log CFU/mL reductions
274 (Le Marc et al., 2009). According to the authors, the efficiency of the aPDT was
275 dependent on the fluence in agreement with the observed by the present study.

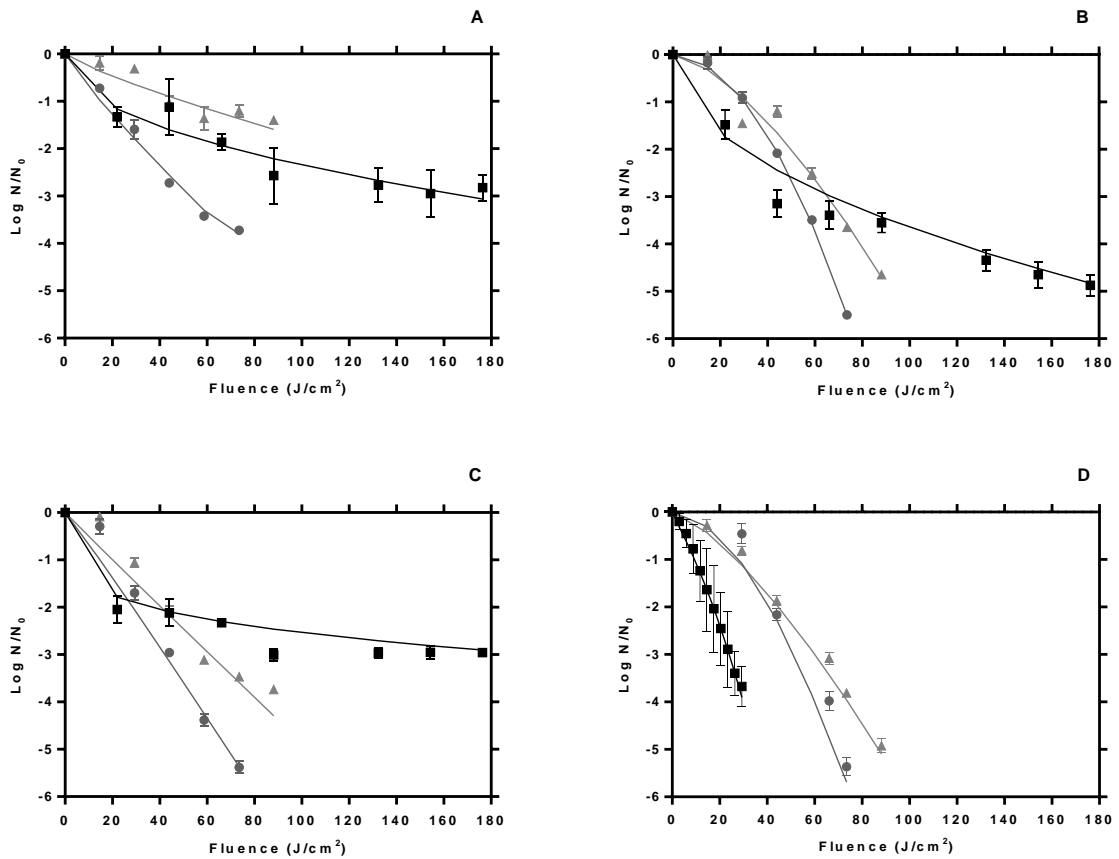
276 The spore inactivation required higher fluences than vegetative cells, which is
277 expected given the high resistance structure, namely exosporium, developed during
278 the sporulation process (Gerhardt & Ribi, 1964; Sanchez-Salas, Setlow, Zhang, Li, &
279 Setlow, 2011). Nevertheless, during the spore inactivation of the most sensitive strain
280 (ATCC 14579; Fig. 4D), it was necessary the same fluence as for vegetative cells
281 (29.40 J/cm^2) to achieve around 4 log spores/mL reductions. However, the
282 concentration required of NMB was higher ($50 \mu\text{M}$) than used for vegetative cells. A
283 small difference between vegetative cells and spores of *B. cereus* in terms of PS
284 concentration was previously cited by Demidova & Hamblin, 2005. The same authors
285 also discussed the differential sensitivity of spores from, *B. subtilis*, *B. atrophaeus*, and
286 *B. megaterium* (Demidova & Hamblin, 2005). A huge difference in terms of aPDT
287 resistance was detected between *B. cereus/B. thuringiensis* and *B. megaterium* which
288 the authors attribute to a structural difference in the spores. The exosporium present
289 in the species *B. cereus/B. thuringiensis* and not in the *B. megaterium* can contribute
290 to the accumulation of PS, allowing the diffusion of the dye inside the spore (Demidova
291 & Hamblin, 2005).

292 The strains B3, B63, and 436 (Fig. 4 A-B-C, respectively) presented similar
293 inactivation curves at all NMB concentrations and fluences. Such less susceptible
294 behavior of these strains was also detected during the spray drying process, where the
295 strain B63 was classified with intermediate resistance and the strains 436 and B3 as
296 less susceptible to the process (Alvarenga et al., 2018). The same authors explored
297 the differences in heat stress tolerance among different *B. cereus* strains at the
298 molecular level with proteomic analysis. The results indicated that the observed
299 variability between *B. cereus* strains could be related to spore coat protein expression
300 (Alvarenga et al., 2018). So far there are no studies in the literature that can explain
301 the variability between *B. cereus* strains related to aPDT which presents different
302 inactivation mechanisms compared to thermal processes.

303 Photoinactivation of *B. cereus* spores mediated by ALA-based, porphyrin
304 derivatives, phenothiazinium dyes, and hypericin-based PS showed significant
305 inactivation results from approximately 2.5 to 6.0 log CFU/mL reductions
306 (Dementavicius, Lukseviciute, Gómez-López, & Luksiene, 2016; Demidova & Hamblin,

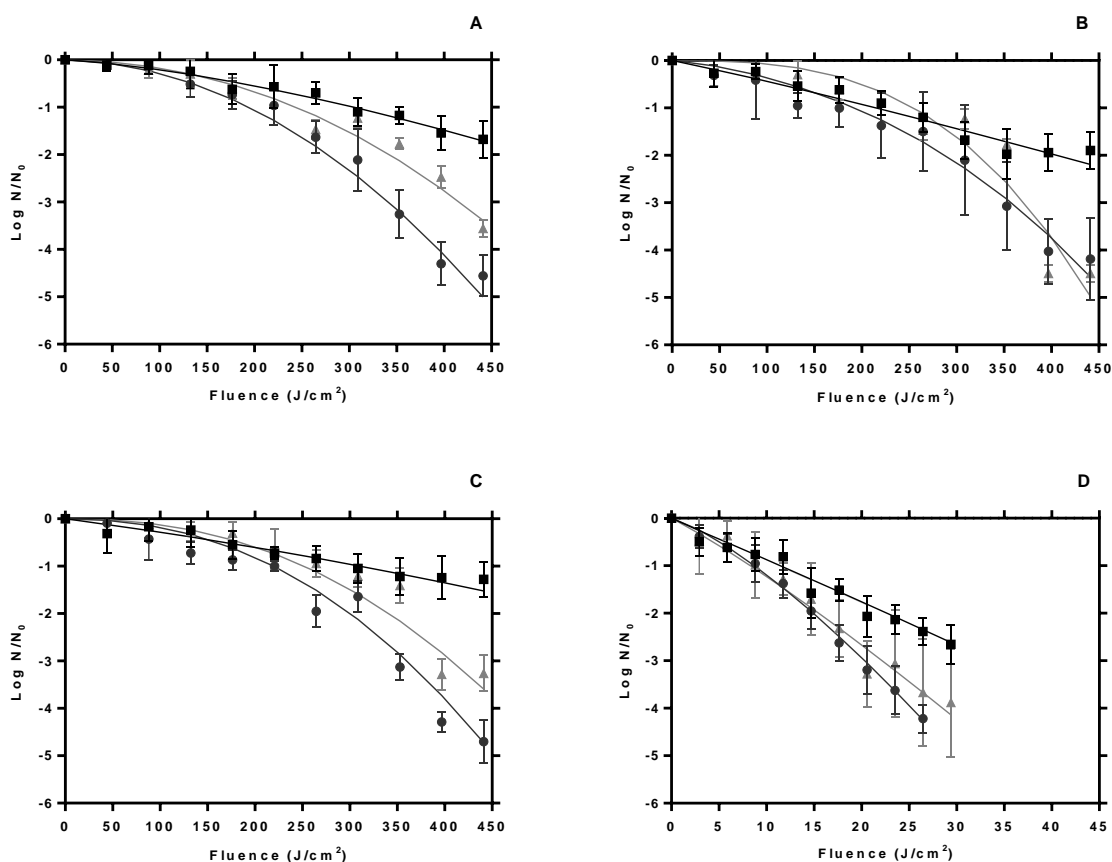
307 2005; Luksiene et al., 2009; Oliveira et al., 2009). TBO is a phenothiazinium dye
308 frequently used for PDT of bacteria and fungi (Demidova & Hamblin, 2005; Gonzales,
309 Da Silva, Roberts, & Braga, 2010; Mahmoudi, Pourhajibagher, Alikhani, & Bahador,
310 2019). Since TBO had presented promising results of *B. cereus* spores inactivation,
311 other types of phenothiazinium dyes were evaluated including NMB (Demidova &
312 Hamblin, 2005). In that study, photoinactivation of *B. cereus* spores mediated by NMB
313 at 50 μ M achieved more than 5 log CFU/mL reductions with half of the fluence used
314 with TBO (40 J/cm²) (Demidova & Hamblin, 2005). It is necessary to consider the time
315 of incubation of the PS of 3 h opposed with 30 min in our study. In addition, it is
316 important to highlight the age of the spores significantly different with 30 days in our
317 study and 3 days declared by Demidova & Hamblin (2005). Such discrepancy in the
318 spore maturation may explain the difference between the present study and the
319 literature (Dementavicius et al., 2016; Demidova & Hamblin, 2005; Luksiene et al.,
320 2009; Oliveira et al., 2009).

321



322

323 **Figure 3.** aPDT inactivation curves of the vegetative cells of different strains of *B.*
 324 *cereus* – B63 (A), 436 (B), B3 (C), and ATCC 14579 (D) – in the presence of NMB at
 325 concentrations of ■ 5, ● 50, and ▲ 100 μM and different fluences (J/cm²). All data
 326 correspond to three independent experiments. —: estimated curve by the Weibull
 327 model. Error bars represent the standard deviation (SD) of three independent
 328 experiments and in some cases are hidden by the symbols.



329

330 **Figure 4.** aPDT inactivation curves of the spores of different strains of *B. cereus* – B63
 331 (A), 436 (B), B3 (C), and ATCC 14579 (D) – in the presence of NMB at concentrations
 332 of ■ 5, ● 50, and ▲ 100 μM and different fluences (J/cm^2). All data correspond to three
 333 independent experiments. —: estimated curve by the Weibull model. Error bars
 334 represent the standard deviation (SD) of three independent experiments and in some
 335 cases are hidden by the symbols.

336

337 Table 2 and 3 gives the fitted photodynamic inactivation kinetics parameters (δ
 338 and p -values) of vegetative cells and spores of the *B. cereus* strains using the Weibull
 339 model. As depicted in Table 2, the highest and smallest δ value (J/cm^2) was found for
 340 the strain B63 (50.24 ± 5.21) and B3 (0.51 ± 0.30) with NMB at 100 and 5 μM ,
 341 respectively ($P < 0.05$). The highest δ values of the strains 436 and ATCC 14579 did
 342 not differ significantly at 50 and 100 μM ($P < 0.05$). Most of the lowest δ values were
 343 observed with NMB at 5 μM suggesting that the minimum concentration of NBMN binds

344 quickly to the cell membrane causing fast inactivation. However, according to the p
345 values presented in Table 2, the strains B3, B63, and 436 become less affected as the
346 fluence increase with NMB 5 μM . This is confirmed by Fig. 3-A-B-C which clearly
347 shows an upward concavity ($p < 1$) of the curves. The only strain with $p > 1$ (downward
348 concavity) for all concentrations of NMB was the ATCC 14579, which indicates that the
349 cells are progressively killed in all conditions. The Weibull model was able to describe
350 the photoinactivation mediated by ALA of *B. cereus* spores with linear, downward, and
351 upward concavity shapes of the inactivation curves (Le Marc et al., 2009). In that study,
352 the authors suggest that the incubation time and concentration of PS impact the p -
353 value increasing the inactivation in the first minutes although remaining cells become
354 less affected (Le Marc et al., 2009).

355 In all conditions tested for *B. cereus* spores, p values were > 1 (Table 3). The
356 downward concavity ($p > 1$) indicates that the microorganisms become increasingly
357 damaged (Van Boekel, 2002). Such behavior can be confirmed by the δ values in all
358 conditions of the *B. cereus* spore inactivation, except in the case of the strain ATCC
359 14579. Among the strains B3, B63, and 436 the smallest and highest δ values (196.23
360 ± 32.27 and 296.88 ± 66.86) were observed for B63 and B3 with NMB at 50 and 5 μM ,
361 respectively. δ values for the strain ATCC 14579 were significantly different in all
362 conditions ($P > 0.05$). Also, the fluence of four decimal reductions (4D) for all strains
363 tested to come up to 400 J/cm^2 at 50 μM of NMB, except for the strain ATCC 14579
364 with 25 J/cm^2 at 50 and 100 μM .

365 **Table 2.** Photoinactivation kinetic parameters of aPDT obtained from Weibull modeling for *B. cereus* vegetative cells.

Strains	NMB (μM)	δ (mean \pm SD) (J/cm^2)	p -value (mean \pm SD)	4D (mean \pm SD) (J/cm^2)	R^2
B3	5	$0.51 \pm 0.30^{\text{c C}}$	$0.21 \pm 0.06^{\text{c B}}$	ND	0.96
	50	$14.81 \pm 0.62^{\text{b C}}$	$1.05 \pm 0.02^{\text{a C}}$	$56.01 \pm 1.45^{\text{b D}}$	0.98
	100	$20.17 \pm 1.15^{\text{a C}}$	$0.99 \pm 0.03^{\text{b C}}$	$82.61 \pm 1.33^{\text{a A}}$	0.96
B63	5	$16.01 \pm 5.15^{\text{b A}}$	$0.46 \pm 0.09^{\text{b B}}$	ND	0.90
	50	$15.32 \pm 1.36^{\text{b C}}$	$0.89 \pm 0.05^{\text{a B}}$	$72.76 \pm 0.46^{\text{D}}$	0.98
	100	$50.24 \pm 5.21^{\text{a A}}$	$0.83 \pm 0.13^{\text{a D}}$	ND	0.87
436	5	$7.67 \pm 3.75^{\text{b B}}$	$0.49 \pm 0.06^{\text{c B}}$	$121.42 \pm 14.82^{\text{a A}}$	0.96
	50	$30.50 \pm 0.29^{\text{a A}}$	$1.94 \pm 0.01^{\text{a A}}$	$62.60 \pm 0.55^{\text{c B}}$	0.99
	100	$31.62 \pm 1.16^{\text{a B}}$	$1.51 \pm 0.04^{\text{b A}}$	$79.38 \pm 0.92^{\text{b B}}$	0.97
ATCC 14579	5	$10.54 \pm 5.53^{\text{b AB}}$	$1.40 \pm 0.57^{\text{a A}}$	$26.46 \pm 0.00^{\text{c B}}$	0.99
	50	$28.21 \pm 1.70^{\text{a B}}$	$1.84 \pm 0.11^{\text{a A}}$	$60.39 \pm 1.18^{\text{b C}}$	0.98
	100	$27.05 \pm 1.62^{\text{a B}}$	$1.38 \pm 0.08^{\text{a B}}$	$74.68 \pm 0.72^{\text{a C}}$	0.99

δ : fluence needed for the first decimal reduction

p -value: shape parameter (dimensionless)

4D: fluence needed to achieve four log reductions

R^2 : determination coefficient

Different lowercase letters in the same column within each strain (B3, B63, 436, and ATCC 14579) indicate significant difference in inactivation kinetic parameters ($P < 0.05$) according to one-way ANOVA followed by post-hoc Tukey test

Different uppercase letters in the same column within each concentration of NMB (5, 50, and 100 μM) indicate significant difference in inactivation kinetic parameters ($P < 0.05$) according to one-way ANOVA followed by post-hoc Tukey test

366

367

368 **Table 3.** Photoinactivation kinetic parameters of aPDT obtained from Weibull modeling of *B. cereus* spores.

Strains	NMB (μM)	δ (mean \pm SD) (J/cm^2)	p -value (mean \pm SD)	4D (mean \pm SD) (J/cm^2)	R^2
B3	5	296.88 \pm 66.86 ^{a A}	1.25 \pm 0.37 ^{b AB}	ND	0.94
	50	219.61 \pm 12.05 ^{b A}	2.24 \pm 0.27 ^{a A}	413.07 \pm 10.10 ^A	0.95
	100	251.67 \pm 11.42 ^{ab A}	2.29 \pm 0.20 ^{a B}	ND	0.91
B63	5	309.07 \pm 56.83 ^{a A}	1.50 \pm 0.32 ^{b A}	ND	0.88
	50	196.23 \pm 32.27 ^{b A}	2.02 \pm 0.38 ^{a A}	395.92 \pm 18.55 ^A	0.98
	100	243.54 \pm 27.57 ^{b A}	2.10 \pm 0.39 ^{a B}	ND	0.91
436	5	222.57 \pm 42.78 ^{a B}	1.09 \pm 0.18 ^{c B}	ND	0.89
	50	202.66 \pm 69.15 ^{a A}	2.13 \pm 0.89 ^{b A}	400.05 \pm 36.01 ^{a A}	0.94
	100	255.20 \pm 14.10 ^{a A}	2.95 \pm 0.32 ^{a A}	411.13 \pm 1.93 ^{a A}	0.90
ATCC 14579	5	11.57 \pm 2.50 ^{a C}	1.04 \pm 0.18 ^{b B}	ND	0.92
	50	8.87 \pm 1.70 ^{b B}	1.33 \pm 0.20 ^{a B}	24.96 \pm 1.15 ^{a B}	0.98
	100	8.56 \pm 1.59 ^{b B}	1.11 \pm 0.21 ^{ab C}	25.09 \pm 0.70 ^{a B}	0.93

δ : fluence needed for the first decimal reduction

p -value: shape parameter (dimensionless)

4D: fluence needed to achieve four log reductions

R^2 : determination coefficient

Different lowercase letters in the same column within each strain (B3, B63, 436, and ATCC 14579) indicate significant difference in inactivation kinetic parameters ($P < 0.05$) according to one-way ANOVA followed by post-hoc Tukey test

Different uppercase letters in the same column within each concentration of NMB (5, 50, and 100 μM) indicate significant difference in inactivation kinetic parameters ($P < 0.05$) according to one-way ANOVA followed by post-hoc Tukey test

370 The spore inactivation kinetic parameters (especially, δ value) of the strain
371 ATCC 14579 (Table 3) confirm that this microorganism has low resistance to the aPDT
372 compared to the other strains.

373 This study evaluated for the first time the effect of aPDT against *B. cereus*
374 strains from different sources. The use of aPDT with NMB and the red light was able
375 to reduce *B. cereus* in both forms (vegetative cells and spores). The variability among
376 strains of *B. cereus* represents a major challenge for food safety. Also, the results of
377 this study indicated that the strain ATCC 14579, widely used as the standard for
378 thermal processing, was the most susceptible to aPDT. Further studies are needed to
379 explain how the variability among strains of the same species occurs. The Weibull
380 model successfully described a non-log-linear photoinactivation of vegetative cells and
381 spores of *B. cereus* as well as the estimation of the kinetic parameters. The
382 mathematical modelling can be a useful tool to determine the ideal conditions for
383 photodynamic inactivation and assist a feasible implementation of aPDT by the
384 industry.

385

386 **Acknowledgment**

387

388 This work was supported by: Conselho Nacional de Desenvolvimento Científico e
389 Tecnológico (CNPq) (Grants #140092/2017-0, #302763/2014-7, and #305804/2017-
390 0); Coordenação de Aperfeiçoamento de Pessoal de Nível Superior (CAPES) -
391 Finance Code 001 for the financial support.

392

393 **Conflict of interest**

394

395 The authors declare no competing interests.

396 **4. References**

- 397 Almeida, A., Faustino, M. A. F., & Tomé, J. P. C. (2015). Photodynamic inactivation of
398 bacteria: finding the effective targets. *Future Medicinal Chemistry*, 7(10), 1221–1224.
399 <https://doi.org/10.4155/fmc.15.59>
- 400 Alvarenga, V. O., Brancini, G. T. P., Silva, E. K., da Pia, A. K. R., Campagnollo, F. B.,
401 Braga, G. Ú. L., Hubinger, M. D., & Sant'Ana, A. S. (2018). Survival variability of 12
402 strains of *Bacillus cereus* yielded to spray drying of whole milk. *International Journal of*
403 *Food Microbiology*, 286, 80–89. <https://doi.org/10.1016/j.ijfoodmicro.2018.07.020>
- 404 Aponiene, K., Paskeviciute, E., Reklaitis, I., & Luksiene, Z. (2015). Reduction of
405 microbial contamination of fruits and vegetables by hypericin-based
406 photosensitization: Comparison with other emerging antimicrobial treatments. *Journal*
407 *of Food Engineering*, 144, 29–35. <https://doi.org/10.1016/j.jfoodeng.2014.07.012>
- 408 Barba, F. J., Koubaa, M., Prado-Silva, L., Orlie, V., & Sant'Ana, A. S. (2017). Mild
409 processing applied to the inactivation of the main foodborne bacterial pathogens: A
410 review. *Trends in Food Science & Technology*, 66, 20–35.
411 <https://doi.org/10.1016/j.tifs.2017.05.011>
- 412 Bottone, E. J. (2010). *Bacillus cereus*, a volatile human pathogen. *Clinical Microbiology*
413 *Reviews*, 23(2), 382–398. <https://doi.org/10.1128/CMR.00073-09>
- 414 Brancini, G. T. P., Rodrigues, G. B., Rambaldi, M. D. S. L., Izumi, C., Yatsuda, A. P.,
415 Wainwright, M., Rosa, J.C., & Braga, G. Ú. L. (2016). The effects of photodynamic
416 treatment with new methylene blue N on the: *Candida albicans* proteome.
417 *Photochemical and Photobiological Sciences*, 15(12), 1503–1513.
418 <https://doi.org/10.1039/c6pp00257a>
- 419 Buchovec, I., Vaitonis, Z., & Luksiene, Z. (2009). Novel approach to control *Salmonella*
420 *enterica* by modern biophotonic technology: Photosensitization. *Journal of Applied*
421 *Microbiology*, 106(3), 748–754. <https://doi.org/10.1111/j.1365-2672.2008.03993.x>
- 422 CDC. (2020). Food safety. Center for Disease Control and Prevention. Retrieved
423 February 23, 2020, from <https://www.cdc.gov/foodsafety/index.html>
- 424 de Menezes, H. D., Tonani, L., Bachmann, L., Wainwright, M., Braga, G. Ú. L., & von

- 425 Zeska Kress, M. R. (2016). Photodynamic treatment with phenothiazinium
426 photosensitizers kills both ungerminated and germinated microconidia of the
427 pathogenic fungi *Fusarium oxysporum*, *Fusarium moniliforme* and *Fusarium solani*.
428 *Journal of Photochemistry and Photobiology B: Biology*, 164, 1–12.
429 <https://doi.org/10.1016/j.jphotobiol.2016.09.008>
- 430 Dementavicius, D., Lukseviciute, V., Gómez-López, V. M., & Luksiene, Z. (2016).
431 Application of mathematical models for bacterial inactivation curves using Hypericin-
432 based photosensitization. *Journal of Applied Microbiology*, 120(6), 1492–1500.
433 <https://doi.org/10.1111/jam.13127>
- 434 Demidova, T. N., & Hamblin, M. R. (2005). Photodynamic inactivation of *Bacillus*
435 spores, mediated by phenothiazinium dyes. *Applied and Environmental Microbiology*,
436 71(11), 6918–6925. <https://doi.org/10.1128/AEM.71.11.6918>
- 437 Geeraerd, A. H., Valdramidis, V. P., & Van Impe, J. F. (2005). GlnaFiT, a freeware tool
438 to assess non-log-linear microbial survivor curves. *International Journal of Food*
439 *Microbiology*, 102(1), 95–105. <https://doi.org/10.1016/j.ijfoodmicro.2004.11.038>
- 440 Gerhardt, P., & Ribí, E. (1964). Ultrastructure Of The Exosporium Enveloping Spores
441 Of *Bacillus cereus*. *Journal of Bacteriology*, 88(6), 1774–1789.
442 <https://doi.org/10.1128/jb.88.6.1774-1789.1964>
- 443 Gonzales, F. P., Da Silva, S. H., Roberts, D. W., & Braga, G. U. L. (2010).
444 Photodynamic inactivation of conidia of the fungi *Metarhizium anisopliae* and
445 *Aspergillus nidulans* with methylene blue and toluidine blue. *Photochemistry and*
446 *Photobiology*, 86(3), 653–661. <https://doi.org/10.1111/j.1751-1097.2009.00689.x>
- 447 Gonzales, J. C., Brancini, G. T. P., Rodrigues, G. B., Silva-Junior, G. J., Bachmann,
448 L., Wainwright, M., & Braga, G. Ú. L. (2017). Photodynamic inactivation of conidia of
449 the fungus *Colletotrichum abscissum* on *Citrus sinensis* plants with methylene blue
450 under solar radiation. *Journal of Photochemistry and Photobiology B: Biology*, 176,
451 54–61. <https://doi.org/10.1016/j.jphotobiol.2017.09.008>
- 452 Heyndrickx, M. (2011). The importance of endospore-forming bacteria originating from
453 soil for contamination of industrial food processing. *Applied and Environmental Soil*
454 *Science*, 2011, 1–11. <https://doi.org/10.1155/2011/561975>

- 455 Izquier, A., & Gómez-López, V. M. (2011). Modeling the pulsed light inactivation of
456 microorganisms naturally occurring on vegetable substrates. *Food Microbiology*, 28(6),
457 1170–1174. <https://doi.org/10.1016/j.fm.2011.03.010>
- 458 Le Marc, Y., Buchovec, I., George, S. M., Baranyi, J., & Luksiene, Z. (2009). Modelling
459 the photosensitization-based inactivation of *Bacillus cereus*. *Journal of Applied*
460 *Microbiology*, 107(3), 1006–1011. <https://doi.org/10.1111/j.1365-2672.2009.04275.x>
- 461 Luksiene, Z., Buchovec, I., & Paskeviciute, E. (2009). Inactivation of food pathogen
462 *Bacillus cereus* by photosensitization in vitro and on the surface of packaging material.
463 *Journal of Applied Microbiology*, 107(6), 2037–2046. <https://doi.org/10.1111/j.1365-2672.2009.04383.x>
- 465 Mafart, P., Couvert, O., Gaillard, S., & Leguerinel, I. (2002). On calculating sterility in
466 thermal preservation methods: application of the Weibull frequency distribution model.
467 *International Journal of Food Microbiology*, 72, 107–113.
468 <https://doi.org/10.17660/ActaHortic.2001.566.11>
- 469 Mahmoudi, H., Pourhajibagher, M., Alikhani, M. Y., & Bahador, A. (2019). The effect
470 of antimicrobial photodynamic therapy on the expression of biofilm associated genes
471 in *Staphylococcus aureus* strains isolated from wound infections in burn patients.
472 *Photodiagnosis and Photodynamic Therapy*, 25, 406–413.
473 <https://doi.org/10.1016/j.pdpdt.2019.01.028>
- 474 Mehta, D. S., Metzger, L. E., Hassan, A. N., Nelson, B. K., & Patel, H. A. (2019). The
475 ability of spore formers to degrade milk proteins, fat, phospholipids, common
476 stabilizers, and exopolysaccharides. *Journal of Dairy Science*, 102(12), 10799–10813.
477 <https://doi.org/10.3168/jds.2019-16623>
- 478 Oliveira, A., Almeida, A., Carvalho, C. M. B., Tomé, J. P. C., Faustino, M. A. F., Neves,
479 M. G. P. M. S., ... Cunha, A. (2009). Porphyrin derivatives as photosensitizers for the
480 inactivation of *Bacillus cereus* endospores. *Journal of Applied Microbiology*, 106(6),
481 1986–1995. <https://doi.org/10.1111/j.1365-2672.2009.04168.x>
- 482 Ölmez, H., & Kretzschmar, U. (2009). Potential alternative disinfection methods for
483 organic fresh-cut industry for minimizing water consumption and environmental impact.

- 484 *LWT - Food Science and Technology*, 42(3), 686–693.
485 <https://doi.org/10.1016/j.lwt.2008.08.001>
- 486 Rodrigues, G. B., Ferreira, L. K. S., Wainwright, M., & Braga, G. U. L. (2012). Journal
487 of Photochemistry and Photobiology B : Biology Susceptibilities of the dermatophytes
488 *Trichophyton mentagrophytes* and *T. rubrum* microconidia to photodynamic
489 antimicrobial chemotherapy with novel phenothiazinium photosensitizers and red light.
490 *Journal of Photochemistry & Photobiology, B: Biology*, 116, 89–94.
491 <https://doi.org/10.1016/j.jphotobiol.2012.08.010>
- 492 Sanchez-Salas, J. L., Setlow, B., Zhang, P., Li, Y. Q., & Setlow, P. (2011). Maturation
493 of released spores is necessary for acquisition of full spore heat resistance during
494 *Bacillus subtilis* sporulation. *Applied and Environmental Microbiology*, 77(19), 6746–
495 6754. <https://doi.org/10.1128/AEM.05031-11>
- 496 Spanu, C. (2016). Sporeforming bacterial pathogens in ready-to-eat dairy products. In
497 *Food Hygiene and Toxicology in Ready-to-Eat Foods*. [https://doi.org/10.1016/B978-0-](https://doi.org/10.1016/B978-0-12-801916-0.00015-7)
498 12-801916-0.00015-7
- 499 Tonani, L., Morosini, N. S., Dantas de Menezes, H., Nadaletto Bonifácio da Silva, M.
500 E., Wainwright, M., Leite Braga, G. Ú., & Regina von Zeska Kress, M. (2018). In vitro
501 susceptibilities of *Neoscytalidium* spp. sequence types to antifungal agents and
502 antimicrobial photodynamic treatment with phenothiazinium photosensitizers. *Fungal*
503 *Biology*, 122(6), 436–448. <https://doi.org/10.1016/j.funbio.2017.08.009>
- 504 Uchida, R., & Silva, F. V. M. (2017). *Alicyclobacillus acidoterrestris* spore inactivation
505 by high pressure combined with mild heat: Modeling the effects of temperature and
506 soluble solids. *Food Control*, 73, 426–432.
507 <https://doi.org/10.1016/j.foodcont.2016.08.034>
- 508 Van Boekel, M. A. J. S. (2002). On the use of the Weibull model to describe thermal
509 inactivation of microbial vegetative cells. *International Journal of Food Microbiology*,
510 74(1–2), 139–159. [https://doi.org/10.1016/S0168-1605\(01\)00742-5](https://doi.org/10.1016/S0168-1605(01)00742-5)
- 511 Wainwright, M. (1998). Photodynamic antimicrobial chemotherapy (PACT). *Journal of*
512 *Antimicrobial Chemotherapy*, 42(1), 13–28. <https://doi.org/10.1093/jac/42.1.13>

- 513 WHO. (2015). World Health Organization. WHO estimates of the global burden of
514 foodborne diseases. Retrieved July 25, 2020, from
515 [https://apps.who.int/iris/bitstream/handle/10665/199350/9789241565165_eng.pdf?se](https://apps.who.int/iris/bitstream/handle/10665/199350/9789241565165_eng.pdf?sequence=1)
516 [quence=1](https://apps.who.int/iris/bitstream/handle/10665/199350/9789241565165_eng.pdf?sequence=1)
- 517 Žudyte, B., & Lukšiene, Ž. (2019). Toward better microbial safety of wheat sprouts:
518 Chlorophyllin-based photosensitization of seeds. *Photochemical and Photobiological*
519 *Sciences*, 18(10), 2521–2530. <https://doi.org/10.1039/c9pp00157c>

1 **Capítulo 3 - Antimicrobial photodynamic treatment as an alternative**
2 **approach for *Alicyclobacillus acidoterrestris* inactivation**

3
4 Leonardo do Prado-Silva^a, Ana T. P. C. Gomes^b, Mariana Q. Mesquita^c, Iramaia A.
5 Neri-Numa^a, Glaucia M. Pastore^a, Maria G. P. M. S. Neves^c, Maria A. F. Faustino^c,
6 Adelaide Almeida^b, Gilberto Ú. L. Braga^d, Anderson S. Sant'Ana^a.

7
8 ^aDepartment of Food Science, Faculty of Food Engineering, University of Campinas
9 (UNICAMP), Campinas, SP, Brazil

10 ^bDepartment of Biology and CESAM, University of Aveiro, Aveiro 3810-193, Portugal

11 ^cDepartment of Chemistry and LAQV-REQUIMTE, University of Aveiro, 3810-193
12 Aveiro, Portugal

13 ^dDepartment of Clinical, Toxicological and Bromatological Analyses, School of
14 Pharmaceutical Sciences of Ribeirão Preto, University of São Paulo, Ribeirão Preto,
15 SP, Brazil

16
17 Original research paper published in the *International Journal of Food*
18 *Microbiology – Elsevier.*

19 <https://doi.org/10.1016/j.ijfoodmicro.2020.108803>

20

21 Abstract

22 *Alicyclobacillus acidoterrestris* is a cause of major concern for the orange juice industry
23 due to its thermal and chemical resistance, as well as its spoilage potential. *A.*
24 *acidoterrestris* spoilage of orange juice is due to off-flavor taints from guaiacol
25 production and some halophenols. The present study aimed to evaluate the
26 effectiveness of antimicrobial photodynamic treatment (aPDT) as an emerging
27 technology to inactivate the spores of *A. acidoterrestris*. The aPDT efficiency towards
28 *A. acidoterrestris* was evaluated using as photosensitizers the tetracationic porphyrin
29 (Tetra-Py⁺-Me) and the phenothiazinium dye new methylene blue (NMB) in
30 combination with white light-emitting diode (LED; 400-740 nm, 65-140 mW/cm²). The
31 spores of *A. acidoterrestris* were cultured on YSG agar plates (pH 3.7 ± 0.1) at 45 °C
32 for 28 days and submitted to the aPDT with Tetra-Py⁺-Me and NMB at 10 µM in
33 phosphate-buffered saline (PBS) in combination with white light (140 mW/cm²). The
34 use of Tetra-Py⁺-Me at 10 µM resulted in a 7.3 ± 0.04 log reduction of the viability of
35 *A. acidoterrestris* spores. No reductions in the viability of this bacterium were observed
36 with NMB at 10 µM. Then, the aPDT with Tetra-Py⁺-Me and NMB at 10 µM in orange
37 juice (UHT; pH 3.9; 11 °Brix) alone and combined with potassium iodide (KI) was
38 evaluated. The presence of KI was able to potentiate the aPDT process in orange
39 juice, promoting the inactivation of 5 log CFU/mL of *A. acidoterrestris* spores after 10
40 h of white light exposition (140 mW/cm²). However, in the absence of KI, both
41 photosensitizers did not promote a significant reduction in the spore viability. The
42 inactivation of *A. acidoterrestris* spores artificially inoculated in orange peels (10⁵
43 spores/mL) was also assessed using Tetra-Py⁺-Me at 10 and 50 µM in the presence
44 and absence of KI in combination with white light (65 mW/cm²). No significant
45 reductions were observed ($p < 0.05$) when Tetra-Py⁺-Me was used at 10 µM, however
46 at the highest concentration (50 µM) a significant spore reduction (≈ 2.8 log CFU/mL
47 reductions) in orange peels was observed after 6 h of sunlight exposition (65 mW/cm²).
48 Although the color, total phenolic content (TPC), and antioxidant capacity of orange
49 juice and peel (only color evaluation) seem to have been affected by light exposition,
50 the impact on the visual and nutritional characteristics of the products remains

51 inconclusive so far. Besides that, the results found suggest that aPDT can be a
52 potential method for the reduction of *A. acidoterrestris* spores on orange groves.

53

54 **Key-words:** aPDT; Emerging technologies; Sporeforming bacteria; Orange juice;
55 Food spoilage; Decontamination

56 Research Highlights

- 57 ○ *Alicyclobacillus acidoterrestris* (AA) inactivation by antimicrobial photodynamic
58 treatment (aPDT)
- 59 ○ AA inactivation using aPDT using two photosensitizers (PS): Tetra-Py⁺-Me and
60 NMB
- 61 ○ aPDT+Tetra-Py⁺-Me caused 7 log CFU/mL reductions of AA under *in vitro*
62 conditions
- 63 ○ aPDT+Tetra-Py⁺-Me+NMB+KI caused 5 log CFU/mL reductions of AA in
64 orange juice
- 65 ○ aPDT+Tetra-Py⁺-Me in sunlight caused 2.8 log CFU/mL reductions of AA in
66 orange peel
- 67

68 **1. Introduction**

69

70 With over three-quarters of global orange juice exports, Brazil is the largest
71 producer of this important commodity (USDA, 2020), demonstrating the importance of
72 this juice for the Brazilian economy. Given this, sustaining the market requires high-
73 quality standards, including those related to the microbiological quality of orange juice.

74 Several microorganisms may represent challenges for the fruit juices industries.
75 Among critical microorganisms impacting the microbiological quality of orange juice,
76 spore-forming bacteria such as *Alicyclobacillus* spp. stand out. As other microbial
77 contaminants, *Alicyclobacillus* spp. is found in the soil (Albuquerque et al., 2000;
78 Groenewald et al., 2008, 2009; Hippchen et al., 1981; Sawaki, 2007). This bacterium
79 is gram-variable, spore-forming, and thermo-acidophilic bacteria that emerged as
80 spoilage bacterium of fruit juices in the 90s (Wisotzkey et al., 1992). *Alicyclobacillus*
81 spp. spoilage of acidic products is characterized by off-flavor taints from guaiacol
82 production and some halophenols without gas production (Siegmond and Pöllinger-
83 Zierler, 2006). Although it is visually difficult to detect the spoilage, these compounds
84 change the organoleptic characteristics of the products causing rejection by
85 consumers and, consequently, economic losses for the industries (Orr and Beuchat,
86 2000). Through direct contact or dust, spores of *Alicyclobacillus* spp. can contaminate
87 the peel of fruits used for juice making. Counts of this bacterium of 10^2 CFU per Kg of
88 fruits collected directly from the trees have been reported (ABECitrus, 1999). Once this
89 contamination occurs, the spores can survive fruit decontamination and heat treatment
90 steps, potentially causing spoilage of finished products (Oteiza et al., 2011).

91 The juice industry widely uses pasteurization (≈ 95 °C) as a microbial inactivation
92 method (Silva et al., 2015). However, depending on the pasteurization conditions,
93 survival, and even stimulation of germination of *Alicyclobacillus* spp. spores may occur,
94 likely resulting in juice spoilage (Gouws et al., 2005; Groenewald et al., 2008). Intense
95 thermal treatments might also modify fruit juices' quality, nutritional, and sensorial
96 characteristics (Evelyn et al., 2016; Uchida and Silva, 2017). Given these facts,
97 alternative strategies to reduce the contamination in fruit surface immediately before
98 juice extraction have been proposed (Lee et al., 2004, 2010), such as fruit washing

99 with disinfectants, e.g., peracetic acid (Friedrich et al., 2009; Osopale et al., 2017).
100 Despite this, this approach seems not to work effectively as spoilage problems caused
101 by *Alicyclobacillus* spp. are frequently reported (Pornpukdeewattana et al., 2020).
102 Additionally, *Alicyclobacillus* spp. spores have also been found in ingredients derived
103 from fruit processing, e.g. flavorings (Oteiza et al., 2014), reinforcing that demand for
104 strategies to reduce contamination before fruit processing.

105 Technologies with potential for fruit peel decontamination must be inexpensive,
106 easy to apply on a large scale, and environmentally friendly. In this way, antimicrobial
107 photodynamic treatment (aPDT) is a light-based technology with the potential for fruit
108 peel decontamination. The antimicrobial effect of aPDT comprises the combination of
109 three non-toxic components *per se*: a photosensitizer (PS), visible light, and molecular
110 oxygen (Deng et al., 2016; Luksiene and Paskeviciute, 2011; Martins et al., 2018;
111 Wainwright et al., 2017). The PS is considered one of the most critical factors of this
112 technique and typically takes non-toxic dyes in the absence of light, like phenothiazines
113 and porphyrins (Maisch, 2009; Oliveira et al., 2009; Wainwright et al., 2017). The
114 activation of an appropriate PS with visible light in the presence of triplet dioxygen
115 ($^3\text{O}_2$), allows the generation of reactive oxygen species (ROS), like singlet oxygen
116 ($^1\text{O}_2$), responsible by the oxidation of microbial targets leading the cell death; these
117 interactions can kill microorganisms through damage in cellular components such as
118 nucleic acid bases (guanine and thymine), amino acids (cysteine, histidine, and
119 tryptophan), proteins, and lipids (Almeida et al., 2015; Brancini et al., 2016; de
120 Menezes et al., 2016; Wainwright et al., 2017; Zudyte and Luksiene, 2019).

121 The efficiency of aPDT using phenothiazines and porphyrins as PS against
122 pathogenic and spoilage microorganisms (de Menezes et al., 2016; Gonzales et al.,
123 2017; Oliveira et al., 2009) and their biofilms (Beirão et al., 2014; Castro et al., 2017;
124 Vieira et al., 2019) have been reported. However, aPDT can be more effective against
125 bacterial spores (negatively charged) if the PS used are positively charged porphyrins
126 (Carvalho et al., 2007; Costa et al., 2008; Minnock et al., 2000; Oliveira et al., 2009;
127 Tomé et al., 2007). Also, to enhance aPDT efficiency, inorganic salts such as
128 potassium iodide (KI) have been proposed (Freire et al., 2016; Huang et al., 2018a;
129 Santos et al., 2019; Vecchio et al., 2015; Wen et al., 2017; Yuan et al., 2020; Zhang et

130 al., 2015). KI has low toxicity and an accepted chemical for medical studies (Hamblin,
131 2017).

132 Therefore, the objective of the present study was to evaluate the effectiveness of
133 aPDT against *A. acidoterrestris* spores in three matrices: phosphate buffer (PBS),
134 orange juice, and orange peel. The treatments were performed in the presence of the
135 tetracationic porphyrin 5,10,15,20-tetrakis(1-methylpyridinium-4-yl) porphyrin tetra-
136 iodide (Tetra-Py⁺-Me) or of new methylene blue (NMB; a phenothiazinium dye) using
137 a white light-emitting diode (LED) to activate the PSs. The combined effect of aPDT
138 and KI in orange juice and peel contaminated with *A. acidoterrestris* spores was also
139 assessed. Lastly, the impact on nutritional and colorimetric characteristics of orange
140 juice and peel after the aPDT was also determined.

141 **2. Materials and Methods**

142 **2.1. Spore cultivation and growth conditions**

143

144 The strain *A. acidoterrestris* (DSM2498) used in this study was obtained from the
145 Leibniz Institute DSMZ – German Collection of Microorganisms and Cell Cultures. The
146 growth of viable cells was performed in two Petri plates containing yeast starch glucose
147 agar (YSG-A; in g/L: yeast extract – 2.0 [Kasvi, Italy]; soluble starch – 2.0 [Merck,
148 Germany]; glucose – 1.0 [Sigma, USA]; pH 3.7 ± 0.1), followed by incubation at 45 °C
149 for up to 3 days. The cells obtained were added to 10 mL of YSG broth (YSG-B)
150 (formulated as YSG-A without agar; pH 3.7 ± 0.1) and incubated at 45 °C for 24 h. One
151 mL from the grown broth was spread on YSG-A Petri plates (pH 3.7 ± 0.1)
152 supplemented with manganese sulfate at 10 ppm (Merck, Germany). After inoculation,
153 the plates were incubated at 45 °C for 28 days as previously described (Pflug, 1999)
154 with modifications. The sporulation progress was frequently verified through malachite
155 green staining. After incubation, the cell mass was gently collected scraping the agar
156 surface with sterile deionized water followed by centrifugation (1500 × *g* for 20 min at
157 4 °C). After five rounds of centrifugation, the spore suspension was resuspended in
158 sterile deionized water and heat-shocked (80 °C for 10 min) to kill any vegetative cells
159 and enumerate the initial concentration of the spores and, finally, stored at – 80 °C
160 (Ultra Freezer MDF U73V; Sanyo, Japan) until further use. The concentration of the
161 spore suspension was 2.0 × 10⁸ spores/mL.

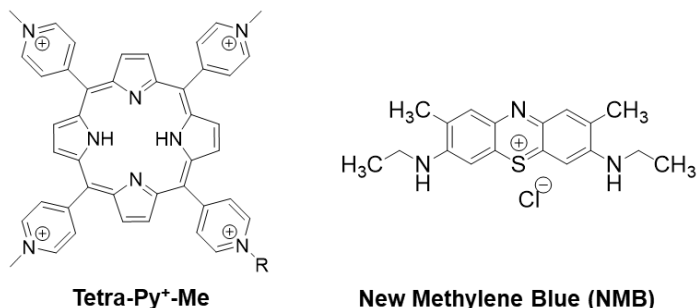
162

163 **2.2. Photosensitizers**

164

165 The photosensitizers (PSs; Figure 1) used in this study were: 5,10,15,20-tetrakis(1-
166 methylpyridinium-4-yl) porphyrin tetraiodide (Tetra-Py⁺-Me) and the phenothiazinium
167 dye new methylene blue N (NMB) which were purchased from Sigma-Aldrich, Inc. (St.
168 Louis, MO, USA). The porphyrin was prepared according to previously reported in the
169 literature, and the purity was confirmed by thin-layer chromatography and ¹H NMR
170 spectroscopy (Simões et al., 2016). For Tetra-Py⁺-Me, a stock solution at 500 μM in
171 dimethyl sulfoxide (DMSO) was prepared while for NMB, the stock solution at the same

172 concentration was prepared in phosphate-buffered saline (PBS; pH 7.4). Before each
173 experiment, the PSs stock solutions were sonicated for 30 min at room temperature
174 (Ultrasonic Bath, Nahita, China).



175

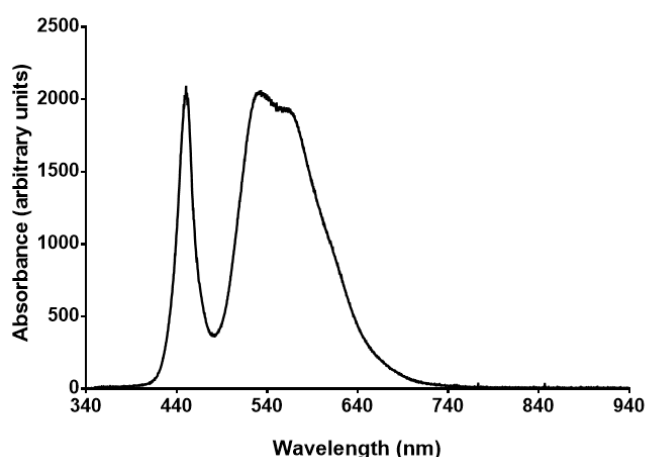
176 **Figure 1.** Chemical structures of the PSs used in this study.

177

178 **2.3. Light source**

179

180 The irradiations during the aPDT assays were performed in the presence of a white
181 light-emitting diode (LED; Inspire, China) at a light irradiance of 140 mW/cm² or 65
182 mW/cm² and a wavelength range between 400 and 740 nm (Figure 2). The aPDT
183 experiments were also carried out under solar radiation. Samples were exposed to
184 natural solar radiation during sunny days at light irradiances ranging from 25 to 65
185 mW/cm². Exposures were conducted during the summer of 2019 in the Faculty of Food
186 Engineering of the University of Campinas – São Paulo, Brazil (22°49'13.2168" S,
187 47°4'3.3924" W). All light measurements were performed using an energy meter
188 (FieldMaxII-TOP; Coherent, USA) combined with a high-sensitivity thermopile sensor
189 (PowerSens – PS19Q; Coherent, USA) as previously detailed (Martins et al., 2018).



190
191 **Figure 2.** The spectrum of absorbance of the white light-emitting diode (LED).
192

193 **2.4. Antimicrobial photodynamic treatments**

194 195 **2.4.1. *In vitro* photoinactivation of *A. acidoterrestris* spores**

196
197 Experiments were performed in sterile 12-well flat-bottomed plates (NEST
198 Biotechnology, China), containing a volume of each PSs to obtain a final concentration
199 of 10 μ M (Tetra-Py⁺-Me and NMB). The wells were inoculated with *A. acidoterrestris*
200 suspension of spores to achieve a final concentration of 10⁷ spores/mL. Plates were
201 kept in the dark for 30 min at 25 °C under agitation (100 rpm) and then exposed for up
202 to 6 h using the white light (140 mW/cm²). Light (LC) and dark controls (DC) were
203 prepared in parallel to determine the effects of the light and PS separately,
204 respectively. After the exposures, samples of 100 μ L were taken every hour and
205 submitted to heat shock (80 °C for 10 min) to stimulate the spore germination (Ferrario
206 and Guerrero, 2018; Prado et al., 2019). The counts of *A. acidoterrestris* spores were
207 determined by pour plating the serial diluted samples onto YSG-A (pH 3.7 \pm 0.1),
208 following incubation at 45 °C for 72 h. The counts of *A. acidoterrestris* were performed
209 in duplicate and expressed as spores/mL. At least three independent experiments
210 were performed for each condition.

211

212 **2.4.2. Photoinactivation of *A. acidoterrestris* spores in orange juice**

213

214 The experiments were performed with orange juice (UHT) purchased from a
215 local market in Aveiro – Portugal. The pH and °Brix values of the juice extracted from
216 the orange were measured using a pH meter (EDGE, Hanna Instruments, USA) and a
217 refractometer (PAL-1, Atago, Japan), respectively. The experiments were conducted
218 as previously described for PBS experiments (section 2.4.1) with some modifications:
219 (i) the PSs were tested in the absence and presence of KI (100 mM); (ii) the plates
220 were irradiated for up to 10 h using the white light provided by the LED at a light
221 irradiance of 140 mW/cm²; and (iii) the LC and DC controls were prepared in the
222 presence of KI (100 mM). The concentration of *A. acidoterrestris* spores in orange juice
223 was 10⁵ spores/mL.

224

225 **2.4.3. Photoinactivation of *A. acidoterrestris* spores on orange peel**

226

227 The experiments were performed with orange peels portions from fresh oranges
228 purchased from a local market in Aveiro – Portugal, under different light sources: an
229 artificial light source (white light) and sunlight, both at light irradiance of 65 mW/cm².

230 The orange peel portions (Figure 3) were cleaned with 70% alcohol and exposed
231 to ultraviolet (UV) irradiation for 15 min inside a laminar flow cabinet, before each
232 experiment. The orange peel portions were placed on sterile 12-well flat-bottomed
233 plates (NEST Biotechnology, China). The suspension of spores of *A. acidoterrestris*
234 and Tetra-Py⁺-Me were spread superficially to each orange peel portion to obtain a
235 final concentration of 10⁶ – 10⁷ spores/mL. Firstly, the aPDT with Tetra-Py⁺-Me at 10
236 μM in the presence and absence of KI was assessed. A higher concentration of Tetra-
237 Py⁺-Me (50 μM) without the addition of KI has also evaluated accordingly to previous
238 studies (Martins et al., 2018). One orange peel sample was used for each time. The
239 orange peels were kept in the dark 30 min for pre-incubation. Light (LC) and dark (DC)
240 controls were carried out simultaneously to the treatment. Sample and LC were
241 irradiated for 6 h while DC was kept in the dark. Three orange peel portions (sample,
242 LC, and DC) were washed in beaker glass with 5 mL of PBS with agitation (100 rpm)

243 for 30 min in the dark before and after exposure. After washing, *A. acidoterrestris*
 244 spores counts in the orange peels portions was performed as previously described in
 245 the section 2.4.1.

246



247

248 **Figure 3.** Representation of the orange peel (A) and the cuts in the 12-well plate
 249 (B).

250

251 2.5. Colorimetric analysis

252

253 Orange juice and peel color coordinates (L^* , a^* , b^*) were measured using a
 254 spectrophotometer (Color Quest II, Hunter Lab, USA) according to Fundo et al., 2019
 255 with adaptations. The equipment was calibrated before every experiment with a blank
 256 calibration tile. A total of 50 mL of orange juice in a glass colorimeter cell or an orange
 257 peel portion ($\varnothing \approx 2.1$ cm) were appropriately placed in the equipment. Three readings
 258 were performed for each sample, always with the same experimental conditions. The
 259 color change was expressed by the coordinates L^* , a^* , and b^* according to the Hunter
 260 Lab color scale. The parameter L^* is responsible for the whiteness value from black
 261 (0) to white (100). The chromaticity from green (-) to red (+) and from blue (-) to yellow
 262 (+) is related to the parameter a^* and b^* , respectively. Total color change (ΔE) was
 263 calculated according to Eq. (1) Furthermore, it is used to evaluate the color changes
 264 of untreated and light-exposed samples (Ihns et al., 2011). Higher ΔE values indicate
 265 a more pronounced color change (Fundo et al., 2019).

266

$$\Delta E = \sqrt{(L_0^* - L^*)^2 + (a_0^* - a^*)^2 + (b_0^* - b^*)^2} \quad Eq. 1$$

267

268 In equation 1, the number "0" is the initial color values from untreated juice

269 samples.

270 **2.6. Total phenolics content and antioxidant capacity of orange juice after**
271 **aPDT.**

272

273 **2.6.1. Total phenolic content**

274

275 The total phenolic content of orange juice after aPDT was measured by the
276 Folin-Ciocalteu method, according to Ainsworth and Gillespie (2007), with minor
277 modification. Aqueous dilutions of orange juice (500 μL) were mixed with 10-fold
278 diluted Folin-Ciocalteu reagent (2.5 mL). After 5 min, 7.5% sodium carbonate solution
279 (2.0 mL) was added, and the absorbance was measured at 750 nm in a
280 spectrophotometer (DU-640TM, Beckman-Coulter, CA, USA). The total phenolic
281 content was quantified using a standard curve of gallic acid, ranging from 15 to 300
282 $\mu\text{g/mL}$. Results were expressed as μg of gallic acid equivalents (GAE) per mL of
283 orange juice.

284

285 **2.6.2. Antioxidant capacity**

286

287 **2.6.2.1. DPPH scavenging activity**

288 2,2-Diphenyl-1-(2,4,6-trinitrophenyl)hydrazyl (DPPH) radical-scavenging
289 activity was measured according to Brand-Williams et al., 1995 method, with
290 modifications. Briefly, 50 μL of ethanolic dilutions of orange juice was mixed with 250
291 μL of DPPH solution (0.004% w/v) in transparent 96-well microplate (Costar,
292 Cambridge, MA, USA). After 30 min reaction, the absorbance was measured at 517
293 nm in a microplate reader (NOVOstar BMG Labtech®, Offenburg, Germany).
294 Antioxidant capacity was determined using a standard curve of 6-hydroxy-2,5,7,8-
295 tetramethylchroman-2-carboxylic acid (Trolox), ranging from 12.5 to 250 μM . Results
296 were expressed as μg of Trolox equivalent per mL of orange juice.

297

298 **2.6.2.2. ABTS^{•+} scavenging capacity**

299

300 The 2,2-azino-bis(3-ethylbenzothiazoline)-6-sulfonic acid (ABTS) scavenging
301 capacity was determined, according to Le et al., (2007). The solution of ABTS^{•+} was
302 prepared by reacting 5 mL of aqueous ABTS solution (7 mM) with 88 µL of potassium
303 persulfate (140 mM) and incubated in the dark at room temperature for 16 h. The assay
304 was performed by mixing 200 µL of the diluted orange juice and 1000 µL of ABTS^{•+}
305 solution. After 6 min of reaction, the solution absorbance was measured at 734 nm in
306 a spectrophotometer (DU-640™, Beckman-Coulter, CA, USA). Antioxidant capacity
307 was determined using a standard curve of Trolox, ranging from 10 to 250 µM. Results
308 were expressed as µg of Trolox equivalent per mL of orange juice.

309

310 **2.6.2.3. Oxygen Radical Absorbance Capacity (ORAC)**

311

312 The Oxygen Radical Absorbance Capacity (ORAC) assay was performed
313 according to Dávalos et al. (2004) and Prior et al. (2003). The reaction was carried out
314 in phosphate buffer (75 mM, pH 7.4), at 37 °C, using fluorescein as a fluorescent probe
315 and 2,2'-azobis(2-methylpropionamide) dihydrochloride (APPH) as a free radical
316 generator. The diluted orange juice (20 µL) was added to a black-walled 96-well
317 microplate, followed by the addition of fluorescein (120 µL, 70 mM) and APPH (60 µL,
318 12 mM). The fluorescence was monitored every 60 s cycle, for 80 cycles, in a
319 microplate reader, at 485 nm of excitation and 520 nm of emission. Results were
320 determined by the difference of the areas under fluorescein decay curves of samples
321 and blank. A calibration curve using Trolox (15 to 1500 µM) was obtained, and the
322 results were expressed as µg of Trolox equivalent per mL of orange juice.

323

324 **2.7. Statistical analysis**

325

326 All graphics and data analyses were performed using GraphPad Prism 6
327 (GraphPad Software, USA). The statistical difference between treatments was
328 analyzed by one-way analysis of variance (ANOVA) followed by Tukey's *post hoc* test
329 and *t*-test at 95% of significance. A value of $p < 0.05$ was considered significant. At
330 least three independent experiments were performed for each condition.

331 3. Results

332

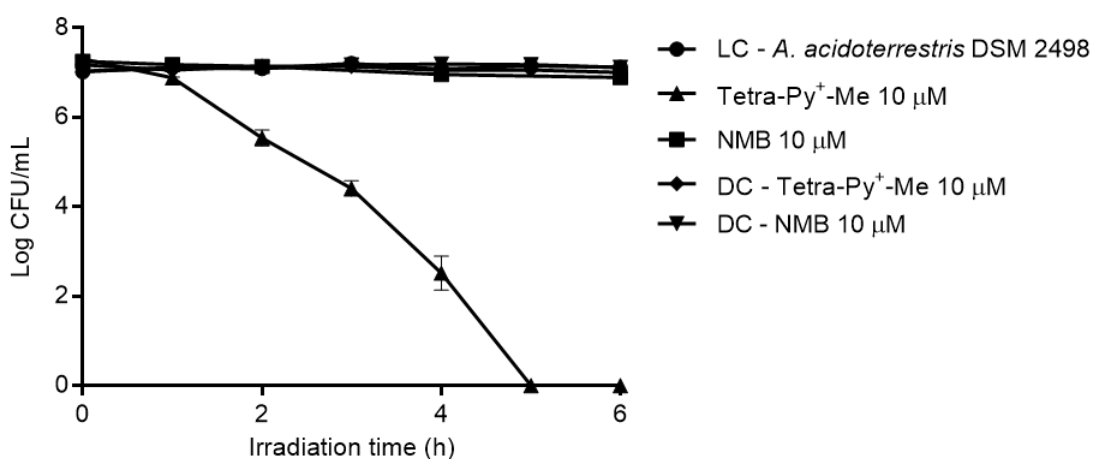
333 3.1. aPDT of *Alicyclobacillus* spores

334

335 3.1.1. *In vitro* photoinactivation of *A. acidoterrestris* spores

336

337 The effect of aPDT with Tetra-Py⁺-Me and NMB on the viability of *A. acidoterrestris*
 338 spores are shown in figure 4. The spores were incubated in the dark with the PSs (10
 339 μM) in PBS for 30 min before exposition to artificial white light (140 mW/cm²). The
 340 inactivation curves were expressed in terms of logarithmic spore viability per milliliter
 341 of PBS (log spores/mL) after heat-shock. Exposure only to the artificial white light
 342 source (LC) did not reduce the viability of *A. acidoterrestris* spores. In the absence of
 343 light (dark control), both PSs at 10 μM also did not affect the viability of the spores.
 344 aPDT with the porphyrin Tetra-Py⁺-Me (at 10 μM) was able to deliver 7 log CFU/mL
 345 reductions ($p < 0.05$) of the spores after 5 h of light exposition. No significant spore
 346 viability reduction was observed after aPDT with NMB at 10 μM (Figure 4; $p > 0.05$).
 347 Additionally, photodegradation of the NMB in the course of aPDT treatment has been
 348 observed through the experiment (data not shown).



349

350 **Figure 4.** Inactivation curve of *A. acidoterrestris* spores in PBS after aPDT with Tetra-
 351 Py⁺-Me and NMB at 10 μM using white LED (400-740 nm) at an irradiance of 140
 352 mW/cm² for up to 6 h. DC: Dark Control; LC: Light Control. Error bars represent the

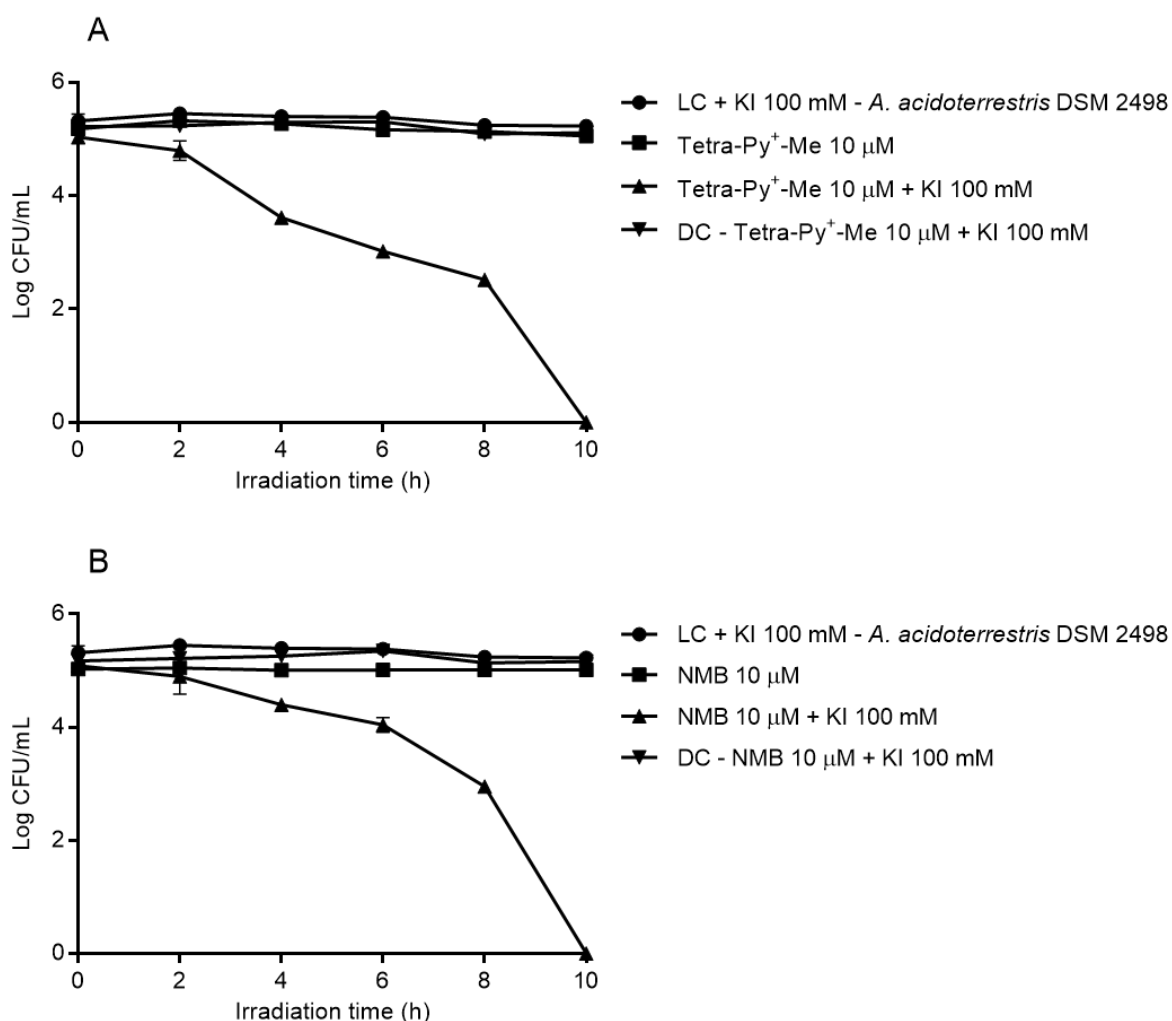
353 standard deviation (SD) of three independent experiments and in some cases are
354 hidden by the symbols.

355

356 **3.1.2. Photoinactivation of *A. acidoterrestris* spores in orange juice**

357

358 Figure 5 shows the aPDT inactivation of *A. acidoterrestris* spores artificially
359 inoculated in orange juice (pH 3.9; 11 °Brix) in the presence and the absence of KI.
360 Also, in this case, the light (LC) and dark (DC) controls in the presence of KI did not
361 affect the viability of *A. acidoterrestris* spores. The results showed no reduction in
362 spore's viability when the aPDT assays were performed in the presence of Tetra-Py⁺-
363 Me or NMB at 10 µM in the absence of KI. It is worth to mention that, the
364 photodegradation of NMB in the absence of KI was detected in the orange juice
365 experiments, as observed in the previous trials in PBS. The inactivation of *A.*
366 *acidoterrestris* spores in orange juice by aPDT was only observed with Tetra-Py⁺-Me
367 and NMB in the presence of KI. The treatment of orange juice inoculated with *A.*
368 *acidoterrestris* spores resulted in 5 log CFU/mL after 10 h of light exposure in the
369 presence of each PS combined with KI (Figure 5).



370

371 **Figure 5.** Inactivation curves of *A. acidoterrestris* spores artificially inoculated in
 372 orange juice during aPDT with Tetra-Py⁺-Me (A) and NMB (B) at 10 µM with or without
 373 KI using white LED (400-740 nm) at an irradiance of 140 mW/cm² for 10 h. DC: Dark
 374 Control with KI; LC: Light Control with KI. Error bars represent the SD of three
 375 independent experiments and in some cases are hidden by the symbols.

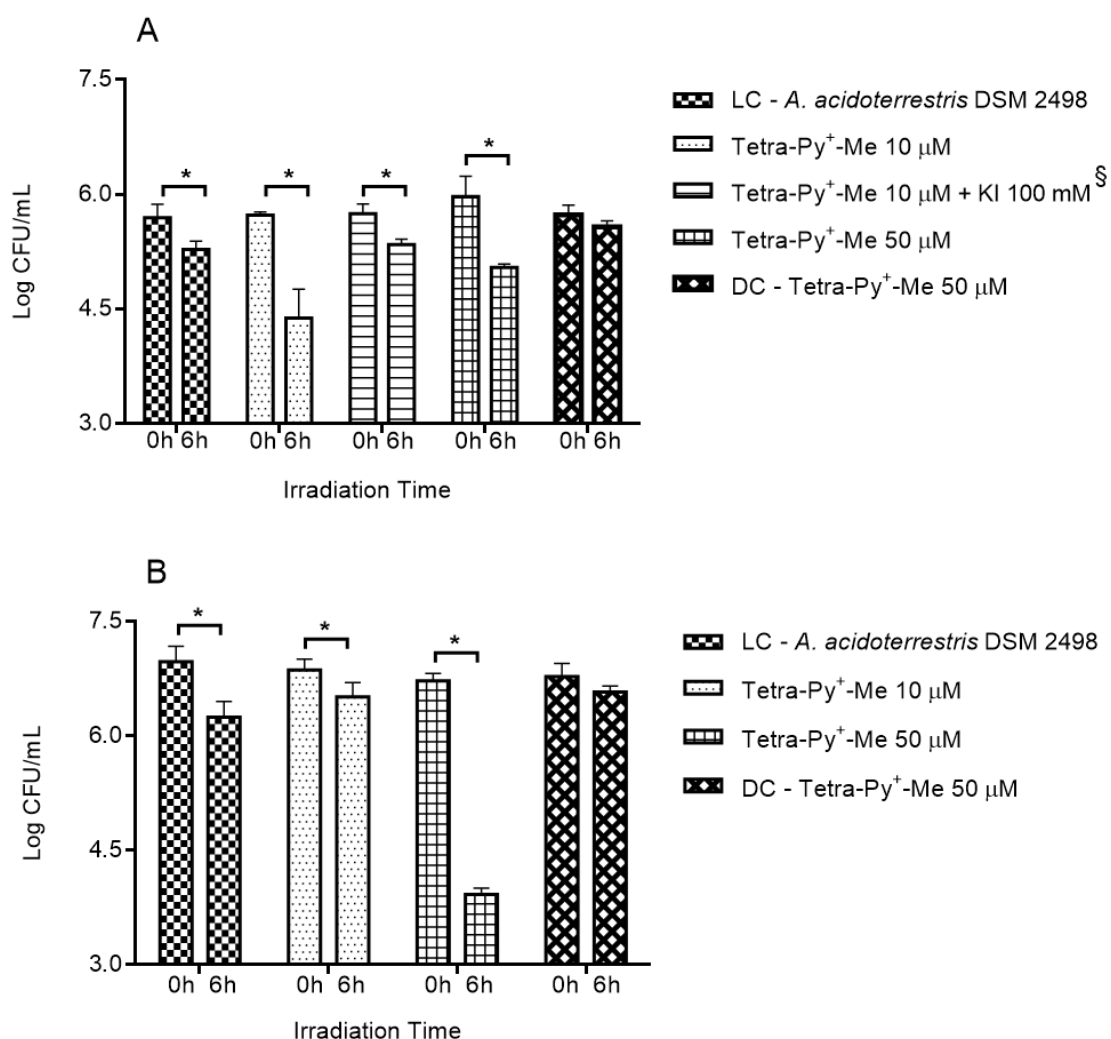
376 **3.1.3. Photoinactivation of *A. acidoterrestris* spores on orange peel**

377

378 Two concentrations of Tetra-Py⁺-Me (10 and 50 μ M) were used to evaluate the
379 photoinactivation *A. acidoterrestris* spores on the surface of orange peels. The higher
380 concentration of this PS was used due to the complexity of the matrix and the condition
381 of the experiment (without agitation) and also based on previous studies (Jesus et al.,
382 2018; Martins et al., 2018). Since in the experiments with PBS and orange juice, it was
383 observed the photodegradation of NMB, this PS was not included in these assays.
384 These studies were conducted using artificial white light and solar radiation at 65
385 mW/cm² (Figure 6A and Figure 6B, respectively).

386 The results achieved with white light had shown that, in the absence of light (DC),
387 Tetra-Py⁺-Me at 50 μ M did not significantly affect the viability of *A. acidoterrestris*
388 spores on orange peel (Figure 6A). However, 1.3 and 0.9 log CFU/mL reductions ($p <$
389 0.05) were achieved with treatments at 10 and 50 μ M of Tetra-Py⁺-Me, respectively.
390 Moreover, in this study, no evidence of the KI potentiation effect was observed.

391 The assays with Tetra-Py⁺-Me at 10 and 50 μ M were also done under sunlight
392 irradiation aiming to assess a possible application of aPDT in orange groves. Thus,
393 orange peels artificially contaminated with *A. acidoterrestris* spores were exposed to
394 aPDT with Tetra-Py⁺-Me at 50 μ M using sunlight (at an irradiance of 65 mW/cm²) as a
395 light source for 6 h. The results are presented in figure 6B and showed that treatment
396 only with the PS (DC) did not reduce the viability of the spores; however, exposures to
397 solar radiation for 6 h reduced the viability of *A. acidoterrestris* spores by 2.8 log
398 CFU/mL ($p <$ 0.05) with Tetra-Py⁺-Me at 50 μ M. A slight significant reduction in spore
399 viability by 0.3 and 0.7 log CFU/mL were observed in aPDT with Tetra-Py⁺-Me at 10
400 μ M and LC, respectively (Figure 6B, $p <$ 0.05).



401

402 **Figure 6.** aPDT of *A. acidoterrestris* spores artificially inoculated in orange peels by
 403 Tetra-Py⁺-Me at 10 and 50 μM using white light (A; 400-740 nm) and sunlight (B)
 404 exposition at an irradiance of 65 mW/cm² for 6 h. DC: Dark Control; LC: Light Control.
 405 Error bars represent the SD of three independent experiments and in some cases are
 406 hidden by the symbols. *Significantly different according to t-test ($p < 0.05$). [§]KI was
 407 tested with Tetra-Py⁺-Me at 10 μM only in white light exposures.

408 3.2. Colorimetric analysis

409

410 The effects of exposure to light, in the absence of PS, are presented in Table 1.

411 The presence of both PS visually altered the characteristics of the juice (data not

412 shown). Moreover, our results clearly showed a significant change in the color

413 coordinates (L^* , a^* , b^*) for orange juice and peel after only light exposure for 6 and 10

414 h. ΔE was calculated to assess the magnitude of the orange juice (20.9 ± 0.314) and

415 peel color changes after white light (8.31 ± 1.25) and sunlight (23.4 ± 0.281) exposures.

416

417 **Table 1.** Estimated color parameters for untreated and light-exposed orange juice

418 and peel during 10 and 6 hours, respectively.

Sample	Treatment	L^*	a^*	b^*	ΔE^\dagger
Orange juice	Untreated	42.0 ± 0.535^b	2.17 ± 0.064^a	21.1 ± 0.488^a	-
	White light	48.7 ± 0.217^a	-3.31 ± 0.021^b	1.98 ± 0.021^b	20.9 ± 0.314
Orange peel	Untreated	61.0 ± 0.467^b	-1.74 ± 1.21^b	52.7 ± 0.022^b	-
	White light	66.0 ± 0.380^a	3.11 ± 0.280^a	57.2 ± 0.353^a	8.31 ± 1.25
	Untreated	59.7 ± 0.137^b	-4.53 ± 0.299^b	52.4 ± 0.615^a	-
	Sunlight	61.6 ± 0.038^a	12.8 ± 0.686^a	36.9 ± 1.46^b	23.4 ± 0.281

419 $\dagger \Delta E$, total color change.

420 The values are average \pm SD. For a given parameter, values with different letters differ significantly ($p < 0.05$)

421

422 3.3. Phenolic content and antioxidant capacity of orange juice exposed to 423 light

424

425 The effect of exposure to light on total phenolic content (TPC) and antioxidant

426 capacity of orange juice are presented in figure 7. Results clearly show that there is a

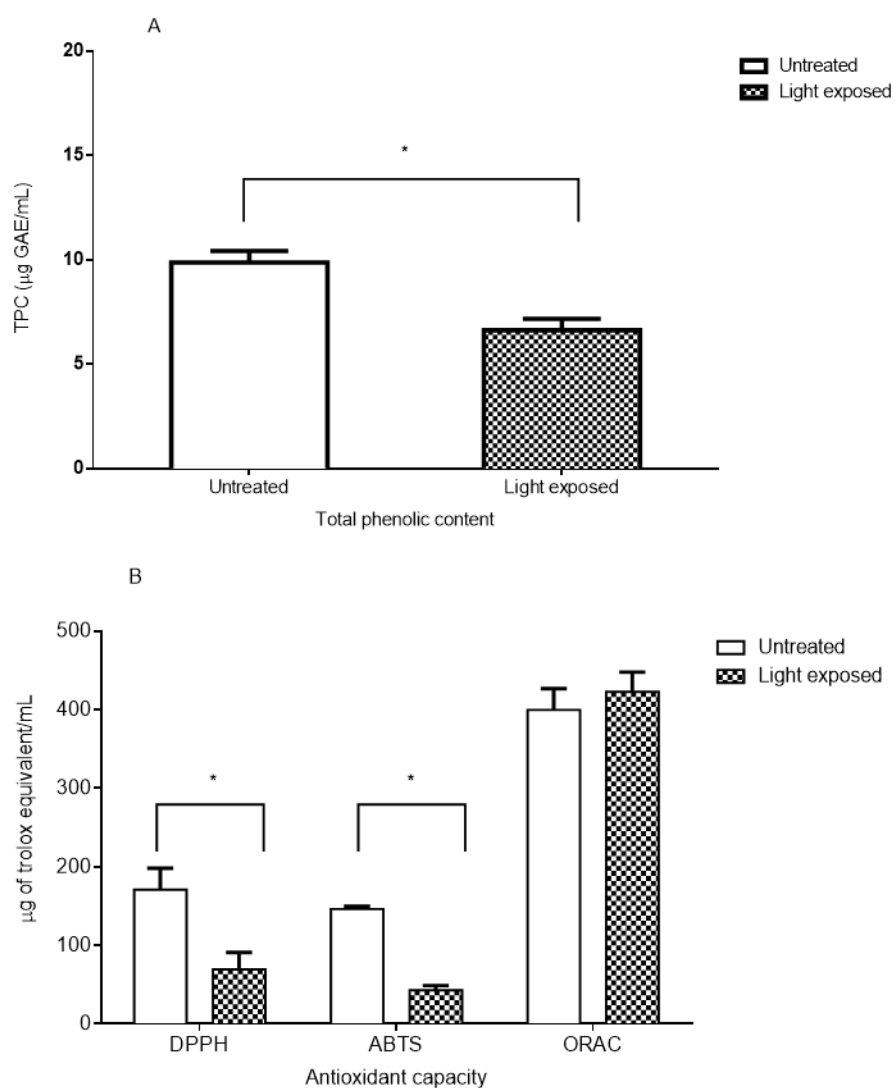
427 significant decrease of $3.25 \mu\text{g GAE/mL}$ in TPC of light exposed orange juice

428 compared to the control (Figure 7-A; $p < 0.05$). The antioxidant capacity of the juice

429 was also significantly reduced in terms of DPPH and ABTS scavenging activity,

430 whereas no significant alteration was detected by the ORAC assay (Figure 7-B; $p >$

431 0.05).



432

433 **Figure 7.** Effect of light exposition using white LED (400-740 nm) on the total phenolic

434 content (A) and antioxidant capacity (B) in orange juice.

435 **4. Discussion**

436

437 In the present study, the inactivation efficiency of aPDT towards *A. acidoterrestris*
438 spores using Tetra-Py⁺-Me and NMB as PSs have been evaluated. As far as the
439 author's best knowledge, this is the first study to demonstrate the application of aPDT
440 towards inactivation of *Alicyclobacillus* spp. spores. This study was initially performed
441 *in vitro* (PBS) under artificial white light irradiation using both PSs at 10 µM. This
442 concentration was chosen based on previous studies which demonstrated its
443 effectiveness against *B. cereus* spores (Oliveira et al., 2009) and prevented the
444 aggregation of the PSs (Fernández-Pérez et al., 2019). The maximum efficiency of *A.*
445 *acidoterrestris* spores inactivation was achieved with Tetra-Py⁺-Me at 10 µM (Figure
446 4). On the contrary, no photoinactivation of *A. acidoterrestris* spores using NMB at the
447 same concentration was observed in PBS (Figure 4). The observed photodegradation
448 of NMB during the long light exposures may be one of the reasons for the low efficiency
449 of aPDT with this PS. The photodegradation of phenothiazine dyes may occur during
450 single oxygen production after exposure to visible light (Nassar et al., 2019).

451 Previous studies have already demonstrated the effectiveness of aPDT to reduce
452 the load of viruses (3-8 log PFU/mL), bacteria (3-8 log CFU/mL) and fungi (0.8-5 log
453 CFU/mL) (Beirão et al., 2014; Castro et al., 2017; da Silva et al., 2012; de Menezes et
454 al., 2016; Freire et al., 2016; Huang et al., 2018b; Oliveira et al., 2009; Santos et al.,
455 2019; Sousa et al., 2019; Vieira et al., 2019; Wen et al., 2017; Wu et al., 2015; Yuan
456 et al., 2020). For instance, aPDT mediated by Tetra-Py⁺-Me caused from 3 to 6 log
457 CFU/mL reductions of single-species and mixed biofilms of *Staphylococcus aureus*,
458 *Pseudomonas aeruginosa*, and *Candida albicans* (Beirão et al., 2014). Biofilms are
459 known as structures of persistence of microorganisms in food processing
460 environments (Galié et al., 2018). When in biofilms, microbial inactivation becomes
461 harder (Bridier et al., 2011). Therefore, the efficiency of aPDT for inactivation of
462 microorganisms in biofilms may suggest this technology may also be effective on
463 spore-forming bacteria inactivation. For instance, studies involving porphyrin
464 derivatives have demonstrated that aPDT using Tetra-Py⁺-Me as PS led to up 3.5 log
465 CFU/mL reductions of *Bacillus cereus* spores (Oliveira et al., 2009). Therefore, given

466 the effectiveness of aPDT towards *A. acidoterrestris* inactivation *in vitro* conditions,
467 further tests were conducted in orange juice.

468 Given the complexity of the orange juice compared to PBS (*e.g.* turbidity), the
469 presence and absence of KI was assessed, since it was expected that the
470 photodynamic effect would be reduced (Sousa et al., 2019). The aPDT treatment with
471 Tetra-Py⁺-Me and NMB at 10 μM in the presence of KI in orange juice resulted in up
472 to 5 log CFU/mL of *A. acidoterrestris* spores (Figure 5).

473 Since the use of KI as a potentiator agent of the aPDT effect was introduced
474 (Vecchio et al., 2015; Zhang et al., 2015), several studies have been conducted to
475 confirm such action on different microorganisms and microbial structures (Freire et al.,
476 2016; Huang et al., 2018a; Vieira et al., 2018, 2019; Wen et al., 2017). In these reports,
477 the authors concluded that KI potentiates the photodynamic effects in most cases,
478 increasing the inactivation of microorganisms for up to 6 log CFU/mL reductions.
479 According to these authors, this potentiation is due to the reaction of KI with ¹O₂
480 affording the production of longer-lived reactive species as free iodine and triiodide (I_2
481 / I_3^-) and also the production of short-lived species such as reactive iodine radicals
482 (I_2^{\bullet}). The production of these species contributes to the remaining microbial
483 inactivation after aPDT (Vieira et al., 2019). In the current study the potentiation effect
484 of KI for both PSs in the inactivation of *A. acidoterrestris* spores was observed since
485 no reduction was detected in the absence of KI (Figure 5). The inefficiency of the aPDT
486 with the PSs in the absence of KI may be explained by the presence of organic
487 compounds in the orange juice. The ROS and ¹O₂ are preferentially acting on the
488 oxidation of organic compounds of the beverage. In the presence of KI, ¹O₂ is
489 consumed to form the iodine species that are capable of destroying *A. acidoterrestris*
490 spores.

491 Even though there is a lack of studies on the use of aPDT for the inactivation of *A.*
492 *acidoterrestris* in fruit juices, other light-based technologies have been employed with
493 that purpose. For instance, UV-C radiation has been found to cause a reduction (log
494 CFU/mL) in *A. acidoterrestris* spores of 2 in apple juice and 5.5 in grape juice by Baysal
495 et al. (2013), 5 in apple juice by Tremarin et al. (2017) and 4.7 in melon juice by Fundo
496 et al. (2019). The differences in inactivation efficiency observed amongst the different

497 juices may be explained by the difference in their turbidity, which may impact on light
498 penetration. For instance, the higher turbidity of apple juice is known to limit light
499 penetration, resulting in overall lower number of decimal reductions of *A.*
500 *acidoterrestris* spores. On the other hand, the lower turbidity of grape juice facilitates
501 the penetration of light and the inactivation of *A. acidoterrestris* spores (Baysal et al.,
502 2013). These findings highlight that aPDT can also deliver up ≈ 5 log CFU/mL
503 reductions of *A. acidoterrestris* spores under *in vitro* conditions, despite the much
504 higher intensity (140 mW/cm²) and exposure time to light (10 h) employed.
505 Furthermore, the similar number of decimal reductions of *A. acidoterrestris* spores
506 obtained by aPDT (Figure 4) and UV-C (Baysal et al., 2013; Fundo et al., 2019;
507 Tremarin et al., 2017), despite the difference in the age (and resistance) of spores
508 used (28 days and 2-10 days, respectively), highlight the potentials of this technology
509 for the inactivation of this bacterium. Despite the longer times to reach similar number
510 of decimal reductions, another advantage of using visible light sources (such in aPDT)
511 is that aPDT does not present risks to the operator's health (Guerrero-Beltrán and
512 Barbosa-Cánovas, 2004). Nonetheless, aPDT efficiency and reduction of exposure
513 time can be further enhanced by the combination of non-toxic compounds with the PS.

514 The use of aPDT as an inactivation method for pathogenic and spoilage
515 microorganisms in fruit juices is rare. However, recently, the combination of ultrasound
516 (US) and aPDT for inactivation of *Escherichia coli* and *S. aureus* in orange juice has
517 been evaluated (Bhavya and Hebbar, 2019). Despite the significant number of decimal
518 reductions of *E. coli* and *S. aureus*, 4.2 and 2.3 log CFU/mL, respectively, a negative
519 impact on the antioxidant capacity has been reported (Bhavya and Hebbar, 2019),
520 corroborating the findings of the current study (Figure 7).

521 The assessment of the light exposures impact on the quality of orange juice was
522 also investigated in order to gain insights into the effects on the color of the juice. The
523 results of this study demonstrated that there was an alteration in all color parameters
524 (L^* , a^* , b^*) of the orange juice after 10 h of white light (LED) exposures, as represented
525 by the ΔE in Table 1. In fact, these analyses were performed aiming to assess the
526 effects of the exposure times to light deemed necessary to result in a certain
527 inactivation of *A. acidoterrestris* spores. Despite this, it has been reported that even a

528 short exposure time (20 min) of melon juice to UV-C radiation resulted in a significant
529 alteration in the L^* coordinate (Fundo et al., 2019). This slight change in the L^*
530 coordinate was linked with the high concentrations of pigments present in the melon
531 juice resulting in a masking effect on the ΔE (Taze et al., 2015). Nevertheless, the
532 impact of aPDT in terms of color varies in the literature depending on the fruit matrix
533 (Bhavya and Hebbar, 2019; Kim et al., 2017; Tao et al., 2019). Whereas a slight
534 change on the color of orange juice was observed with curcumin and blue light (Bhavya
535 and Hebbar, 2019), a positive effect on fresh-cut apples by the use of the same PS
536 (Tao et al., 2019). Contrarily, the absence of the PS allowed change in L^* , a^* , b^*
537 parameters of fresh-cut papaya (Kim et al., 2017). Previous studies also evaluated the
538 impact of aPDT on the antioxidant profile of strawberries, apricots, plums,
539 cauliflowers, and orange juice (Aponiene et al., 2015; Luksiene and Paskeviciute,
540 2011). Although such studies did not show any adverse effect on total phenolic content
541 or antioxidant capacity after only 30 min of light exposure. However, none of these
542 studies have applied the aPDT for long period of light exposure in liquid substrate as
543 in the current study.

544 Given the results obtained from the orange juice experiments, the photoinactivation
545 of *A. acidoterrestris* spores on the surface of orange peels was performed.
546 Remarkably, aPDT caused a reduction ($p < 0.05$) of *A. acidoterrestris* spores (≈ 2.8
547 log CFU/mL) on orange peels when carried out under solar radiation. In other studies,
548 aPDT with LED-light resulted in 1.8 log CFU/mL, 0.95 log CFU/g and 0.6-0.7 log CFU/g
549 reductions of *L. monocytogenes* in artificially inoculated on the surface of strawberries
550 (Luksiene & Pakeuviciute, 2011), *E. coli* on apple slices (Tao et al., 2019) and of *B.*
551 *cereus* on the surface of apricots, cauliflowers, and plums (Aponiene et al., 2015),
552 respectively. However, very high reduction (> 6 log CFU/mL) of *Pseudomonas*
553 *syringae* pv. *actinidiae* has been reported on kiwifruit leaves submitted to aPDT
554 treatment done under solar radiation for 2 cycles of 90 min (Martins et al., 2018). This
555 finding reinforces that solar radiation seems to be crucial in enhancing the inactivation
556 efficiency of aPDT with PSs. The higher efficiency of aPDT with sunlight for inactivation
557 of *A. acidoterrestris* spores on orange peel than aPDT with white light (LED) can be
558 explained by antimicrobial properties of each source of light. If on one hand, white light

559 (LED) contains only the visible spectrum, which is known to not present antimicrobial
560 effects (Santos et al., 2020), on the other hand, the full-spectrum of solar radiation
561 contains UV rays with known antimicrobial activity (Dias et al., 2018).

562 It is known that the counts of *Alicyclobacillus* spp. in fruits in the trees may reach
563 up to 10^2 spores/Kg (ABECitrus, 1999). As a result, a step of fruit disinfection is
564 currently used to reduce *Alicyclobacillus* spp. spores loads at the beginning of fruit
565 processing. Nonetheless, this step is not able to deliver more than 2 log CFU/mL
566 reductions of *Alicyclobacillus* spp. spores (Orr and Beuchat, 2000). Thus, counts of
567 *Alicyclobacillus* spp. spores in fruit products after processing of up to 10^2 - 10^3
568 spores/mL have been reported (ABECitrus, 1999). Consequently, this level of
569 contamination is enough for this bacterium to germinate, grow and further cause juice
570 spoilage if storage conditions are appropriate leading to severe losses (Spinelli et al.,
571 2009), highlighting that controlling strategies to reduce the counts of this bacterium
572 prior to processing are needed. Therefore, the ≈ 3 log CFU/mL reductions of *A.*
573 *acidoterrestris* spores on orange peels caused by aPDT under solar radiation
574 comprises a remarkable finding. This technology could be applied in practice directly
575 in the fruits in the trees exposed to abundant sunlight. As such, it emerges as a feasible
576 strategy to reduce the counts of *Alicyclobacillus* spp. spores prior to fruit processing.
577 As such aPDT under solar radiation may contribute to the overall reduction of
578 *Alicyclobacillus* spp. spores throughout the production chain required for the
579 production of shelf-stable orange juice and derived beverages. Besides, with further
580 refinements and enhancements in the inactivation efficiency, aPDT under solar
581 radiation could favor the decrease in the use/concentration of chemical sanitizers. In
582 practice, this technology would allow the reduction of costs as well as contribute with
583 an environmental friendly processing. The current work is the first to evaluate the
584 potential of aPDT as an emerging technology towards inactivation of *A. acidoterrestris*
585 spores.

586 **Acknowledgements**

587

588 This work was supported by: Conselho Nacional de Desenvolvimento Científico e
589 Tecnológico (CNPq; Grants: #140092/2017-0, #302763/2014-7, and #305804/2017-
590 0); Coordenação de Aperfeiçoamento de Pessoal de Nível Superior (CAPES) -
591 Finance Code 001 for the financial support. Thanks are due for the financial support to
592 CESAM Research Unit (UID/AMB/50017/2019 and
593 UIDB/50017/2020+UIDP/50017/2020), QOPNA Research Unit (FCT
594 UID/QUI/00062/2019) and LAQV-REQUIMTE Research Unit (UIDB/50006/2020), to
595 FCT/MCTES through national funds, and the co-funding by the FEDER, within the
596 PT2020 Partnership Agreement and Compete 2020.

597

598 **Conflict of interest**

599

600 The authors declare no competing interests.

601

602 **5. References**

603 ABECitrus, 1999. Acidothermophilic sporeforming bacteria (ATSB) in orange juices:
604 Detection methods, ecology, and involvement in the deterioration of fruit juices. Assoc.
605 Bras. dos Export. Cítricos. URL [http://www.citrusbr.com.br/exportadores-](http://www.citrusbr.com.br/exportadores-citricos/sobre-citrusbr/imagens/ATSB_Abecitrus.pdf)
606 [citricos/sobre-citrusbr/imagens/ATSB_Abecitrus.pdf](http://www.citrusbr.com.br/exportadores-citricos/sobre-citrusbr/imagens/ATSB_Abecitrus.pdf) (accessed 5.15.20).

607 Ainsworth, E.A., Gillespie, K.M., 2007. Estimation of total phenolic content and other
608 oxidation substrates in plant tissues using Folin–Ciocalteu reagent. *Nat. Protoc.* 2,
609 875–877. <https://doi.org/10.1038/nprot.2007.102>

610 Albuquerque, L., Rainey, F.A., Chung, A.P., Sunna, A., Nobre, M.F., Grote, R.,
611 Antranikian, G., Da Costa, M.S., 2000. *Alicyclobacillus hesperidum* sp. nov. and a
612 related genomic species from solfataric soils of Sao Miguel in the Azores. *Int. J. Syst.*
613 *Evol. Microbiol.* 50, 451–457. <https://doi.org/10.1099/00207713-50-2-451>

614 Almeida, A., Faustino, M.A.F., Tomé, J.P.C., 2015. Photodynamic inactivation of
615 bacteria: finding the effective targets. *Future Med. Chem.* 7, 1221–1224.

- 616 <https://doi.org/10.4155/fmc.15.59>
- 617 Aponiene, K., Paskeviciute, E., Reklaitis, I., Luksiene, Z., 2015. Reduction of microbial
618 contamination of fruits and vegetables by hypericin-based photosensitization:
619 Comparison with other emerging antimicrobial treatments. *J. Food Eng.* 144, 29–35.
620 <https://doi.org/10.1016/j.jfoodeng.2014.07.012>
- 621 Baysal, A.H., Molva, C., Unluturk, S., 2013. UV-C light inactivation and modeling
622 kinetics of *Alicyclobacillus acidoterrestris* spores in white grape and apple juices. *Int.*
623 *J. Food Microbiol.* 166, 494–498. <https://doi.org/10.1016/j.ijfoodmicro.2013.08.015>
- 624 Beirão, S., Fernandes, S., Coelho, J., Faustino, M.A.F., Tomé, J.P.C., Neves,
625 M.G.P.M.S., Tomé, A.C., Almeida, A., Cunha, A., 2014. Photodynamic inactivation of
626 bacterial and yeast biofilms with a cationic porphyrin. *Photochem. Photobiol.* 90, 1387–
627 1396. <https://doi.org/10.1111/php.12331>
- 628 Bhavya, M.L., Hebbar, H.U., 2019. Sono-photodynamic inactivation of *Escherichia coli*
629 and *Staphylococcus aureus* in orange juice. *Ultrason. Sonochem.* 57, 108–115.
630 <https://doi.org/10.1016/j.ultsonch.2019.05.002>
- 631 Brancini, G.T.P., Rodrigues, G.B., Rambaldi, M.D.S.L., Izumi, C., Yatsuda, A.P.,
632 Wainwright, M., Rosa, J.C., Braga, G.Ú.L., 2016. The effects of photodynamic
633 treatment with new methylene blue N on the *Candida albicans* proteome. *Photochem.*
634 *Photobiol. Sci.* 15, 1503–1513. <https://doi.org/10.1039/C6PP00257A>
- 635 Brand-Williams, W., Cuvelier, M.E., Berset, C., 1995. Use of a free radical method to
636 evaluate antioxidant activity. *LWT - Food Sci. Technol.* 28, 25–30.
637 [https://doi.org/10.1016/S0023-6438\(95\)80008-5](https://doi.org/10.1016/S0023-6438(95)80008-5)
- 638 Bridier, A., Briandet, R., Thomas, V., Dubois-Brissonnet, F., 2011. Resistance of
639 bacterial biofilms to disinfectants: a review. *Biofouling* 27, 1017–1032.
640 <https://doi.org/10.1080/08927014.2011.626899>
- 641 Carvalho, C.M.B., Gomes, A.T.P.C., Fernandes, S.C.D., Prata, A.C.B., Almeida, M.A.,
642 Cunha, M.A., Tomé, J.P.C., Faustino, M.A.F., Neves, M.G.P.M.S., Tomé, A.C.,
643 Cavaleiro, J.A.S., Lin, Z., Rainho, J.P., Rocha, J., 2007. Photoinactivation of bacteria
644 in wastewater by porphyrins: Bacterial β -galactosidase activity and leucine-uptake as

- 645 methods to monitor the process. *J. Photochem. Photobiol. B Biol.* 88, 112–118.
646 <https://doi.org/10.1016/j.jphotobiol.2007.04.015>
- 647 Castro, K.A.D.F., Moura, N.M.M., Fernandes, A., Faustino, M.A.F., Simões, M.M.Q.,
648 Cavaleiro, J.A.S., Nakagaki, S., Almeida, A., Cunha, Â., Silvestre, A.J.D., Freire,
649 C.S.R., Pinto, R.J.B., Neves, M. da G.P.M.S., 2017. Control of *Listeria innocua* biofilms
650 by biocompatible photodynamic antifouling chitosan based materials. *Dye. Pigment.*
651 137, 265–276. <https://doi.org/10.1016/j.dyepig.2016.10.020>
- 652 Costa, L., Alves, E., Carvalho, C.M.B., Tomé, J.P.C., Faustino, M.A.F., Neves,
653 M.G.P.M.S., Tomé, A.C., Cavaleiro, J.A.S., Cunha, Â., Almeida, A., 2008. Sewage
654 bacteriophage photoinactivation by cationic porphyrins: A study of charge effect.
655 *Photochem. Photobiol. Sci.* 7, 415–422. <https://doi.org/10.1039/b712749a>
- 656 da Silva, R.N., Tomé, A.C., Tomé, J.P.C., Neves, M.G.P.M.S., Faustino, M.A.F.,
657 Cavaleiro, J.A.S., Oliveira, A., Almeida, A., Cunha, Â., 2012. Photo-inactivation of
658 *Bacillus* endospores: inter-specific variability of inactivation efficiency. *Microbiol.*
659 *Immunol.* 56, 692–699. <https://doi.org/10.1111/j.1348-0421.2012.00493.x>
- 660 Dávalos, A., Gómez-Cordovés, C., Bartolomé, B., 2004. extending applicability of the
661 oxygen radical absorbance capacity (ORAC–Fluorescein) assay. *J. Agric. Food Chem.*
662 52, 48–54. <https://doi.org/10.1021/jf0305231>
- 663 de Menezes, H.D., Tonani, L., Bachmann, L., Wainwright, M., Braga, G.Ú.L., von
664 Zeska Kress, M.R., 2016. Photodynamic treatment with phenothiazinium
665 photosensitizers kills both ungerminated and germinated microconidia of the
666 pathogenic fungi *Fusarium oxysporum*, *Fusarium moniliforme* and *Fusarium solani*. *J.*
667 *Photochem. Photobiol. B Biol.* 164, 1–12.
668 <https://doi.org/10.1016/j.jphotobiol.2016.09.008>
- 669 Deng, X., Tang, S., Wu, Q., Tian, J., Riley, W.W., Chen, Z., 2016. Inactivation of *Vibrio*
670 *parahaemolyticus* by antimicrobial photodynamic technology using methylene blue. *J.*
671 *Sci. Food Agric.* 96, 1601–1608. <https://doi.org/10.1002/jsfa.7261>
- 672 Dias, L.P., Araújo, C.A.S., Pupin, B., Ferreira, P.C., Braga, G.Ú.L., Rangel, D.E.N.,
673 2018. The Xenon Test Chamber Q-SUN® for testing realistic tolerances of fungi

- 674 exposed to simulated full spectrum solar radiation. *Fungal Biol.* 122, 592–601.
675 <https://doi.org/10.1016/j.funbio.2018.01.003>
- 676 Evelyn, Kim, H.J., Silva, F.V.M., 2016. Modeling the inactivation of *Neosartorya fischeri*
677 ascospores in apple juice by high pressure, power ultrasound and thermal processing.
678 *Food Control* 59, 530–537. <https://doi.org/10.1016/j.foodcont.2015.06.033>
- 679 Fernández-Pérez, A., Valdés-Solís, T., Marbán, G., 2019. Visible light spectroscopic
680 analysis of Methylene Blue in water; the resonance virtual equilibrium hypothesis. *Dye.*
681 *Pigment.* 161, 448–456. <https://doi.org/10.1016/j.dyepig.2018.09.083>
- 682 Ferrario, M.I., Guerrero, S.N., 2018. Inactivation of *Alicyclobacillus acidoterrestris*
683 ATCC 49025 spores in apple juice by pulsed light. Influence of initial contamination
684 and required reduction levels. *Rev. Argent. Microbiol.* 50, 3–11.
685 <https://doi.org/10.1016/j.ram.2017.04.002>
- 686 Freire, F., Ferraresi, C., Jorge, A.O.C., Hamblin, M.R., 2016. Photodynamic therapy of
687 oral *Candida* infection in a mouse model. *J. Photochem. Photobiol. B Biol.* 159, 161–
688 168. <https://doi.org/10.1016/j.jphotobiol.2016.03.049>
- 689 Friedrich, L.M., Goodrich-Schneider, R., Parish, M.E., Danyluk, M.D., 2009. Mitigation
690 of *Alicyclobacillus* spp. spores on food contact surfaces with aqueous chlorine dioxide
691 and hypochlorite. *Food Microbiol.* 26, 936–941.
692 <https://doi.org/10.1016/j.fm.2009.06.011>
- 693 Fundo, J.F., Miller, F.A., Mandro, G.F., Tremarin, A., Brandão, T.R.S., Silva, C.L.M.,
694 2019. UV-C light processing of Cantaloupe melon juice: Evaluation of the impact on
695 microbiological, and some quality characteristics, during refrigerated storage. *LWT -*
696 *Food Sci. Technol.* 103, 247–252. <https://doi.org/10.1016/j.lwt.2019.01.025>
- 697 Galié, S., García-Gutiérrez, C., Miguélez, E.M., Villar, C.J., Lombó, F., 2018. Biofilms
698 in the food industry: health aspects and control methods. *Front. Microbiol.* 9.
699 <https://doi.org/10.3389/fmicb.2018.00898>
- 700 Gonzales, J.C., Brancini, G.T.P., Rodrigues, G.B., Silva-Junior, G.J., Bachmann, L.,
701 Wainwright, M., Braga, G.Ú.L., 2017. Photodynamic inactivation of conidia of the
702 fungus *Colletotrichum abscissum* on *Citrus sinensis* plants with methylene blue under

- 703 solar radiation. *J. Photochem. Photobiol. B Biol.* 176, 54–61.
704 <https://doi.org/10.1016/j.jphotobiol.2017.09.008>
- 705 Gouws, P. A., Gie, L., Pretorius, A., Dhansay, N., 2005. Isolation and identification of
706 *Alicyclobacillus acidocaldarius* by 16S rDNA from mango juice and concentrate. *Int. J.*
707 *Food Sci. Technol.* 40, 789–792. <https://doi.org/10.1111/j.1365-2621.2005.01006.x>
- 708 Groenewald, W.H., Gouws, P.A., Witthuhn, R.C., 2008. Isolation and identification of
709 species of *Alicyclobacillus* from orchard soil in the Western Cape, South Africa.
710 *Extremophiles* 12, 159–163. <https://doi.org/10.1007/s00792-007-0112-z>
- 711 Groenewald, W.H., Gouws, P.A., Witthuhn, R.C., 2009. Isolation, identification and
712 typification of *Alicyclobacillus acidoterrestris* and *Alicyclobacillus acidocaldarius* strains
713 from orchard soil and the fruit processing environment in South Africa. *Food Microbiol.*
714 26, 71–76. <https://doi.org/10.1016/j.fm.2008.07.008>
- 715 Guerrero-Beltrán, J.A., Barbosa-Cánovas, G. V., 2004. Review: Advantages and
716 limitations on processing foods by UV light. *Food Sci. Technol. Int.* 10, 137–147.
717 <https://doi.org/10.1177/1082013204044359>
- 718 Hamblin, M.R., 2017. Potentiation of antimicrobial photodynamic inactivation by
719 inorganic salts. *Expert Rev. Anti. Infect. Ther.* 15, 1059–1069.
720 <https://doi.org/10.1080/14787210.2017.1397512>
- 721 Hippchen, B., Alfred, R., Poralla, K., 1981. Occurrence in soil of thermo-acidophilic
722 bacilli possessing ω -cyclohexane fatty acids and hopanoids. *Arch. Microbiol.* 129, 53–
723 55.
- 724 Huang, L., El-Hussein, A., Xuan, W., Hamblin, M.R., 2018a. Potentiation by potassium
725 iodide reveals that the anionic porphyrin TPPS4 is a surprisingly effective
726 photosensitizer for antimicrobial photodynamic inactivation. *J. Photochem. Photobiol.*
727 *B Biol.* 178, 277–286. <https://doi.org/10.1016/j.jphotobiol.2017.10.036>
- 728 Huang, Y.Y., Wintner, A., Seed, P.C., Brauns, T., Gelfand, J.A., Hamblin, M.R., 2018b.
729 Antimicrobial photodynamic therapy mediated by methylene blue and potassium iodide
730 to treat urinary tract infection in a female rat model. *Sci. Rep.* 8, 1–9.
731 <https://doi.org/10.1038/s41598-018-25365-0>

- 732 Ihns, R., Diamante, L.M., Savage, G.P., Vanhanen, L., 2011. Effect of temperature on
733 the drying characteristics, colour, antioxidant and beta-carotene contents of two apricot
734 varieties. *Int. J. Food Sci. Technol.* 46, 275–283. [https://doi.org/10.1111/j.1365-
735 2621.2010.02506.x](https://doi.org/10.1111/j.1365-2621.2010.02506.x)
- 736 Jesus, V., Martins, D., Branco, T., Valério, N., Neves, M.G.P.M.S., Faustino, M.A.F.,
737 Reis, L., Barreal, E., Gallego, P.P., Almeida, A., 2018. An insight into the photodynamic
738 approach: Versus copper formulations in the control of *Pseudomonas syringae* pv.
739 *Actinidiae* in kiwi plants. *Photochem. Photobiol. Sci.* 17, 180–191.
740 <https://doi.org/10.1039/c7pp00300e>
- 741 Kim, M.J., Tang, C.H., Bang, W.S., Yuk, H.G., 2017. Antibacterial effect of 405±5nm
742 light emitting diode illumination against *Escherichia coli* O157:H7, *Listeria*
743 *monocytogenes*, and *Salmonella* on the surface of fresh-cut mango and its influence
744 on fruit quality. *Int. J. Food Microbiol.* 244, 82–89.
745 <https://doi.org/10.1016/j.ijfoodmicro.2016.12.023>
- 746 Le, K., Chiu, F., Ng, K., 2007. Identification and quantification of antioxidants in *Fructus*
747 *lycii*. *Food Chem.* 105, 353–363. <https://doi.org/10.1016/J.FOODCHEM.2006.11.063>
- 748 Lee, S.-Y., Gray, P.M., Dougherty, R.H., Kang, D.-H., 2004. The use of chlorine dioxide
749 to control *Alicyclobacillus acidoterrestris* spores in aqueous suspension and on apples.
750 *Int. J. Food Microbiol.* 92, 121–127. <https://doi.org/10.1016/j.ijfoodmicro.2003.09.003>
- 751 Lee, S.-Y., Ryu, S.-R., Kang, D.-H., 2010. Treatment with chlorous acid to inhibit
752 spores of *Alicyclobacillus acidoterrestris* in aqueous suspension and on apples. *Lett.*
753 *Appl. Microbiol.* no-no. <https://doi.org/10.1111/j.1472-765X.2010.02874.x>
- 754 Luksiene, Z., Paskeviciute, E., 2011. Novel approach to the microbial decontamination
755 of strawberries: Chlorophyllin-based photosensitization. *J. Appl. Microbiol.* 110, 1274–
756 1283. <https://doi.org/10.1111/j.1365-2672.2011.04986.x>
- 757 Maisch, T., 2009. A new strategy to destroy antibiotic resistant microorganisms:
758 antimicrobial photodynamic treatment. *Mini-Reviews Med. Chem.* 9, 974–983.
759 <https://doi.org/10.2174/138955709788681582>
- 760 Martins, D., Mesquita, M.Q., Neves, M.G.P.M.S., Faustino, M.A.F., Reis, L., Figueira,

- 761 E., Almeida, A., 2018. Photoinactivation of *Pseudomonas syringae* pv. *actinidiae* in
762 kiwifruit plants by cationic porphyrins. *Planta* 248, 409–421.
763 <https://doi.org/10.1007/s00425-018-2913-y>
- 764 Minnock, A., Vernon, D.I., Schofield, J., Griffiths, J., Parish, J.H., Brown, S.B., 2000.
765 Mechanism of uptake of a cationic water-soluble pyridinium zinc phthalocyanine across
766 the outer membrane of *Escherichia coli*. *Antimicrob. Agents Chemother.* 44, 522–527.
767 <https://doi.org/10.1128/AAC.44.3.522-527.2000>
- 768 Nassar, S.J.M., Wills, C., Harriman, A., 2019. Inhibition of the photobleaching of
769 methylene blue by association with urea. *ChemPhotoChem* 3, 1042–1049.
770 <https://doi.org/10.1002/cptc.201900141>
- 771 Oliveira, A., Almeida, A., Carvalho, C.M.B., Tomé, J.P.C., Faustino, M.A.F., Neves,
772 M.G.P.M.S., Tomé, A.C., Cavaleiro, J.A.S., Cunha, A., 2009. Porphyrin derivatives as
773 photosensitizers for the inactivation of *Bacillus cereus* endospores. *J. Appl. Microbiol.*
774 106, 1986–1995. <https://doi.org/10.1111/j.1365-2672.2009.04168.x>
- 775 Orr, R.V., Beuchat, L.R., 2000. Efficacy of disinfectants in killing spores of
776 *Alicyclobacillus acidotorrestris* and performance of media for supporting colony
777 development by survivors. *J. Food Prot.* 63, 1117–1122. [https://doi.org/10.4315/0362-](https://doi.org/10.4315/0362-028X-63.8.1117)
778 [028X-63.8.1117](https://doi.org/10.4315/0362-028X-63.8.1117)
- 779 Osopale, B.A., Witthuhn, C.R., Albertyn, J., Oguntinyinbo, F.A., 2017. Inhibitory
780 spectrum of diverse guaiacol-producing *Alicyclobacillus acidoterrestris* by poly
781 dimethyl ammonium chloride disinfectant. *LWT - Food Sci. Technol.* 84, 241–247.
782 <https://doi.org/10.1016/j.lwt.2017.05.052>
- 783 Oteiza, J.M., Ares, G., Sant'Ana, A.S., Soto, S., Giannuzzi, L., 2011. Use of a
784 multivariate approach to assess the incidence of *Alicyclobacillus* spp. in concentrate
785 fruit juices marketed in Argentina: Results of a 14-year survey. *Int. J. Food Microbiol.*
786 151, 229–234. <https://doi.org/10.1016/j.ijfoodmicro.2011.09.004>
- 787 Oteiza, J.M., Soto, S., Alvarenga, V.O., Sant'Ana, A.S., Giannuzzi, L., 2014. Flavorings
788 as new sources of contamination by deteriorogenic *Alicyclobacillus* of fruit juices and
789 beverages. *Int. J. Food Microbiol.* 172, 119–124.

- 790 <https://doi.org/10.1016/j.ijfoodmicro.2013.12.007>
- 791 Pflug, I.J., 1999. Microbiology and engineering of sterilization process., 10th ed.
792 University of Minnesota, Minneapolis, MN.
- 793 Pornpukdeewattana, S., Jindaprasert, A., Massa, S., 2020. Alicyclobacillus spoilage
794 and control - a review. Crit. Rev. Food Sci. Nutr. 60, 108–122.
795 <https://doi.org/10.1080/10408398.2018.1516190>
- 796 Prado, D.B. do, Szczerepa, M.M. dos A., Capeloto, O.A., Astrath, N.G.C., Santos,
797 N.C.A. dos, Previdelli, I.T.S., Nakamura, C.V., Mikcha, J.M.G., Abreu Filho, B.A. de,
798 2019. Effect of ultraviolet (UV-C) radiation on spores and biofilms of Alicyclobacillus
799 spp. in industrialized orange juice. Int. J. Food Microbiol. 305.
800 <https://doi.org/10.1016/j.ijfoodmicro.2019.108238>
- 801 Prior, R.L., Hoang, H., Gu, L., Wu, X., Bacchiocca, M., Howard, L., Hampsch-Woodill,
802 M., Huang, D., Ou, B., Jacob, R., 2003. Assays for hydrophilic and lipophilic antioxidant
803 capacity (oxygen radical absorbance capacity (orac fl) of plasma and other biological
804 and food samples. J. Agric. Food Chem. 51, 3273–3279.
805 <https://doi.org/10.1021/jf0262256>
- 806 Santos, A.R., Batista, A.F.P., Gomes, A.T.P.C., Neves, M. G.P.M.S., Faustino, M.A.F.,
807 Almeida, A., Hioka, N., Mikcha, J.M.G., 2019. The remarkable effect of potassium
808 iodide in eosin and rose bengal photodynamic action against Salmonella Typhimurium
809 and Staphylococcus aureus. Antibiotics 8. <https://doi.org/10.3390/antibiotics8040211>
- 810 Santos, A.R., da Silva, A.F., Batista, A.F.P., Freitas, C.F., Bona, E., Sereia, M.J.,
811 Caetano, W., Hioka, N., Mikcha, J.M.G., 2020. Application of response surface
812 methodology to evaluate photodynamic inactivation mediated by eosin y and 530 nm
813 led against Staphylococcus aureus. Antibiotics 9, 125.
814 <https://doi.org/10.3390/antibiotics9030125>
- 815 Sawaki, T., 2007. Introduction, in: Yokota, A., Fujii, T., Goto, K. (Eds.), Alicyclobacillus:
816 Thermophilic acidophilic bacilli. Springer, Japan, Tokyo, pp. 1–5.
817 https://doi.org/10.1007/978-4-431-69850-0_1
- 818 Siegmund, B., Pöllinger-Zierler, B., 2006. Odor thresholds of microbially induced off-

- 819 flavor compounds in apple juice. *J. Agric. Food Chem.* 54, 5984–5989.
820 <https://doi.org/10.1021/jf060602n>
- 821 Silva, L.P., Gonzales-Barron, U., Cadavez, V., Sant'Ana, A.S., 2015. Modeling the
822 effects of temperature and pH on the resistance of *Alicyclobacillus acidoterrestris* in
823 conventional heat-treated fruit beverages through a meta-analysis approach. *Food*
824 *Microbiol.* 46, 541–552. <https://doi.org/10.1016/j.fm.2014.09.019>
- 825 Simões, C., Gomes, M.C., Neves, M.G.P.M.S., Cunha, A., Tomé, J.P.C., Tomé, A.C.,
826 Cavaleiro, J.A.S., Almeida, A., Faustino, M.A.F., 2016. Photodynamic inactivation of
827 *Escherichia coli* with cationic meso-tetraarylporphyrins - The charge number and
828 charge distribution effects. *Catal. Today* 266, 197–204.
829 <https://doi.org/10.1016/j.cattod.2015.07.031>
- 830 Sousa, V., Gomes, A.T.P.C., Freitas, A., Faustino, M.A.F., Neves, M.G.P.M.S.,
831 Almeida, A., 2019. Photodynamic Inactivation of *Candida albicans* in Blood Plasma
832 and Whole Blood. *Antibiotics* 8, 221. <https://doi.org/10.3390/antibiotics8040221>
- 833 Spinelli, A.C.N.F., Sant'Ana, A.S., Rodrigues-Junior, S., Massaguer, P.R., 2009.
834 Influence of different filling, cooling, and storage conditions on the growth of
835 *Alicyclobacillus acidoterrestris* CRA7152 in orange juice. *Appl. Environ. Microbiol.* 75,
836 7409–7416. <https://doi.org/10.1128/AEM.01400-09>
- 837 Tao, R., Zhang, F., Tang, Q. Juan, Xu, C. shan, Ni, Z.J., Meng, X. hong, 2019. Effects
838 of curcumin-based photodynamic treatment on the storage quality of fresh-cut apples.
839 *Food Chem.* 274, 415–421. <https://doi.org/10.1016/j.foodchem.2018.08.042>
- 840 Taze, B.H., Unluturk, S., Buzrul, S., Alpas, H., 2015. The impact of UV-C irradiation on
841 spoilage microorganisms and colour of orange juice. *J. Food Sci. Technol.* 52, 1000–
842 1007. <https://doi.org/10.1007/s13197-013-1095-7>
- 843 Tomé, J.P.C., Silva, E.M.P., Pereira, A.M.V.M., Alonso, C.M.A., Faustino, M.A.F.,
844 Neves, M.G.P.M.S., Tomé, A.C., Cavaleiro, J.A.S., Tavares, S.A.P., Duarte, R.R.,
845 Caeiro, M.F., Valdeira, M.L., 2007. Synthesis of neutral and cationic tripyridylporphyrin-
846 D-galactose conjugates and the photoinactivation of HSV-1. *Bioorganic Med. Chem.*
847 15, 4705–4713. <https://doi.org/10.1016/j.bmc.2007.05.005>

- 848 Tremarin, A., Brandão, T.R.S., Silva, C.L.M., 2017. Inactivation kinetics of
849 *Alicyclobacillus acidoterrestris* in apple juice submitted to ultraviolet radiation. *Food*
850 *Control* 73, 18–23. <https://doi.org/10.1016/j.foodcont.2016.07.008>
- 851 Uchida, R., Silva, F.V.M., 2017. *Alicyclobacillus acidoterrestris* spore inactivation by
852 high pressure combined with mild heat: Modeling the effects of temperature and
853 soluble solids. *Food Control* 73, 426–432.
854 <https://doi.org/10.1016/j.foodcont.2016.08.034>
- 855 USDA, 2020. United States Department of Agriculture. Foreign Agricultural Service.
856 Citrus: World Markets and Trade. January. [https://www.fas.usda.gov/data/citrus-world-](https://www.fas.usda.gov/data/citrus-world-markets-and-trade)
857 [markets-and-trade](https://www.fas.usda.gov/data/citrus-world-markets-and-trade) (accessed 4.23.20).
- 858 Vecchio, D., Gupta, A., Huang, L., Landi, G., Avci, P., Rodas, A., Hamblin, M.R., 2015.
859 Bacterial photodynamic inactivation mediated by methylene blue and red light is
860 enhanced by synergistic effect of potassium iodide. *Antimicrob. Agents Chemother.*
861 59, 5203–5212. <https://doi.org/10.1128/AAC.00019-15>
- 862 Vieira, C., Gomes, A.T.P.C., Mesquita, M.Q., Moura, N.M.M., Neves, M.G.P.M.S.,
863 Faustino, A.F., Almeida, A., 2018. An insight into the potentiation effect of potassium
864 iodide on APDT efficacy. *Front. Microbiol.* 9, 1–16.
865 <https://doi.org/10.3389/fmicb.2018.02665>
- 866 Vieira, C., Santos, A., Mesquita, M.Q., Gomes, A.T.P.C., Neves, M.G.P.M.S.,
867 Faustino, M.A.F., Almeida, A., 2019. Advances in aPDT based on the combination of
868 a porphyrinic formulation with potassium iodide: Effectiveness on bacteria and fungi
869 planktonic/biofilm forms and viruses. *J. Porphyr. Phthalocyanines* 23, 534–545.
870 <https://doi.org/10.1142/S1088424619500408>
- 871 Wainwright, M., Maisch, T., Nonell, S., Plaetzer, K., Almeida, A., Tegos, G.P., Hamblin,
872 M.R., 2017. Photoantimicrobials—*are we afraid of the light?* *Lancet Infect. Dis.* 17,
873 e49–e55. [https://doi.org/10.1016/S1473-3099\(16\)30268-7](https://doi.org/10.1016/S1473-3099(16)30268-7)
- 874 Wen, X., Zhang, X., Szewczyk, G., El-Hussein, A., Huang, Y.-Y., Sarna, T., Hamblin,
875 M.R., 2017. Potassium iodide potentiates antimicrobial photodynamic inactivation
876 mediated by rose bengal in in vitro and in vivo studies. *Antimicrob. Agents Chemother.*

877 61, 1–15.

878 Wisotzkey, J.D., Jurtshuk, P., Fox, G.E., Deinhard, G., Poralla, K., 1992. Comparative
879 sequence analyses on the 16S rRNA (rDNA) of *Bacillus acidocaldarius*, *Bacillus*
880 *acidoterrestris*, and *Bacillus cycloheptanicus* and proposal for creation of a new genus,
881 *Alicyclobacillus* gen. nov. *Int. J. Syst. Bacteriol.* 42, 263–269.
882 <https://doi.org/10.1099/00207713-42-2-263>

883 Wu, J., Hou, W., Cao, B., Zuo, T., Xue, C., Leung, A.W., Xu, C., Tang, Q.J., 2015.
884 Virucidal efficacy of treatment with photodynamically activated curcumin on murine
885 norovirus bio-accumulated in oysters. *Photodiagnosis Photodyn. Ther.* 12, 385–392.
886 <https://doi.org/10.1016/j.pdpdt.2015.06.005>

887 Yuan, L., Lyu, P., Huang, Y.Y., Du, N., Qi, W., Hamblin, M.R., Wang, Y., 2020.
888 Potassium iodide enhances the photobactericidal effect of methylene blue on
889 *Enterococcus faecalis* as planktonic cells and as biofilm infection in teeth. *J.*
890 *Photochem. Photobiol. B Biol.* 203, 111730.
891 <https://doi.org/10.1016/j.jphotobiol.2019.111730>

892 Zhang, Y., Dai, T., Wang, M., Vecchio, D., Chiang, L.Y., Hamblin, M.R., 2015.
893 Potentiation of antimicrobial photodynamic inactivation mediated by a cationic
894 fullerene by added iodide: in vitro and in vivo studies. *Nanomedicine* 10, 603–614.
895 <https://doi.org/10.2217/nnm.14.131>

896 Zudyte, B., Luksiene, Z., 2019. Toward better microbial safety of wheat sprouts:
897 Chlorophyllin-based photosensitization of seeds. *Photochem. Photobiol. Sci.* 18,
898 2521–2530. <https://doi.org/10.1039/c9pp00157>

Discussão geral

A partir da revisão de literatura disponível no capítulo 1 observou-se uma grande quantidade de estudos envolvendo a inativação fotodinâmica de células vegetativas e biofilmes de origem bacteriana (HUANG et al., 2020; SANTOS et al., 2019; SILVA et al., 2019; VIEIRA et al., 2019; YASSUNAKA et al., 2015). Assim, neste estudo uma maior atenção foi direcionada para a avaliação dos efeitos de aPDT em esporos de *B. cereus* e *A. acidoterrestris*.

No capítulo 2 foram avaliadas 12 diferentes cepas de *B. cereus* em relação aos efeitos do TFA com NMB e um aparato de luz vermelha (Figura 1 – A). A partir dos resultados da análise de concentração mínima inibitória (MIC) ao NMB, foi possível determinar a resistência das cepas de *B. cereus* ao tratamento fotodinâmico. Embora algumas cepas fossem da mesma origem essa condição não determinou a resistência ao processo fotodinâmico. A formação de quatro grupos de diferentes níveis de resistência à TFA revelou uma importante variabilidade entre as cepas estudadas. Este comportamento também foi observado durante o processo de secagem de leite por *spray drying* com as mesmas cepas utilizadas neste estudo (ALVARENGA et al., 2018) e confirmado entre cepas de *B. subtilis* por outro estudo (DEN BESTEN et al., 2017).

Desta forma, uma cepa de *B. cereus* de cada grupo foi selecionada de acordo com a sua resistência (B63 > 436 > B3 > ATCC 14579) para a determinação dos parâmetros cinéticos de inativação fotodinâmica. O processo de TFA na presença de NMB combinado com luz vermelha foi avaliado em células vegetativas e esporos de cada uma das cepas. Os resultados demonstraram que a inativação fotodinâmica das células vegetativas e esporos das 4 cepas selecionadas não obedeceu a uma cinética de inativação linear. Assim, o modelo de Weibull (não-linear) foi usado para ajustar os dados observados e estimar os parâmetros cinéticos de fotoinativação. O modelo de Weibull já havia sido usado para descrever a inativação fotodinâmica de células vegetativas de *B. cereus* (LE MARC et al., 2009). Outro estudo também investigou os efeitos de TFA na viabilidade celular de *B. cereus* e observou que a eficiência do

tratamento era dependente da fluência aplicada (APONIENE et al., 2015). O mesmo comportamento também foi observado neste estudo.

Como era esperado, a inativação fotodinâmica dos esporos exigiu doses de luz mais elevadas do que as células vegetativas. A estrutura da capa dos esporos, principalmente de esporos envelhecidos, elevou a resistência térmica e ao hipoclorito de sódio de *B. subtilis* em estudos anteriores (SANCHEZ-SALAS et al., 2011). Entretanto, a cepa mais sensível identificada neste estudo (ATCC 14579) apresentou resultados semelhantes entre células vegetativas e esporos. A sensibilidade entre células vegetativas e esporos de *B. cereus* foi comparada anteriormente, onde os esporos foram ligeiramente mais resistentes do que as células vegetativas usando compostos fenotiazínicos (DEMIDOVA; HAMBLIN, 2005).

Curiosamente, os valores mais baixos de δ (J/cm^2) para as células vegetativa foram observados na presença de NMB à 5 μM , sugerindo que nesta concentração a primeira redução decimal ocorreu mais rápido do que em concentrações mais elevadas. No entanto, de acordo com os valores de p apresentados na Tabela 2 do Capítulo 2, as cepas B63, 436 e B3 tornam-se resistentes à medida que a fluência aumenta com NMB 5 μM . Este comportamento confirmou-se pelas curvas de inativação côncavas ($p < 1$) apresentadas nas figuras 3-A-B-C. A única cepa com curvas de inativação convexas ($p > 1$) para todas as concentrações de NMB foi a ATCC 14579, indicando que essa cepa foi progressivamente inativada em todas as condições.

Em todas as condições testadas para esporos de *B. cereus*, os valores de p foram maiores do que 1 (Tabela 3; Capítulo 1). Curvas de inativação convexas ($p > 1$) indicam que os micro-organismos se tornam cada vez mais susceptíveis ao tratamento aplicado (VAN BOEKEL, 2002). Desta forma, observou-se que os esporos de *B. cereus* forma progressivamente inativados ao longo do tempo. Além disso, a fluência necessária para atingir 4 reduções decimais (4D) para todas as cepas testadas chegou a 400 J/cm^2 e 50 μM de NMB, exceto para a cepa mais susceptível ATCC 14579 com 25 J/cm^2 a 50 e 100 μM .

No capítulo 3, a eficiência de tratamento fotodinâmico para a inativação de esporos de *A. acidoterrestris* usando Tetra-Py⁺-Me e NMB foi investigada. Até onde

se sabe, este é o primeiro estudo que demonstrou a aplicação de TFA em esporos de *Alicyclobacillus* sp. Este estudo foi realizado inicialmente *in vitro* (PBS) para ambos os FS a 10 μ M de concentração combinados com luz branca artificial do tipo LED (Figura 1 – B). O tratamento fotodinâmico com a porfirina Tetra-Py⁺-Me (10 μ M) foi capaz de reduzir em 7 ciclos logarítmicos a população de esporos de *A. acidoterrestris* após 5 horas de exposição à luz. Entretanto, não foi observada fotoinativação dos esporos de *A. acidoterrestris* utilizando NMB na mesma concentração (Figura 4; Capítulo 3). Este resultado, pode ser atribuído ao processo de degradação ou fotobranqueamento de corantes fenotiazínicos já observado em estudos anteriores pela reação com o oxigênio singlete (GALSTYAN; DOBRINDT, 2019; NASSAR; WILLS; HARRIMAN, 2019).

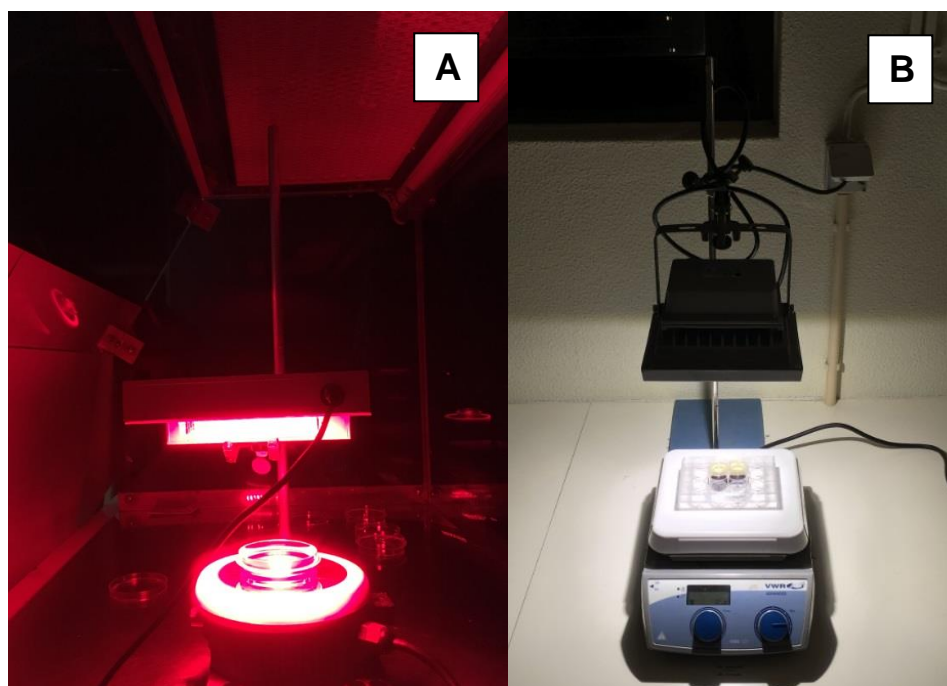


Figura 1. Aparato de 96 LEDs emissores de luz vermelha (400-700 nm; máximo: 631 nm; **A**) e aparato de LED emissor de luz branca (400-700 nm; máximo: ~ 440 nm e 540 nm; **B**)

Estudos anteriores já haviam demonstrado a eficiência do tratamento fotodinâmico em reduzir a carga de bactérias e vírus (3-8 ciclos logarítmicos) e fungos (0,8-5 ciclos logarítmicos) (BEIRÃO et al., 2014; DE MENEZES et al., 2016; VIEIRA et al., 2019; YUAN et al., 2020). Por exemplo, a porfirina Tetra-Py⁺-Me também causou de 3 a 6 reduções logarítmicas durante a fotoinativação de biofilmes (mono- e multi-

espécies) de *Staphylococcus aureus*, *Pseudomonas aeruginosa* e *Candida albicans* (BEIRÃO et al., 2014). A formação de biofilmes em ambientes de processamento de alimentos dificulta a inativação microbiana já que são estruturas que aderem fortemente à uma determinada superfície (BRIDIER et al., 2011; GALIÉ et al., 2018). Portanto, a eficiência da inativação fotodinâmica de microrganismos em biofilmes pode sugerir que essa tecnologia também pode ser eficaz na inativação de bactérias formadoras de esporos. Por exemplo, estudos envolvendo derivados de porfirinas já demonstraram que o uso de Tetra-Py⁺-Me como FS reduziu em até 3,5 ciclos logarítmicos as populações de esporos de *B. cereus* (OLIVEIRA et al., 2009).

A partir dos resultados *in vitro* de inativação fotodinâmica dos esporos de *A. acidoterrestris*, outros testes foram realizados em matrizes reais de alimentos como o suco de laranja. O uso do suco de laranja justifica-se pelos impactos negativos causados pela presença da bactéria *Alicyclobacillus* neste alimento, descritos anteriormente neste trabalho.

Dada a complexidade do suco de laranja em relação ao PBS (por exemplo, turbidez), a presença e a ausência de iodeto de potássio (KI) foram avaliadas, pois era esperado que o efeito fotodinâmico fosse reduzido (SOUSA et al., 2019). O tratamento TFA com Tetra-Py⁺-Me e NMB (10 µM) na presença de KI no suco de laranja resultou em até 5 reduções logarítmicas de esporos de *A. acidoterrestris* (Figura 5).

Desde que foi introduzido o uso de KI como agente potenciador do efeito fotodinâmico (VECCHIO et al., 2015; ZHANG et al., 2015), vários estudos foram conduzidos para confirmar essa ação em diferentes micro-organismos e estruturas microbianas (FREIRE et al., 2016; HUANG et al., 2018; VIEIRA et al., 2018, 2019; WEN et al., 2017). Nestes estudos, os autores concluíram que o KI potencializa os efeitos fotodinâmicos na maioria dos casos, aumentando a inativação de microrganismos em até 6 reduções logarítmicas.

Embora nenhum relato de estudo sobre o uso de TFA para a inativação de *A. acidoterrestris* em bebidas tenha sido identificado, outras tecnologias baseadas em exposição à luz foram utilizadas com esse objetivo. Por exemplo, verificou-se que a radiação UV-C foi capaz de causar entre 2 – 5,5 reduções logarítmicas na população

de esporos de *A. acidoterrestris* em sucos de maçã, uva e melão (BAYSAL; MOLVA; UNLUTURK, 2013; FUNDO et al., 2019; TREMARIN; BRANDÃO; SILVA, 2017). As diferenças de eficiência de inativação observadas entre os diferentes sucos podem ser explicadas pelo grau de turbidez de cada suco, que pode influenciar a penetração da luz.

O número semelhante de reduções decimais de esporos de *A. acidoterrestris* obtidas pelo presente estudo (Figura 4 e 5) e UV-C (Baysal et al., 2013; Fundo et al., 2019; Tremarin et al., 2017), apesar da diferença na idade dos esporos utilizados (28 e 2-10 dias, respectivamente), destacam os potenciais do tratamento fotodinâmico para a inativação dessa bactéria. Apesar do tempo mais longo para atingir um número semelhante de reduções decimais, outra vantagem do uso de fontes de luz visível (como no TFA) é que o tratamento fotodinâmico não apresenta riscos à saúde do operador (GUERRERO-BELTRÁN; BARBOSA-CÁNOVAS, 2004). No entanto, a eficiência do TFA e a redução do tempo de exposição podem ser aprimoradas pela combinação de compostos não tóxicos com o FS.

Como parte do processo de avaliação do impacto de TFA nas características do suco de laranja, também foram avaliados os efeitos na cor do suco. Os resultados demonstraram que houve alteração em todos os parâmetros de cor (L^* , a^* , b^*) do suco de laranja após 10 h de tratamento. Entretanto, estudos recentes mostraram que até mesmo períodos curtos (20 min) de exposição à radiação UV-C, foi observada uma alteração significativa na coordenada L^* em suco de melão (FUNDO et al., 2019). Além disso, o impacto da exposição à UV-C e LED em termos de alteração de cor diferem na literatura (BHAVYA; HEBBAR, 2019; TAO et al., 2019). Estudos anteriores também avaliaram o impacto da TFA na qualidade nutricional de morangos, damascos, ameixas, couve-flor e suco de laranja (APONIENE et al., 2015; BHAVYA; HEBBAR, 2019; LUKSIENE; PASKEVICIUTE, 2011). Embora esses estudos não tenham demonstrado nenhum efeito adverso significativo na capacidade antioxidante do alimento, nenhum desses estudos aplicou o TFA por um período tão longo ou avaliou a inativação de esporos bacterianos como o presente estudo.

A partir dos resultados obtidos nos experimentos com suco de laranja, avaliou-se a aplicação do tratamento fotodinâmico superficialmente em laranjas artificialmente

contaminadas com esporos de *A. acidoterrestris*. Os resultados mostraram uma diminuição significativa de esporos ($\approx 2,8$ reduções logarítmicas) durante o tratamento sob luz solar. Este é um resultado importante, visto que a contaminação de *Alicyclobacillus* spp. é de até 10^2 - 10^3 esporos/mL em produtos finais (ABECITRUS, 1999; OTEIZA et al., 2011). Portanto, os resultados de inativação de esporos de *A. acidoterrestris* em cascas de laranja obtidas pelo tratamento fotodinâmico sob radiação solar constituem um notável avanço tecnológico. Essa tecnologia pode ser aplicada na prática diretamente nos frutos das árvores expostas à luz solar abundante. Como tal, surge como uma estratégia viável para reduzir as contagens de esporos de *Alicyclobacillus* spp. antes do processamento de frutas.

Conclusão geral

Neste estudo foram avaliadas duas das principais espécies bacterianas envolvidas em processos de DTAs e deterioração de alimentos e bebidas. Por meio de uma nova abordagem de inativação microbiana voltada para o setor agroalimentar, foi possível determinar parâmetros cinéticos de inativação e a aplicação tecnológica em matrizes reais de alimentos.

Inicialmente nos ensaios de CIM com as 12 cepas de *B. cereus* foi observado que existe, inclusive, variabilidade entre cepas da mesma origem em relação ao processo de inativação fotodinâmica. Este fato é extremamente relevante visto que os processos industriais estabelecem parâmetros de inativação referentes a uma determinada espécie microbiana. As cepas de *B. cereus* utilizadas nos estudos subsequentes, como mencionado anteriormente, são oriundas de diferentes origens como refeições prontas (B63), chocolate (436) e leite (B3), além de uma cepa padrão (ATCC 14579). Tais cepas podem causar doenças e deterioração em produtos lácteos. O uso de TFA mediado por NMB e luz vermelha foi capaz de reduzir as populações de células vegetativas e esporos de *B. cereus*. O uso da modelagem matemática por meio do modelo de Weibull foi capaz de descrever o comportamento não-linear das curvas de inativação, bem como estimar os parâmetros cinéticos de inativação fotodinâmica. Essa ferramenta poderá contribuir com a otimização de ensaios de TFA como, por exemplo, determinando as concentrações de FS e tempo de exposição à luz.

Assim como foi observado no capítulo 2 que o processo de TFA inativou células vegetativas e esporos de *B. cereus*, o capítulo 3 elucidou a inativação de esporos de *A. acidoterrestris* em diferentes matrizes. Além disso, este estudo confirmou o efeito potencializador do KI em processos fotodinâmicos e o uso da radiação solar, sugerindo que a técnica poderia ser aplicada em campos de plantações. Comprovadamente TFA trata-se de uma tecnologia emergente que poderá em um futuro próximo substituir métodos tradicionais, como é o caso da pasteurização e sanitização. No entanto, existem gargalos que podem afetar o processo de aplicação tecnológica da TFA na indústria de alimentos, como por exemplo, efeitos indesejáveis

de alteração de cor e redução do valor nutricional dos alimentos. A otimização do processo de TFA, como o uso de FS e fontes de luz que não alterem o valor nutricional bem como as características organolépticas dos alimentos surgem como uma próspera tendência para trabalhos futuros.

Referências

- ABECITRUS. Acidothermophilic sporeforming bacteria (ATSB) in orange juices: Detection methods, ecology, and involvement in the deterioration of fruit juices. Disponível em: <http://www.citrusbr.com.br/exportadores-citricos/sobre-citrusbr/imagens/ATSB_Abecitrus.pdf>. Acesso em: 15 maio. 2020.
- ALVARENGA, V. O. et al. Survival variability of 12 strains of *Bacillus cereus* yielded to spray drying of whole milk. **International Journal of Food Microbiology**, v. 286, p. 80–89, 2018.
- APONIENE, K. et al. Reduction of microbial contamination of fruits and vegetables by hypericin-based photosensitization: Comparison with other emerging antimicrobial treatments. **Journal of Food Engineering**, v. 144, p. 29–35, 2015.
- BARBA, F. J. et al. Mild processing applied to the inactivation of the main foodborne bacterial pathogens: A review. **Trends in Food Science & Technology**, v. 66, p. 20–35, 2017.
- BARTOLOMEU, M. et al. Effect of photodynamic therapy on the virulence factors of *Staphylococcus aureus*. **Frontiers in Microbiology**, v. 7, p. 1–11, 2016.
- BAYSAL, A. H.; MOLVA, C.; UNLUTURK, S. UV-C light inactivation and modeling kinetics of *Alicyclobacillus acidoterrestris* spores in white grape and apple juices. **International Journal of Food Microbiology**, v. 166, n. 3, p. 494–498, 2013.
- BEIRÃO, S. et al. Photodynamic inactivation of bacterial and yeast biofilms with a cationic porphyrin. **Photochemistry and Photobiology**, v. 90, n. 6, p. 1387–1396, 2014.
- BHAVYA, M. L.; HEBBAR, H. U. Sono-photodynamic inactivation of *Escherichia coli* and *Staphylococcus aureus* in orange juice. **Ultrasonics sonochemistry**, v. 57, n. February, p. 108–115, 2019.
- BOTTONE, E. J. *Bacillus cereus*, a volatile human pathogen. **Clinical Microbiology Reviews**, v. 23, n. 2, p. 382–398, 2010.
- BRIDIER, A. et al. Resistance of bacterial biofilms to disinfectants: a review.

Biofouling, v. 27, n. 9, p. 1017–1032, 2011.

CARLIN, F. Origin of bacterial spores contaminating foods. **Food Microbiology**, v. 28, n. 2, p. 177–182, 2011.

CEBRIÁN, G.; MAÑAS, P.; CONDÓN, S. Comparative resistance of bacterial foodborne pathogens to non-thermal technologies for food preservation. **Frontiers in Microbiology**, v. 7, p. 1–17, 2016.

CERNY, G.; HENNLICH, W.; PORALLA, K. Fruchtsaftverderb durch Bacillen: Isolierung und charakterisierung des verderbserregers. **Zeitschrift für Lebensmittel-Untersuchung und -Forschung**, v. 179, n. 3, p. 224–227, 1984.

CHANG, S.-S.; KANG, D.-H. *Alicyclobacillus* spp. in the fruit juice industry: history, characteristics, and current isolation/detection procedures. **Critical reviews in microbiology**, v. 30, n. 2, p. 55–74, 2004.

DE MENEZES, H. D. et al. Photodynamic treatment with phenothiazinium photosensitizers kills both ungerminated and germinated microconidia of the pathogenic fungi *Fusarium oxysporum*, *Fusarium moniliforme* and *Fusarium solani*. **Journal of Photochemistry and Photobiology B: Biology**, v. 164, p. 1–12, 2016.

DEMIDOVA, T. N.; HAMBLIN, M. R. Photodynamic inactivation of *Bacillus* spores, mediated by phenothiazinium dyes. **Applied and Environmental Microbiology**, v. 71, n. 11, p. 6918–6925, 2005.

DEN BESTEN, H. M. W. et al. Microbial variability in growth and heat resistance of a pathogen and a spoiler: All variabilities are equal but some are more equal than others. **International Journal of Food Microbiology**, v. 240, p. 24–31, 2017.

FAO. Food and Agricultural Organization. Global food losses and food waste – Extent, causes and prevention. Disponível em: <<http://www.fao.org/3/a-i2697e.pdf>>. Acesso em: 18 abr. 2020.

FERRARIO, M. I.; GUERRERO, S. N. Inactivation of *Alicyclobacillus acidoterrestris* ATCC 49025 spores in apple juice by pulsed light. Influence of initial contamination and required reduction levels. **Revista Argentina de Microbiologia**, v. 50, n. 1, p. 3–11, 2018.

FREIRE, F. et al. Photodynamic therapy of oral *Candida* infection in a mouse model. **Journal of Photochemistry and Photobiology B: Biology**, v. 159, p. 161–168, 2016.

FUNDO, J. F. et al. UV-C light processing of Cantaloupe melon juice: Evaluation of the impact on microbiological, and some quality characteristics, during refrigerated storage. **LWT - Food Science and Technology**, v. 103, p. 247–252, 2019.

GALIÉ, S. et al. Biofilms in the food industry: Health aspects and control methods. **Frontiers in Microbiology**, v. 9, n. 898, 2018.

GALSTYAN, A.; DOBRINDT, U. Determining and unravelling origins of reduced photoinactivation efficacy of bacteria in milk. **Journal of Photochemistry and Photobiology B: Biology**, v. 197, p. 111554, 2019.

GUERRERO-BELTRÁN, J. A.; BARBOSA-CÁNOVAS, G. V. Review: Advantages and limitations on processing foods by UV light. **Food Science and Technology International**, v. 10, n. 3, p. 137–147, 2004.

HAMBLIN, M. R.; ABRAHAMSE, H. Oxygen-independent antimicrobial photoinactivation: Type III photochemical mechanism? **Antibiotics**, v. 9, n. 53, 2020.

HEYNDRICKX, M. The importance of endospore-forming bacteria originating from soil for contamination of industrial food processing. **Applied and Environmental Soil Science**, v. 2011, p. 1–11, 2011.

HIPPCHEN, B.; RÖLL, A.; PORALLA, K. Occurrence in soil of thermo-acidophilic bacilli possessing ω -cyclohexane fatty acids and hopanoids. **Archives of Microbiology**, v. 129, p. 53–55, 1981.

HU, X. et al. Factors affecting *Alicyclobacillus acidoterrestris* growth and guaiacol production and controlling apple juice spoilage by lauric arginate and ϵ -polylysine. **LWT**, v. 119, p. 108883, fev. 2020.

HUANG, J. et al. Enhanced antibacterial and antibiofilm functions of the curcumin-mediated photodynamic inactivation against *Listeria monocytogenes*. **Food Control**, v. 108, n. July 2019, p. 106886, fev. 2020.

HUANG, L. et al. Potentiation by potassium iodide reveals that the anionic porphyrin TPPS4 is a surprisingly effective photosensitizer for antimicrobial photodynamic inactivation. **Journal of Photochemistry and Photobiology B: Biology**, v. 178, n. August 2017, p. 277–286, jan. 2018.

JESIONEK, A.; VON TAPPEINER, H. Zur behandlung der hautcarcinome mit fluorescierenden stoffen. **Arch Klin Med**, v. 82, n. (in German), p. 223, 1905.

KIM, M.-J. et al. Antibacterial effect of 405±5nm light emitting diode illumination against Escherichia coli O157:H7, Listeria monocytogenes, and Salmonella on the surface of fresh-cut mango and its influence on fruit quality. **International Journal of Food Microbiology**, v. 244, p. 82–89, 2017.

LE MARC, Y. et al. Modelling the photosensitization-based inactivation of Bacillus cereus. **Journal of Applied Microbiology**, v. 107, n. 3, p. 1006–1011, 2009.

LUKSIENE, Z.; PASKEVICIUTE, E. Novel approach to the microbial decontamination of strawberries: chlorophyllin-based photosensitization. **Journal of applied microbiology**, v. 110, n. 5, p. 1274–83, maio 2011.

MANSOORI, B. et al. Photodynamic therapy for cancer: Role of natural products. **Photodiagnosis and Photodynamic Therapy**, v. 26, p. 395–404, 2019.

MEHTA, D. S. et al. The ability of spore formers to degrade milk proteins, fat, phospholipids, common stabilizers, and exopolysaccharides. **Journal of Dairy Science**, v. 102, n. 12, p. 10799–10813, 2019.

NASSAR, S. J. M.; WILLS, C.; HARRIMAN, A. Inhibition of the Photobleaching of Methylene Blue by Association with Urea. **ChemPhotoChem**, v. 3, n. 10, p. 1042–1049, 10 out. 2019.

ODEYEMI, O. A. et al. Understanding spoilage microbial community and spoilage mechanisms in foods of animal origin. **Comprehensive Reviews in Food Science and Food Safety**, v. 19, n. 2, p. 311–331, 2020.

OLIVEIRA, A. et al. Porphyrin derivatives as photosensitizers for the inactivation of Bacillus cereus endospores. **Journal of Applied Microbiology**, v. 106, n. 6, p. 1986–1995, jun. 2009.

ÖLMEZ, H.; KRETZSCHMAR, U. Potential alternative disinfection methods for organic fresh-cut industry for minimizing water consumption and environmental impact. **LWT - Food Science and Technology**, v. 42, n. 3, p. 686–693, 2009.

ORR, R. V. et al. Detection of guaiacol produced by *Alicyclobacillus acidoterrestris* in apple juice by sensory and chromatographic analyses, and comparison with spore and vegetative cell populations. **Journal of Food Protection**, v. 63, n. 11, p. 1517–1522, 2000.

OTEIZA, J. M. et al. Use of a multivariate approach to assess the incidence of *Alicyclobacillus* spp. in concentrate fruit juices marketed in Argentina: Results of a 14-year survey. **International Journal of Food Microbiology**, v. 151, n. 2, p. 229–234, dez. 2011.

PASKEVICIUTE, E.; ZUDYTE, B.; LUKŠIENE, Ž. Innovative Nonthermal Technologies: Chlorophyllin and Visible Light Significantly Reduce Microbial Load on Basil. **Food technology and biotechnology**, v. 57, n. 1, p. 126–132, mar. 2019.

RAAB, O. Über die Wirkung fluoreszcierender Stoffe aus Infusorien. **Ztg. Biol.**, v. 39, n. (in German), p. 524, 1900.

REVERTER-CARRIÓN, L. et al. Inactivation study of *Bacillus subtilis*, *Geobacillus stearothermophilus*, *Alicyclobacillus acidoterrestris* and *Aspergillus niger* spores under Ultra-High Pressure Homogenization, UV-C light and their combination. **Innovative Food Science and Emerging Technologies**, v. 48, n. June 2017, p. 258–264, 2018.

RODRIGUES, G. B. et al. Photodynamic inactivation of *Candida albicans* and *Candida tropicalis* with aluminum phthalocyanine chloride nanoemulsion. **Fungal Biology**, n. xxxx, p. 4–10, 2019.

SANCHEZ-SALAS, J. L. et al. Maturation of released spores is necessary for acquisition of full spore heat resistance during *Bacillus subtilis* sporulation. **Applied and Environmental Microbiology**, v. 77, n. 19, p. 6746–6754, 2011.

SANTOS, A. R. et al. The remarkable effect of potassium iodide in eosin and rose bengal photodynamic action against *salmonella typhimurium* and *staphylococcus aureus*. **Antibiotics**, v. 8, n. 4, 2019.

SIEGMUND, B.; PÖLLINGER-ZIERLER, B. Odor thresholds of microbially induced off-flavor compounds in apple juice. **Journal of Agricultural and Food Chemistry**, v. 54, n. 16, p. 5984–5989, 2006.

SILVA, A. F. et al. Xanthene Dyes and Green <scp>LED</scp> for the Inactivation of Foodborne Pathogens in Planktonic and Biofilm States. **Photochemistry and Photobiology**, v. 95, n. 5, p. 1230–1238, 16 set. 2019.

SMIT, Y. et al. Alicyclobacillus spoilage and isolation – A review. **Food Microbiology**, v. 28, n. 3, p. 331–349, maio 2011.

SOUSA, V. et al. Photodynamic Inactivation of *Candida albicans* in Blood Plasma and Whole Blood. **Antibiotics**, v. 8, n. 4, p. 221, 13 nov. 2019.

SPANU, C. **Sporeforming bacterial pathogens in ready-to-eat dairy products**. [s.l.] Elsevier Inc., 2016.

SPINELLI, A. C. N. F. et al. Influence of different filling, cooling, and storage conditions on the growth of *Alicyclobacillus acidoterrestris* CRA7152 in orange juice. **Applied and Environmental Microbiology**, v. 75, n. 23, p. 7409–7416, 2009.

TAO, R. et al. Effects of curcumin-based photodynamic treatment on the storage quality of fresh-cut apples. **Food Chemistry**, v. 274, n. April 2018, p. 415–421, 2019.

TORLAK, E. Inactivation of *Alicyclobacillus acidoterrestris* spores in aqueous suspension and on apples by neutral electrolyzed water. **International Journal of Food Microbiology**, v. 185, p. 69–72, ago. 2014.

TREMARIN, A.; BRANDÃO, T. R. S.; SILVA, C. L. M. Inactivation kinetics of *Alicyclobacillus acidoterrestris* in apple juice submitted to ultraviolet radiation. **Food Control**, v. 73, p. 18–23, 2017.

UCHIDA, R.; SILVA, F. V. M. *Alicyclobacillus acidoterrestris* spore inactivation by high pressure combined with mild heat: Modeling the effects of temperature and soluble solids. **Food Control**, v. 73, p. 426–432, 2017.

VAN BOEKEL, M. On the use of the Weibull model to describe thermal inactivation of microbial vegetative cells. **International Journal of Food Microbiology**, v. 74, n. 1–

2, p. 139–159, 25 mar. 2002.

VAN LUONG, T. S. et al. Diversity and guaiacol production of *Alicyclobacillus* spp. from fruit juice and fruit-based beverages. **International Journal of Food Microbiology**, v. 311, n. August, p. 108314, 2019.

VECCHIO, D. et al. Bacterial photodynamic inactivation mediated by methylene blue and red light is enhanced by synergistic effect of potassium iodide. **Antimicrobial Agents and Chemotherapy**, v. 59, n. 9, p. 5203–5212, 2015.

VEIRA, C. et al. An insight into the potentiation effect of potassium iodide on APDT efficacy. **Frontiers in Microbiology**, v. 9, n. NOV, p. 1–16, 2018.

VIEIRA, C. et al. Advances in aPDT based on the combination of a porphyrinic formulation with potassium iodide: Effectiveness on bacteria and fungi planktonic/biofilm forms and viruses. **Journal of Porphyrins and Phthalocyanines**, v. 23, n. 4–5, p. 534–545, 2019.

WAINWRIGHT, M. et al. Photoantimicrobials—are we afraid of the light? **The Lancet Infectious Diseases**, v. 17, n. 2, p. e49–e55, 2017.

WEN, X. et al. Potassium Iodide Potentiates Antimicrobial Photodynamic Inactivation Mediated by Rose Bengal in In Vitro and In Vivo Studies. **Antimicrobial Agents and Chemotherapy**, v. 61, n. 7, p. 1–15, 2017.

WHO. **World Health Organization. WHO estimates of the global burden of foodborne diseases.** [s.l.: s.n.]. Disponível em: <https://apps.who.int/iris/bitstream/handle/10665/199350/9789241565165_eng.pdf?sequence=1>.

WISOTZKEY, J. D. et al. Comparative Sequence Analyses on the 16S rRNA (rDNA) of *Bacillus acidocaldarius*, *Bacillus acidoterrestris*, and *Bacillus cycloheptanicus* and Proposal for Creation of a New Genus, *Alicyclobacillus* gen. nov. **International Journal of Systematic Bacteriology**, v. 42, n. 2, p. 263–269, 1 abr. 1992.

WORLD BANK. **The Safe Food Imperative: Accelerating Progress in Low- and Middle-Income Countries.** Disponível em: <<https://openknowledge.worldbank.org/bitstream/handle/10986/30568/97814648134>

50.pdf?sequence=6&isAllowed=y>. Acesso em: 24 abr. 2020.

YAMAZAKI, K.; TEDUKA, H.; SHINANO, H. Isolation and Identification of Alicyclobacillus acidoterrestris from Acidic Beverages. **Bioscience, Biotechnology, and Biochemistry**, v. 60, n. 3, p. 543–545, 12 jan. 1996.

YASSUNAKA, N. N. et al. Photodynamic Inactivation Mediated by Erythrosine and its Derivatives on Foodborne Pathogens and Spoilage Bacteria. **Current Microbiology**, v. 71, n. 2, p. 243–251, 2015.

YUAN, L. et al. Potassium iodide enhances the photobactericidal effect of methylene blue on Enterococcus faecalis as planktonic cells and as biofilm infection in teeth. **Journal of Photochemistry and Photobiology B: Biology**, v. 203, n. December 2019, p. 111730, 2020.

ZHANG, Y. et al. Potentiation of antimicrobial photodynamic inactivation mediated by a cationic fullerene by added iodide: In vitro and in vivo studies. **Nanomedicine**, v. 10, n. 4, p. 603–614, 2015.

ŽUDYTE, B.; LUKŠIENE, Ž. Toward better microbial safety of wheat sprouts: Chlorophyllin-based photosensitization of seeds. **Photochemical and Photobiological Sciences**, v. 18, n. 10, p. 2521–2530, 2019.

Anexos

Anexo 1. Confirmação de aceite de publicação de artigo original referente ao Capítulo 3 entítulado: “Antimicrobial photodynamic treatment as an alternative approach for *Alicyclobacillus acidoterrestris* inactivation”.

16/09/2020

Fwd: Your Submission - prado.leonardo27@gmail.com - Gmail

De: **Luca Cocolin** <eesserver@eesmail.elsevier.com>
Date: seg., 27 de jul. de 2020 às 08:11
Subject: Your Submission
To: <and@unicamp.br>
Cc: <ubarron@ijpb.pt>

Ms. Ref. No.: FOOD-D-20-00511R1
Title: Antimicrobial photodynamic treatment as an alternative approach for *Alicyclobacillus acidoterrestris* inactivation
International Journal of Food Microbiology

Dear Anderson,

I am pleased to inform you that your paper "Antimicrobial photodynamic treatment as an alternative approach for *Alicyclobacillus acidoterrestris* inactivation" has been accepted for publication in International Journal of Food Microbiology.

Your accepted manuscript will now be transferred to our production department and work will begin on creation of the proof. If we need any additional information to create the proof, we will let you know. If not, you will be contacted again in the next few days with a request to approve the proof and to complete a number of online forms that are required for publication.

Further information on the handling of your manuscript as well as the scheduled time of publication may be obtained at: <http://authors.elsevier.com>

Yours sincerely,

Luca Cocolin, Ph.D
Editor In Chief
International Journal of Food Microbiology

Anexo 2. Comprovante de cadastro de acesso ao Patrimônio Genético/CTA no Sisgen.



Ministério do Meio Ambiente
CONSELHO DE GESTÃO DO PATRIMÔNIO GENÉTICO
 SISTEMA NACIONAL DE GESTÃO DO PATRIMÔNIO GENÉTICO E DO CONHECIMENTO TRADICIONAL ASSOCIADO

Comprovante de Cadastro de Acesso
 Cadastro nº A276CB6

A atividade de acesso ao Patrimônio Genético, nos termos abaixo resumida, foi cadastrada no SisGen, em atendimento ao previsto na Lei nº 13.123/2015 e seus regulamentos.

Número do cadastro: **A276CB6**
 Usuário: **UNICAMP**
 CPF/CNPJ: **46.068.425/0001-33**
 Objeto do Acesso: **Patrimônio Genético**
 Finalidade do Acesso: **Pesquisa**

Espécie

Bacillus cereus

Título da Atividade: **Inativação microbiana por tratamento fotodinâmico: da cinética de inativação à aplicações em vegetais**

Equipe

Leonardo do Prado Silva **UNICAMP**
Anderson de Souza Sant'Ana **UNICAMP**

Data do Cadastro: **22/06/2020 11:33:49**
 Situação do Cadastro: **Concluído**

Conselho de Gestão do Patrimônio Genético
 Situação cadastral conforme consulta ao SisGen em **11:35** de **22/06/2020**.



SISTEMA NACIONAL DE GESTÃO
 DO PATRIMÔNIO GENÉTICO
 E DO CONHECIMENTO TRADICIONAL
 ASSOCIADO - **SISGEN**